

Formation of carbonyl compounds during ozonation of wastewater: Method development for non-target screening and precursor evaluation

Master Thesis

Author(s):

Gebhardt, Isabelle

Publication date:

2021

Permanent link:

<https://doi.org/10.3929/ethz-b-000641262>

Rights / license:

[In Copyright - Non-Commercial Use Permitted](#)

ETH

Eidgenössische Technische Hochschule Zürich
Swiss Federal Institute of Technology Zurich

Swiss Federal Institute of Technology (ETH)
8006 Zürich
Department of Environmental Systems Science
Institute of Biogeochemistry and Pollutant Dynamics

eawag
aquatic research 000

Swiss Federal Institute of Aquatic Science (EAWAG)
8600 Dübendorf
Department of Water Resources and Drinking Water
Research Group Drinking Water Chemistry

Master's thesis

Master's degree programme in Environmental Sciences

Formation of carbonyl compounds during ozonation of wastewater: Method development for non-target screening and precursor evaluation

Supervisor: Prof. Dr. Urs von Gunten
Eawag, Department Water Resources & Drinking Water

Co-Supervisors: Joanna Houska
Eawag, Department Water Resources & Drinking Water

Dr. Tarek Manasfi
Eawag, Department Environmental Chemistry

submitted by: Isabelle Gebhardt
(15-915-937)
8006 Zurich

January 10, 2021

Abstract

The identification of unknown carbonyls in complex matrices remains to be a bottleneck in analytical chemistry. In this study, a method for the derivatization and non-target analysis of carbonyls in different water matrices including wastewater (WW) was optimized. The method involved derivatization of carbonyls with *p*-toluenesulfonylhydrazine (TSH) and the resulting TSH-hydrazone were analyzed by liquid chromatography coupled to electrospray ionization high-resolution mass spectrometry (LC-ESI-HRMS). The following derivatization parameters were optimized: TSH concentration, acid concentration, and reaction time. Along with target analysis of 16 carbonyls, non-target analysis of unknown carbonyls was conducted by tracking signature fragments originating from the derivatizing agent in laboratory-ozonated WW, lake-water (LW), Suwannee River Fulvic acid (SRFA) and selected model compounds with and without OH radical scavenger. Formaldehyde, acetaldehyde, glyoxylic acid and pyruvic acid were observed at relatively high concentrations (total concentration of 3.7-6.3 μM) in WW after ozonation at a specific ozone dose (0.5 $\text{mgO}_3/\text{mgDOC}$) without quenching of OH radicals. The non-target analysis of ozonated samples using the developed workflow allowed the detection of over 70 unknown carbonyls in some ozonated wastewater samples. Possible and probable structures were proposed for some unknown carbonyls. Olefins, phenols and β -diketones and presumably such structures within DOM were precursors of carbonyls formed during ozonation of WW. The ozonation of such precursors (e.g. sorbic acid, phenol) provided further information for the structure elucidation of unknown carbonyls.

Table of Contents

List of Figures	1
List of Tables.....	3
1. Introduction	4
1.1 Ozonation in wastewater treatment	4
1.2 Toxicity of carbonyls.....	4
1.3 Analysis of carbonyls	5
1.4 Carbonyl formation mechanisms.....	6
1.5 Goals and approach	7
2. Materials and methods.....	8
2.1 Reagents and solutions	8
2.1.1 Chemicals	8
2.1.2 Stock solutions	9
2.2 Ozonation of different water matrices and carbonyl precursor evaluation.....	10
2.2.1 Preparation of ozone stock solution	10
2.2.2 Ozonation of DOM, wastewater and lake water.....	10
2.2.3 Ozonation of carbonyl precursors	12
2.3 LC-ESI-HRMS method.....	13
2.4 Optimization of derivatization.....	13
2.4.1 Influence of TSH concentration	14
2.4.2 Influence of acid addition.....	15
2.4.3 Influence of reaction time.....	15
2.4.4 Influence of derivatization on the detectability of carbonyl compounds.....	15
2.5 Method performance characteristics.....	16
2.5.1 Linearity ranges, limits of detection and quantification	16
2.5.2 Analytical matrix effects	16
2.5.3 Stability of derivatized carbonyl compounds	17
2.6 Data analysis and non-target workflow	17
3. Results and discussion.....	19
3.1 Optimization of derivatization.....	19
3.1.1 Influence of TSH concentration	19
3.1.2 Influence of acid concentration and reaction time.....	20
3.1.3 Influence of derivatization on the detectability of carbonyls	21
3.2 Identification of unknown carbonyls by non-target analysis.....	22

3.3 Carbonyl precursor evaluation and structure elucidation	25
3.3.1 Olefinic carbonyl precursors	25
3.3.2 Phenolic carbonyl precursors	33
3.4 Ozonation of different water matrices	36
3.4.1 Quantification of target carbonyl compounds	36
3.4.2 Identification of non-target carbonyl compounds	39
3.5 Limitations.....	43
4. Conclusions and outlook	43
5. Acknowledgements	46
6. References	47
Supporting Information (SI).....	51
Section S.1 Abbreviations	51
Section S.2 Impurities in TSH chemical	51
Section S.3 Volumes of ozone stock solution spiked to different water matrices.....	53
Section S.4 Linearity ranges, limits of detection and quantification.....	53
Section S.5 Analytical matrix effects	54
Section S.6 Stability of derivatized carbonyl compounds.....	55
Section S.7 Repeatability of internal standard spiking.....	56
Section S.8 Dilution factors applied for correction for quantification of target carbonyl compounds	56
Section S.9 Applied ozone doses for ozonation of carbonyl precursors	56
Section S.10 Compound Discoverer workflow	57
Section S.11 Input files, grouping and ratios in Compound Discoverer	58
Section S.12 Influence of TSH concentration on derivatization efficiencies in different water matrices	59
Section S.13 Quantified concentrations of target carbonyl compounds in different water matrices.	61
Section S.14 Identified (using non-target workflow) carbonyl compounds in different ozonated waters with OH radical scavenging	64
Section S.15 Carbonyl compounds that were formed in the ozonolysis of model compounds as a function of applied ozone dose.....	65
Section S.16 Drawings of carbonyl compound products formed during ozonolysis of model compounds according to Criegee mechanism	68
Section S.17 Identified (using non-target workflow) N-containing carbonyl compounds in different water matrices.....	72
Declaration of originality	73

List of Figures

Figure 1. Acid-catalyzed hydrazone formation from the reaction of TSH with benzaldehyde.....	6
Figure 2. Criegee mechanism for reactions of olefins with ozone in aqueous solutions. Modified from von Sonntag & von Gunten, 2012.	7
Figure 3. Scheme of sample preparation of a blank that was derivatized (TSH 200 μ M, HCl 0.02 M), a benzaldehyde-TSH/cinnamaldehyhde-TSH (B/C-TSH) calibration standard (200 nM) and a sample spiked with benzaldehyde/cinnamaldejyde (B/C) (200 nM) that was derivatized. All samples were spiked with the two internal standards benzaldehyde-d6 (B-d6) and tramadol-d6 (T-d6) and had a total volume of 1.5 mL.	15
Figure 4. Signature fragments for derivatized carbonyl compounds originating from the derivatizing agent TSH with exact masses of 139.0212, 155.0161 and 157.0318 Da and structures in positive ESI.	18
Figure 5. Influence of TSH concentration on the derivatization efficiency (%) of (a) benzaldehyde and (b) cinnamaldehyde in different water matrices.	19
Figure 6. (a) Influence of HCl concentration on the derivatization efficiency for 13 target carbonyl compounds; (b) influence of reaction time at room temperature on the derivatization efficiency for 16 target carbonyl compounds.	20
Figure 7. Detectability of 16 target carbonyl compounds in positive and negative ESI modes. The pink (negative mode) and magenta (positive mode) coloured bars refer to non-derivatized samples. The lightblue (negative mode) and blue (positive mode) coloured bars refer to derivatized samples.	21
Figure 8. Scheme of the criteria applied to the outcome of the Compound Discoverer analysis for WW Neugut samples (without OH radical scavenging). With five criteria, 42 results were selected from initially 1405 results.	22
Figure 9. Scheme of workflow for assignment of possible and probable structures for unknown carbonyls. Confidence levels of identification according to Schymanski et al., 2014.	23
Figure 10. Scheme of product formation from reactions of sorbic acid with ozone according to the Criegee mechanism. Reaction arrows indicate an attack of ozone at the carbon double bond highlighted in the same color.	26
Figure 11. Scheme of tentative (not solely according to the Criegee mechanism) product formation from reactions of sorbic acid with ozone. Reaction mechanism is adapted from mechanism of ozonolysis of acrylic acid shown in von Sonntag & von Gunten (2012).	30
Figure 12. Scheme of possible and probable structures for carbonyl compounds that were formed during ozonolysis of 3-buten-2-ol in the presence of the OH radical scavenger DMSO. The tentative candidates in grey are less likely than the ones in black color (based on the structure of the precursor 3-buten-2-ol).....	31
Figure 13. Scheme of possible and probable structures for carbonyl compounds that were formed during ozonolysis of acetylacetone in the presence of the OH radical scavenger DMSO. The tentative candidates in grey are less likely than the ones in black color (based on the structure of the precursor acetylacetone).....	33
Figure 14. Tentative candidates for $H_6H_8O_2$ and $C_6H_8O_3$ formed during the ozonolysis of 4-ethylphenol based on the Criegee mechanism.....	34
Figure 15. Tentative candidates for $C_3H_4O_3$ and $C_7H_8O_4$ formed during the ozonolysis of 4-methoxyphenol based on the Criegee mechanism.....	35
Figure 16. Quantification of formaldehyde, acetaldehyde, glyoxylic acid, pyruvic acid, glyoxal and glutaraldehyde in different ozonated water samples (without and with DMSO). The red horizontal line indicates the LOQ for each target carbonyl compound. The blue vertical line is drawn at a specific	

ozone dose of 0.5 mgO₃ / mgDOC, which is typically applied in WWTPs. The specific ozone dose (mgO₃ / mgDOC) is shown on the x-axis and the concentration on the y-axis (nM or μM). The y-axis for formaldehyde is presented in a logarithmic scale. Concentrations below the LODs are not shown.

.....	37
Figure 17. Peak areas (arbitrary units, y-axis) of eight carbonyl compounds that were identified in ozonated WW, LW and SRFA (without DMSO) as a function of the specific ozone dose (mgO ₃ /mgDOC, x-axis). The blue vertical line is drawn at a specific ozone dose of 0.5 mgO ₃ / mgDOC, which is typically applied in WWTPs.	42
Figure S.1. Contamination with acetaldehyde-, acetone-, butyraldehyde-, formaldehyde- and 3-pentanone-TSH hydrazones as a function of increasing TSH concentrations (μM) spiked to blanks (NP water).....	52
Figure S.2. Stability of 13 derivatized target carbonyl compounds in a sample stored at 4 °C in the autosampler that was analysed every day during a measurement series of five days.	55
Figure S.3. Nodes and description of pre-defined Compound Discoverer workflow template “Untargeted environmental research ID workflow with statistics: Detect and identify unknown compounds with differential analysis”.....	57
Figure S.4. Input files, sample type and treatment for analysis of SRFA (exemplary) samples in Compound Discoverer analysis.	58
Figure S.5. Generated ratios for treatments in Compound Discoverer analysis.....	59
Figure S.6. Influence of TSH concentration on the derivatization efficiencies of several target carbonyl compounds in different water matrices.	60
Figure S.7. Peak areas for a selection of carbonyl compounds that were formed during ozonolysis (with DMSO) of sorbic acid as a function of ozone dose (μM).....	65
Figure S.8. Peak areas for all of carbonyl compounds that were formed during ozonolysis (with DMSO) of 3-buten-2-ol as a function of ozone dose (μM).....	66
Figure S.9. Peak areas for a selection of carbonyl compounds that were formed during ozonolysis (with DMSO) of acetylacetone as a function of ozone dose (μM).....	66
Figure S.10. Peak areas for a selection of carbonyl compounds that were formed during ozonolysis (with DMSO) of phenol as a function of ozone dose (μM).	67
Figure S.11. Peak areas for a selection of carbonyl compounds that were formed during ozonolysis (with DMSO) of 4-ethylphenol as a function of ozone dose (μM).	67
Figure S.12. Peak areas for a selection of carbonyl compounds that were formed during ozonolysis (with DMSO) of 4-methoxyphenol as a function of ozone dose (μM).	68
Figure S.13. Carbonyl compounds formed during ozonolysis of cinnamic acid, sorbic acid, 3-buten-2-ol and acetylacetone according to Criegee mechanism.	68
Figure S.14. Carbonyl compounds formed during ozonolysis of 4-ethylphenol according to Criegee mechanism.....	69
Figure S.15. Carbonyl compounds formed during ozonolysis of 4-methoxyphenol according to Criegee mechanism.	69
Figure S. 16. Carbonyl compounds formed during ozonolysis of phenol (ozonide 1) according to Criegee mechanism.	70
Figure S.17. Carbonyl compounds formed during ozonolysis of phenol (ozonide 2) according to Criegee mechanism.	70
Figure S. 18. Carbonyl compounds formed during ozonolysis of phenol (ozonide 3) according to Criegee mechanism.	71

List of Tables

Table 1. Target carbonyl compounds used in this study, including name, purity or weight percent, molecular formula, carbonyl class, CAS number and supplier.	9
Table 2. Selected model compounds for carbonyl precursor evaluation, including name, purity, molecular formula, CAS number and supplier of the chemicals.	9
Table 3. Water quality parameters measured for each water sample included conductivity, pH, alkalinity, hardness, ammonium concentration (NH_4^+), nitrite concentration (NO_2^-), dissolved organic carbon content (DOC), and dissolved total nitrogen content. ND (not determined) indicates that this value was not measured.	11
Table 4. Applied specific ozone doses ($\text{mgO}_3/\text{mgDOC}$) and respective DOC (mg/L) of different samples.	12
Table 5. Overview on the total carbonyl content (μM) and TSH concentrations (μM) used in the experiments for derivatization optimization and assessment.	14
Table 6. Summary of molecular formulas and retention times for carbonyl compounds (excluding <i>N</i> -containing) that were identified (using non-target workflow) in ozonated WWs, SRFA and LW without OH radical scavenging (without DMSO) and from the ozonated model compounds (excluding cinnamic acid) with OH radical scavenging (with DMSO).	27
Table 7. Count of total compounds (including <i>N</i> -containing) and <i>N</i> -containing results for the different ozonated water samples (without DMSO and with DMSO). ND (not determined) indicates that this value was not obtained.	40
Table S.1. Volumes (μL) of ozone stock solution (1.69 mM) spiked to different water matrices.	53
Table S.2. R^2 , LODs, LOQs and linearity ranges for all target carbonyl compounds.	54
Table S.3. Analytical matrix effects (%) for benzaldehyde- and cinnamaldehyde-TSH hydrazones in different water matrices.	55
Table S.4. Dilution factor for correction of concentrations of target carbonyls in different water matrices that were spiked with specific ozone doses.	56
Table S.5. Spiked volumes (theoretical values) (μL) of ozone stock solution (1.59 mM), applied ozone doses (theoretical) (μM), actual ozone doses in samples (μM) and molar ratio ozone to compound spiking.	56
Table S.6. Modifications to pre-defined workflow from Compound Discoverer.	58
Table S.7. Quantified formaldehyde concentrations (μM) in different water matrices.	61
Table S.8. Quantified acetaldehyde concentrations (μM) in different water matrices.	61
Table S.9. Quantified glyoxilic acid concentrations (μM) in different water matrices.	62
Table S.10. Quantified pyruvic acid concentrations (μM) in different water matrices.	62
Table S.11. Quantified glyoxal concentrations (nM) in different water matrices.	63
Table S.12. Quantified glutaraldehyde concentrations (nM) in different water matrices.	63
Table S.13. Summary of molecular formulas and retention times for carbonyl compounds (excluding <i>N</i> -containing) that were identified (using non-target workflow) in ozonated WWs and SRFA with OH radical scavenging (with DMSO).	64
Table S.14. Molecular formulas and RTs of identified (using non-target workflow) <i>N</i> -containing carbonyl compounds in different water matrices.	72

1. Introduction

1.1 Ozonation in wastewater treatment

Chemical oxidants such as ozone are applied in water treatment for (i) disinfection, and (ii) the enhanced abatement of organic micropollutants. Ozone is very effective in inactivating viruses, bacteria, fungi and protozoa and was first used as a disinfectant for drinking water in the beginning of the 20th century (von Sonntag & von Gunten, 2012). Ozonation is used in drinking water and wastewater (WW) treatment and is also widely discussed as a treatment step for municipal water reuse, which aims to increase water security and reduce water scarcity issues in arid regions (von Gunten, 2018). In Switzerland, due to Art. 60b in the Waters Protection Act (WPA) adopted in January 2016, about 100 out of 700 Swiss wastewater treatment plants (WWTPs) have to be upgraded with an advanced treatment step (e.g. ozonation) for micropollutant abatement (Bourgin et al., 2018). The WPA aims to improve surface water quality by reducing the load of micropollutants discharged from conventional WWTPs where they are insufficiently eliminated. An average 80% of organic micropollutants should be abated over the whole WWTP from influent to effluent (Eggen et al., 2014).

Ozone is a strong oxidant that reacts with water matrix components and micropollutants and leads to the formation of ozonation byproducts (OBP) and ozonation transformation products (OTP) respectively, among which some might be toxic (von Gunten, 2018). In WW, the largest fraction of ozone is consumed by dissolved organic matter (DOM), for the most part by phenolic moieties (von Gunten, 2018). Numerous OBPs have been identified so far, but further investigations are needed to reveal the full range of OBPs. More specifically, some carbonyl-containing byproducts are analytically challenging to detect and could be undetected without derivatization. Besides ozone, also OH radicals play a role, which are produced from various ozone decomposition reactions (von Sonntag & von Gunten, 2012). While OH radicals contribute to the abatement of micropollutants, they may also contribute to the formation of undesired OBPs. Carbonyl compounds such as potentially toxic aldehydes, ketones, diketones and ketoacids may be formed from reactions of ozone and/or OH radicals with DOM. Relatively high concentrations of carbonyl compounds ($> 7 \mu\text{M}$) were measured after ozonation of WW (Marron et al., 2020). Since these carbonyl-containing OBPs are often easily biodegradable, a biological post-treatment step is typically implemented after an oxidation in drinking or WW treatment (Von Gunten, 2018). Marron et al., 2020 studied the formation and fate of carbonyls in potable water reuse systems. The authors measured the concentrations of six saturated aldehydes, seven α,β -unsaturated aldehydes, and one ketone in several water reuse facilities. In facilities where biological filtration or biologically active carbon filtration was applied after ozone treatment, the observed carbonyl concentrations were reduced by over 90% by those biological post-treatment steps (Marron et al., 2020).

1.2 Toxicity of carbonyls

Carbonyls elicit toxicity by forming covalent bonds with nucleophilic sites on biological targets such as enzymes, proteins, DNA and other macromolecules (Feron et al., 1991; Lopachin & Gavin, 2014). The resulting adduct formation thereby impairs cellular processes and may lead to cytotoxicity (Lopachin & Gavin, 2014). Exposure to carbonyls has been associated with

health risks such as cancer, cardiovascular diseases, diabetes or Alzheimer's disease (Lopachin & Gavin, 2014). Carbonyls in the environment originate both from natural and anthropogenic sources (Lopachin & Gavin, 2014). More than 300 unsaturated aldehydes (such as cinnamaldehyde or cinnamaldehyde) are naturally contained in various foods such as fish or potatoes (Lopachin & Gavin, 2014). It is estimated that the daily intake of α,β -unsaturated aldehydes through drinking water and food consumption is about 5 mg/kg body weight (Lopachin & Gavin, 2014). α,β -unsaturated aldehydes are more toxic than their saturated analogues because of an increased electrophilicity due to a double bond between the carbonyl groups (Benigni et al., 2005; Lopachin & Gavin, 2014). α,β -unsaturated carbonyls such as acrolein or methylvinyl ketone for example are associated with toxicity of most major organs including the hepatic, renal, respiratory, and nervous systems (Lopachin et al., 2008). Saturated aldehydes such as acetaldehyde and formaldehyde are probable human carcinogens classified by the US EPA (group B2 and B1 respectively). Acetaldehyde and formaldehyde are produced during ozonation as well as during disinfection with chlorine and chlorine dioxide in water treatment (Weinberg et al., 1993). In ozonated drinking water formaldehyde concentrations of up to 30 $\mu\text{g/L}$ have been found (Tomkins et al., 1989). Concentrations of these carbonyls in treated waters should be monitored to prevent undesired health risks. California for example has set a notification level of 100 $\mu\text{g/L}$ for formaldehyde in treated water (Cal/EPA, 2010). Oxoaldehydes such as glyoxal and methylglyoxal or unsaturated aldehydes may also be generated endogenously during oxidative stress, and possibly interact with other environmental aldehydes amplifying the oxidative damage to cells (Lopachin & Gavin, 2014). Due to the abundance of carbonyls in dietary components, drinking water and the environment, further investigations regarding the toxicity mechanisms of these compounds merit consideration.

1.3 Analysis of carbonyls

Carbonyls are difficult to analyse with liquid chromatography coupled to electrospray ionization high-resolution mass spectrometry (LC-ESI-HRMS) for several reasons (Siegel et al., 2014). Firstly, they are insufficiently retained on a C18 column due to their hydrophilicity. Secondly, they show a poor ionization in ESI due to the absence of ionizable functional groups. Thirdly, they produce no selective fragment ions that help deduce their structure. Thus, the identification and quantification of carbonyls remain a major bottleneck in LC-ESI-HRMS, especially in complex matrices such as WW (Siegel et al., 2014). As a measure against poor ionizability, derivatization of carbonyls needs to be carried out prior to analysis. The following are two derivatizing agents among many phenylhydrazines that have been used in the past: 2,4-dinitrophenylhydrazine (DNPH) (Liu et al., 2020; Richardson et al., 2000) and *p*-toluenesulfonylhydrazine (TSH) (Marron et al., 2020; Siegel et al., 2014). When used with LC-MS analysis, DNPH derivatization suffers from several disadvantages such as a limited solubility in aqueous samples, explosiveness, and enhanced deposition in the MS ion-source (Siegel et al., 2014). In a screening for other commercially available derivatizing agents, Siegel et al., 2014 identified TSH as a good alternative to DNPH claiming that TSH showed a higher solubility and higher volatility compared to DNPH. At higher temperatures (about 150 °C), TSH decomposes to gaseous species, which reduces its deposition in the MS ion-source and allows for injection of an excess of TSH in a sample (Siegel et al., 2014). Due to these advantages, TSH was chosen as a derivatizing agent in this study. This approach facilitates the identifications of

unknown carbonyls in WW based on the detection of signature fragment ions originating from the derivatizing agent. Carbonyls and TSH (hydrazine) form a carbonyl-TSH-hydrazone catalysed by acid (Siegel et al., 2014). There is a possibility of E/Z isomer formation. The reaction proceeds exclusively via aldehyde/keto-carbonyls, carbonyl groups conjugated to heteroatoms as found in carboxylic acids or esters are not reactive (Siegel et al., 2014). The acid-catalyzed hydrazone formation from the reaction of TSH with benzaldehyde is shown in Figure 1.

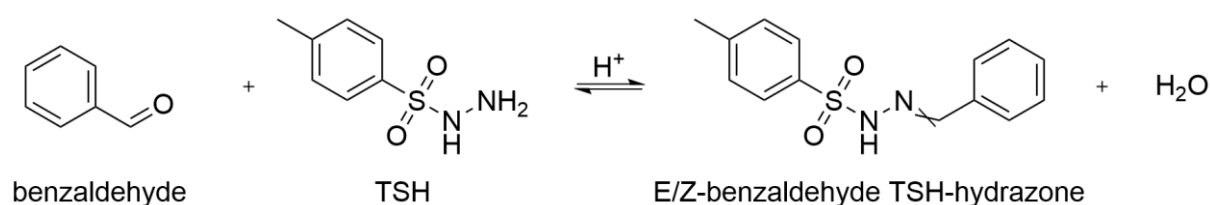


Figure 1. Acid-catalyzed hydrazone formation from the reaction of TSH with benzaldehyde.

1.4 Carbonyl formation mechanisms

Ozone reacts readily with electron rich moieties of organic compounds (von Sonntag & von Gunten, 2012). For the carbonyl formation, the two major ozone-reactive sites are olefins and activated aromatic compounds. Olefins react with ozone mainly according to the Criegee mechanism, which describes the classical reaction mechanism between ozone and a carbon-carbon double bond. According to the Criegee mechanism (Figure 2) an ozonide is formed followed by the cleavage of a carbon-carbon double bond (Criegee, 1975). The products from this cleavage are a zwitterion and a carbonyl. In aqueous solutions, an α -hydroxyalkylhydroperoxide is formed from the zwitterion. The α -hydroxyalkylhydroperoxide is in equilibrium with hydrogen peroxide and a carbonyl. Ozone in reaction with olefins that consist of two distinct alkyl groups (R1 and R2) may form two different carbonyls in aqueous solution (containing R1 or R2) (Figure 2).

Similar to olefins, aromatic compounds can also form an ozonide in reactions with ozone and then react according to the Criegee mechanism. However, an adduct is formed in the reactions of aromatic compounds with ozone prior to the formation of an ozonide (von Sonntag & von Gunten, 2012). In aromatic systems, the positive charge that develops upon adduct formation is distributed over the entire aromatic ring and thus stabilizes the chemical intermediate. From this chemical intermediate, several other reaction pathways can occur (Ramseier & von Gunten, 2009; Tentscher et al., 2018). Thus, the Criegee mechanism is only one of many reaction mechanisms that occur in reactions of aromatic compounds with ozone (von Sonntag & von Gunten, 2012).

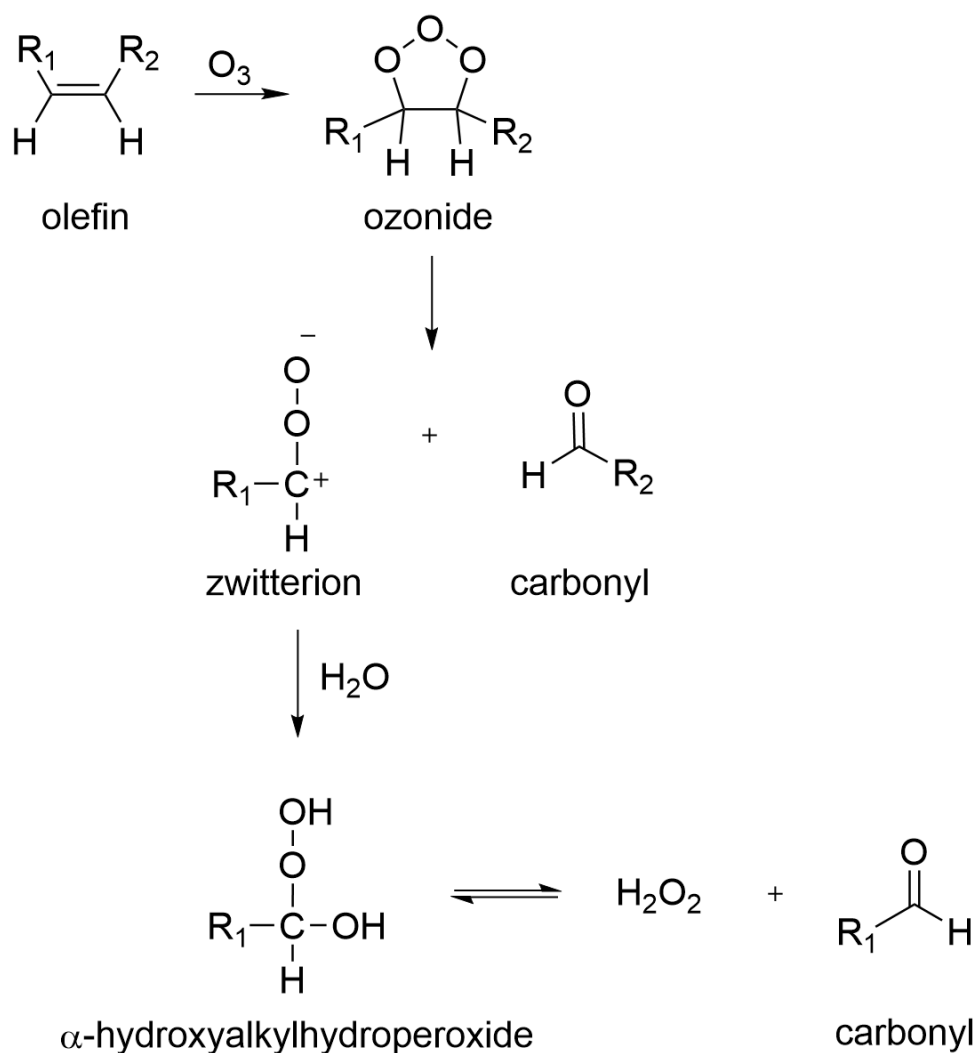


Figure 2. Criegee mechanism for reactions of olefins with ozone in aqueous solutions. Modified from von Sonntag & von Gunten, 2012.

1.5 Goals and approach

The two main goals of this thesis were (i) developing a method for the derivatization and non-target analysis of carbonyl-containing compounds in WW and (ii) understanding the formation of carbonyls from reactions of DOM with ozone. So far, little data exist regarding the applicability of derivatization methods for carbonyl identification in complex water matrices such as WW.

Method development was based on (i) optimizing the TSH derivatization conditions (concentration of the derivatizing agent, acid concentration, reaction time and stability of derivatized carbonyls), (ii) application of a non-target workflow which allows screening for carbonyls. Samples were analysed with LC-ESI-HRMS, and carbonyls were identified by tracking signature fragments originating from the derivatizing agent TSH. To achieve a better understanding of the formation of carbonyls from DOM during ozonation, the developed method was applied to investigate the formation of carbonyls during ozonation of DOM from WW and surface waters. Three WWs (Neugut, Werdhölzli and Glarnerland), a LW (Greifensee), and Suwannee River Fulvic acid (SRFA) as a model for Dissolved Organic Matter (DOM) were ozonated and

analysed. An array of target carbonyls was quantified in samples which were ozonated at different doses, along with non-target screening to detect unknown carbonyls. Moreover, model compounds (three phenols, three olefins and one β -diketone), which are typically contained in DOM were ozonated and analysed. This allowed the assess some precursors, which may contribute to the formation of carbonyls during ozonation.

2. Materials and methods

2.1 Reagents and solutions

2.1.1 Chemicals

In total, 16 different carbonyl compounds were selected as target compounds including saturated and unsaturated aldehydes, unsaturated and cyclic ketones, diketones and ketoacids (Table 1). Such compounds of different characteristics were chosen to cover a wide range of potentially formed carbonyls during ozonation. Benzaldehyde-d₆ (Sigma-Aldrich, CAS: 17901-93-8, 99% purity, 98% deuterated) and tramadol-d₆ hydrochloride (tramadol-d₆, TRC Canada, CAS: 1109217-84-6) were used as internal standards. Furthermore, benzaldehyde tosylhydrazone (benzaldehyde-TSH, CAS: 1666-17-7, 98% purity) was purchased from Sigma-Aldrich. Cinnamaldehyde tosylhydrazone (cinnamaldehyde-TSH, >99.9% purity) was prepared by Dr. Samuel Derrer at Eawag (Dübendorf). The derivatizing agent *p*-toluenesulfonylhydrazide (TSH, CAS: 1576-35-8, 97% purity, LOT: WXBC9979V) was purchased from Sigma-Aldrich. SRFA was purchased from the International Humic Substances Society (SRFA II, Cat. No.: 2S10IF, 52.34 % C, 0.67 % N).

Furthermore, the following substances and solvents were used for the stock and sample solutions: NanoPure (NP) water ($\geq 18\text{M}\Omega$, ASTM type 1) from arium® pro Ultrapure Laboratory Water Systems from Sartorius, acetonitrile (ACN, LC/MS grade, Optima®, Fisher Chemical), methanol (MeOH, LC/MS grade, Optima®, Fisher Chemical), formic acid (FA, LC/MS grade, Optima®, Fisher Chemical), sodium phosphate dibasic dihydrate (Sigma-Aldrich, 98.5-101.0% purity), sodium phosphate monobasic dihydrate (Sigma-aldrich, 99 % purity), hypochloric acid (32 wt. %, Emsure®), dimethylsulfoxide (DMSO, LC/MS grade, Sigma-Aldrich, 99.9% purity) and phosphoric acid (Sigma-Aldrich, 85% purity).

Table 1. Target carbonyl compounds used in this study, including name, purity or weight percent, molecular formula, carbonyl class, CAS number and supplier.

Chemicals	Molecular formula	Carbonyl class	CAS number	Supplier
Formaldehyde, 37 wt.%	CH ₂ O	Aldehyde, saturated	50-00-0	Sigma-Aldrich
Acetaldehyde, 99.5%	C ₂ H ₄ O	Aldehyde, saturated	75-07-0	Acros organics
Decanal, 95%	C ₁₀ H ₂₀ O	Aldehyde, saturated	112-31-2	Sigma-Aldrich
Benzaldehyde, 99%	C ₇ H ₆ O	Aldehyde, saturated	100-52-7	Fluka
Indole-3-carboxaldehyde, 97%	C ₉ H ₇ NO	Aldehyde, saturated, N-containing	487-89-8	Sigma-Aldrich
4-Hydroxy-2-methoxybenzaldehyde, 98%	C ₈ H ₈ O ₃	Aldehyde, saturated	673-22-3	Sigma-Aldrich
Crotonaldehyde (cis/trans), 99.5%	C ₄ H ₆ O	Aldehyde, unsaturated	4170-30-3	Sigma-Aldrich
Cinnamaldehyde, 95%	C ₉ H ₈ O	Aldehyde, unsaturated	104-55-2	Sigma-Aldrich
Methacrolein, 95%	C ₄ H ₆ O	Aldehyde, unsaturated	78-85-3	Sigma-Aldrich
Cyclopentanone, 99%	C ₅ H ₈ O	Ketone, cyclic	120-92-3	Fluka
1-Acetyl-1-cyclohexen, 97%	C ₈ H ₁₂ O	Ketone, unsaturated	932-66-1	Sigma-Aldrich
3,5-Heptanedione, 97%	C ₇ H ₁₂ O ₂	Diketone	7424-54-6	Sigma-Aldrich
Glyoxal, 40 wt. %	C ₂ H ₂ O ₂	Diketone	107-22-2	Sigma-Aldrich
Glutaraldehyde, 50 wt. %	C ₅ H ₈ O ₂	Diketone	111-30-8	Sigma-Aldrich
Glyoxylic acid, 98%	C ₂ H ₂ O ₃	Ketoacid	563-96-2	Sigma-Aldrich
Pyruvic acid, 98%	C ₃ H ₄ O ₃	Ketoacid	127-17-3	Sigma-Aldrich

Seven model compounds (three phenols, three olefins and one β -diketone) from Sigma-Aldrich were used for the study as possible carbonyl precursors (Table 2). These model compounds were: phenol, 4-ethylphenol, 4-methoxyphenol, trans-cinnamic acid, sorbic acid, 3-buten-2-ol, acetylacetone.

Table 2. Selected model compounds for carbonyl precursor evaluation, including name, purity, molecular formula, CAS number and supplier of the chemicals.

Chemicals	Molecular formula	CAS number	Supplier
Phenol, 99.5%	C ₆ H ₆ O	108-95-2	Fluka
4-Ethylphenol, 99%	C ₈ H ₁₀ O	123-07-9	Sigma-Aldrich
4-Methoxyphenol, 99%	C ₇ H ₈ O ₂	150-76-5	Sigma-Aldrich
Trans-cinnamic acid, 99%	C ₉ H ₈ O ₂	140-10-3	Sigma-Aldrich
Sorbic acid, 99%	C ₆ H ₈ O ₂	110-44-1	Fluka
3-Buten-2ol, 97%	C ₄ H ₈ O	598-32-3	Sigma-Aldrich
Acetylacetone, 99%	C ₅ H ₈ O ₂	123-54-6	Sigma-Aldrich

2.1.2 Stock solutions

Carbonyl compound stock solutions at concentrations in the range of 10 to 100 mM were prepared in ACN with the exception of glyoxylic acid, which was prepared in MeOH due to its low solubility in ACN. The carbonyl compound stock solutions were stored in amber vials with

no or little headspace and kept in the freezer at $-20\text{ }^{\circ}\text{C}$ for up to 4 months. Volatile compounds such as methacrolein or crotonaldehyde were pipetted using a multipipette (Multipipette[®] plus, Eppendorf). Acetaldehyde was transferred into the stock solution with a syringe, to avoid losses of the chemical due to its high volatility. Acetaldehyde and formaldehyde intermediate solutions were prepared freshly every time from a stock solution of 105.7 mM and 100 mM, respectively. Other intermediate solutions containing carbonyl compounds in a range of 0.1-1 mM were prepared in ACN and kept stored to one week in amber vials at $-20\text{ }^{\circ}\text{C}$. All other solutions were prepared freshly on a daily basis in ACN or NP water. The stock solution of the derivatizing agent TSH was prepared in ACN at a concentration of 10 mM and stored up to one month at $-20\text{ }^{\circ}\text{C}$ in a vial without headspace. Caps of vials containing stock solutions were wrapped with parafilm (Parafilm M, Bemis) to provide a better sealing during storage.

2.2 Ozonation of different water matrices and carbonyl precursor evaluation

2.2.1 Preparation of ozone stock solution

To prepare ozone stock solution, ozone-containing gas was produced using an ozone generator (BMT 803 BT, BMT Messtechnik, Berlin) from pure oxygen (Carbagas) and bubbled into ice-cooled NP water. To determine the concentration of the ozone stock solutions, 500 μL of the ozone stock solution were added to 2 mL of phosphoric acid (50 mM) in a 1-cm pathlength quartz cuvette, and then the UV absorbance was measured with a spectrophotometer (Cary 100, Varian, USA) at 260 nm. The UV absorbance was measured twice for each ozone stock solution in a short period of time and an average UV absorbance was used to calculate the ozone concentration according to the following formula (Equation 1):

$$[\text{O}_3] \text{ (mM)} = \frac{\text{Abs} \times 2.5 \text{ mL} \times 1000}{3200 \text{ M}^{-1}\text{cm}^{-1} \times 0.5 \text{ mL} \times 1 \text{ cm}} \quad (1)$$

Abs: average absorbance, 2.5 mL: total volume of the sample consisting of 2 mL phosphoric acid and 0.5 mL ozone stock; 1000: correction factor for converting concentration from M to mM; $3200 \text{ M}^{-1} \text{ cm}^{-1}$: molar absorptivity of ozone at 260 nm (von Sonntag & von Gunten, 2012); 0.5 mL: volume of ozone stock solution in the sample; 1 cm: width of quartz cuvette.

2.2.2 Ozonation of DOM, wastewater and lake water

SRFA solutions, lake water (LW) from Lake Greifensee (16.07.2020), and secondary treatment effluent WW samples collected from WWTPs Neugut (17.09.2020), Werdhölzli (15.09.2020) and Glarnerland (22.06.2017) were ozonated at different ozone doses in laboratory-controlled experiments. Water quality parameters including conductivity, pH, alkalinity, hardness, ammonium, nitrite, dissolved organic carbon (DOC) and dissolved nitrogen concentrations were measured by the “Ausbildungs und Analytiklabor” (AuA) at Eawag (Dübendorf) (Table 3). SRFA was prepared at a DOC concentration of 5.5 mg/L in NP water, equivalent to the DOC measured for the WW Werdhölzli. The WWs were stored in the refrigerator ($4\text{-}8\text{ }^{\circ}\text{C}$) and were filtered using pre-rinsed cellulose-nitrate membranes with a pore size of $0.45\text{ }\mu\text{m}$ prior to the experiments. All samples contained phosphate buffer (5 mM) and were adjusted to $\text{pH } 7.0 \pm 0.1$ using 1 M solutions of HCl and NaOH.

WW Neugut is constituted of communal and industrial WW from several municipalities. About 8 million m³ WW are treated annually in the WWTP Neugut, of which about 48% originate from inhabitants and commuters (about 55 000 people) and about 52% from trade and industry (ARANEugut, 2020). The ARA Werdhölzli is the biggest WWTP in Switzerland and treats the WW of the city of Zurich (about 450 000 inhabitants) amounting to about 80 million m³ per year (Swisswater AG, 2020; Stadt Zürich, 2020). About 69% of the WW in the ARA Werdhölzli originate from inhabitants and about 31% from trade and industry (Micropoll, 2019). The WW of about 43 000 inhabitants are treated in ARA Glarnerland and about 6-8 million m³ WW are treated annually, of which about 40% originate from industrial discharges (Abwasserverband Glarnerland, 2020).

Table 3. Water quality parameters measured for each water sample included conductivity, pH, alkalinity, hardness, ammonium concentration (NH₄⁺), nitrite concentration (NO₂⁻), dissolved organic carbon content (DOC), and dissolved total nitrogen content. ND (not determined) indicates that this value was not measured.

Matrix	Conductivity (µS/cm at 20 °C)	pH	Alkalinity (mmol/L)	Hardness (mmol/L)	NH ₄ ⁺ (µg/L)	NO ₂ ⁻ (µg/L)	DOC (mg/L)	Dissolved total nitrogen content (mg/L)
WW Neugut	1014	8.15	5.14	2.82	42.35	5.81	5.06	10.66
WW Werdhölzli	ND	7.90	3.59	ND	109.60	43.00	5.50	4.15
WW Glarnerland	ND	8.73	1.76	ND	ND	227.50	10.97	ND
LW Lake Greifensee	273	8.42	3.36	1.62	18.40	26.88	3.40	2.00

To determine the effect of OH radicals on the formation of carbonyls during ozonation, two sets of samples were prepared, one containing OH radical scavenger DMSO (0.5 mM) and the other without DMSO. By adding an OH radical scavenger, direct reactions attributed to ozone rather than to ozone and OH radicals could be studied (Ramseier & von Gunten, 2009). Tertiary-butanol is a common scavenger, but it forms substantial amounts of formaldehyde in reaction with OH radicals (von Sonntag & von Gunten, 2012). In an ozonated system tertiary-butanol yields up to 30 % formaldehyde and also other carbonyls such as acetone and 2-hydroxy-2-methylpropanal are produced (Flyunt et al., 2003). However, formaldehyde was one of the target analytes to be measured, thus another suitable OH radical scavenger had to be used. DMSO reacts only slowly with ozone ($k = 1.8 \text{ M}^{-1} \text{ s}^{-1}$), while its reaction with OH radicals is fast ($k = 7 \times 10^9 \text{ M}^{-1} \text{ s}^{-1}$) (von Sonntag & von Gunten, 2012), wherefore it is a suitable candidate for scavenging OH radicals. A product from reactions of ozone with DMSO is formaldehyde (Yurkova et al., 1999). Yurkova et al., 1999 found that when using a DMSO concentration of 10 mM at pH 7 about 85 µM formaldehyde were formed. This is equivalent to a formaldehyde yield of about 0.85%, and thus much smaller than the yield that has been reported for tertiary-butanol. When using a higher DMSO concentration of 100 mM at pH 7 a higher formaldehyde yield was observed amounting to about 455 µM (Yurkova et al., 1999). Assuming that the relation between the DMSO and formaldehyde concentration is linear, we would estimate a yield of about 2 µM formaldehyde for a DMSO concentration of 0.5 mM, which was used in the experiments in this thesis. The concentration of DMSO (0.5mM) was chosen as low as possible

(to avoid formaldehyde formation from ozonolysis of DMSO) but high enough so that reactions of DMSO with OH radicals were at least 10 times faster than reactions of phenol with OH radicals. Phenol was used as a proxy for WW. The rate constant for DMSO with OH radicals is $7 \times 10^9 \text{ M}^{-1}\text{s}^{-1}$ (Buxton et al., 1968). For phenol a similar rate constant was assumed (around $7 \times 10^9 \text{ M}^{-1}\text{s}^{-1}$). Based on the generous assumption that the whole DOC in WW is constituted by phenol, the DOC of a typical WW (around 5 mg/L) could be expressed as a phenol concentration of 50 μM . Therefore, a concentration ten times higher (0.5 mM) was chosen for DMSO.

Samples were ozonated at different specific ozone doses (Table 4). Volumes of ozone stock solution (1.69 mM) spiking are listed in the Supporting Information (SI) (Section S.3). DOC concentrations are typically higher in WW than in surface water, invoking faster O₃ decomposition rates and higher OH radical exposures (Buffle et al., 2006). The applied ozone doses were lower for the WW Glarnerland compared to the other water samples, due to an initial estimate of DOC at 6 mg/L instead of the later measured 10.97 mg/L.

Before derivatization, samples were spiked with 100 nM benzaldehyde-d₆, which was used as a surrogate to determine the derivatization efficiency based on which the peak areas were corrected. The carbonyl concentrations in the samples were quantified based on external calibrations of the target carbonyl compounds in NP water standard solutions. As a blank, NP water containing phosphate buffer (5 mM) with and without addition of DMSO (0.5 mM) was measured before and after ozonation (with 107 μM O₃). Concentrations in the blanks were subtracted from the measured concentrations of the target carbonyl compounds. Additionally, the measured concentrations of the target carbonyl compounds were corrected based on correction factors taking into account dilution factors from the ozone spiking and from spiking of TSH and HCl. The dilution factors are shown in the SI (Section S.8).

Table 4. Applied specific ozone doses (mgO₃/mgDOC) and respective DOC (mg/L) of different samples.

Matrix	Specific ozone dose (mgO ₃ /mgDOC)						DOC (mg/L)
	Dose 0	Dose 1	Dose 2	Dose 3	Dose 4	Dose 5	
SRFA	0	0.25	0.48	0.94	1.8	2.5	5.5
WW Neugut	0	0.25	0.49	0.94	1.8	2.5	5.1
WW Werdhölzli	0	0.25	0.48	0.94	1.8	2.5	5.5
WW Glarnerland	0	0.13	0.26	0.51	1.0	1.3	10.1
LW Greifensee	0	0.25	0.49	0.96	1.9	2.7	3.4

2.2.3 Ozonation of carbonyl precursors

Stock solutions containing 50 μM of the model compounds, namely phenol, 4-ethylphenol, 4-methoxyphenol, cinnamic acid, sorbic acid, 3-buten-2-ol and acetylacetone covering three compounds classes (phenols, olefins and β -diketones) were prepared in NP water. The stock solutions contained phosphate buffer (5 mM) and were adjusted to pH 7.0 ± 0.1 . Compounds were ozonated at five ozone doses with a molar ratio of ozone to compound of about 0.5, 1, 2, 4 and 6 (SI Section S.9). Cinnamic acid was only ozonated at three ozone doses with a molar ratio of

ozone to compound of about 0.5, 1 and 2. DMSO (1 mM) was added to all samples. Additionally, a sample at an intermediate ozone dose (molar ratio of ozone to compound of 2) was ozonated without addition of DMSO. The ozonated cinnamic acid solution was diluted by a factor 50 with NP water and the rest of the ozonated compound solutions by a factor 5. These diluted solutions were derivatized with 50 μ M TSH and 0.02 M HCl.

2.3 LC-ESI-HRMS method

Samples were analyzed using high-performance liquid chromatography (UltiMate 3000 UHPLC system, Dionex) coupled to high-resolution hybrid quadrupole-orbitrap mass spectrometer (Q Exactive Plus, Thermo Scientific). Separation was performed using an Atlantis column (3 μ m particle size, 3 x 150 mm) at 30 °C and a flow of 300 μ L/min. An autosampler (PAL HTS-xt system, McKinley scientific) was used for sample injection (50 μ L sample injected into a 100 μ L loop) and for sample storage at 4 °C during measurement sequences. Eluents consisted of NP water (A) and MeOH (B) each containing 0.1% FA. The LC method ran for 29 min and the LC gradient started with 95% A. After 1 min, B increased gradually from 5% to reach 95% at 17 min and stayed constant until 25 min. Afterwards, A increased to reach 95% (starting gradient) at 27 min and then remained constant until the end of the run. During the first 5 min of the run, the LC flow was diverted to waste to avoid contaminating the MS with phosphate buffer, which was present in most samples, and the ESI spray voltage was meanwhile set to 0. Moreover, the intense peak of the derivatizing agent (RT: 11.9 minutes) was cut out by diverting the LC flow to waste between about 11.8 and 12.3 min to avoid any contamination of the MS. A NP water blank was injected after each derivatized sample to avoid carry-over of derivatized carbonyls from one sample into another.

Acquisition was achieved by performing an initial MS full-scan (resolution 140'000 at m/z 200) followed by data-dependent fragmentation MS/MS experiments (resolution 17'500 at m/z 200) in the positive polarity mode. The latter was selected since it provided better detection of the derivatized carbonyls than the negative polarity mode (details in Section 3.1.4). MS conditions were the following: spray voltage 4000 V, capillary temperature 350 °C, sheath gas 40 arbitrary units, and auxiliary gas 10 arbitrary units, mass range from 100 to 1000 Da (exception: 55 to 550 Da, Section 2.4.4). When charging issues were experienced in the MS, a full scan in the negative mode with low resolution (17'500) was added from 5 to 10 min and again from 26 to 29 min to the MS method. These time windows were selected since no derivatized carbonyls eluted within and therefore any decline in peak areas related to the additional scans in the negative mode could be avoided.

Properties of the data-dependent (top 5) MS/MS scans included an Automatic Gain Control (AGC) of 2×10^5 , isolation window of 1.0 m/z, and normalized collision energy (NCE) of 30. The masses of the 16 derivatized target carbonyls in positive ESI were added to an inclusion list to ensure their fragmentation.

2.4 Optimization of derivatization

To optimize the derivatization procedure several factors were studied: the influence of (i) the TSH concentration, (ii) the acid addition and (iii) the reaction time. The experiments performed for the optimization of the derivatization method were conducted at the initial stages of this

study. Thus, the carbonyl compound and TSH concentrations that were spiked to the samples were not consistent over all experiments (Table 5). Moreover, an experiment was performed to compare the detectability of carbonyl compounds with derivatization using the optimized procedure to that without derivatization. Table 5 provides an overview of the total carbonyl compound content and TSH concentrations that were used in experiments, in which different conditions for derivatization optimization and assessment were investigated.

Table 5. Overview on the total carbonyl content (μM) and TSH concentrations (μM) used in the experiments for derivatization optimization and assessment.

Investigated condition	Total carbonyl content (μM)	TSH concentration (μM)	Ratio (TSH/carbonyls)
TSH concentration (Section 2.4.1)	0.4 to > 20 *	100, 200, 300	<5 to 750
Acid addition (0-0.05 M HCl) (Section 2.4.2)	1.6	30	19
Reaction time (10-120 min) (Section 2.4.3)	8	200	25

* In NP blanks 0.4 μM carbonyls was contained. In ozonated WW and SRFA a minimum of 20 μM carbonyl compounds were contained (based on the quantification of target carbonyls in this study).

2.4.1 Influence of TSH concentration

The influence of the TSH concentration on the derivatization efficiency was studied by comparing the derivatization efficiencies at different TSH concentrations (100, 200 and 300 μM) for benzaldehyde and cinnamaldehyde. Calibration standards for a mix of benzaldehyde-TSH and cinnamaldehyde-TSH were prepared in NP water. Ozonated and non-ozonated WW Neugut and SRFA samples were spiked with 200 nM benzaldehyde and cinnamaldehyde, and derivatized with 100, 200 and 300 μM TSH and an addition of 0.02 M HCl. NP water was spiked and derivatized in the same manner as a blank. All samples additionally contained 32.7 nM tramadol-d6 and 100 nM benzaldehyde-d6 as internal standards. The sample preparation of a blank that was derivatized, a benzaldehyde-TSH/cinnamaldehyde-TSH calibration standard and a sample spiked with benzaldehyde/cinnamaldehyde that was derivatized are shown in Figure 3. Additionally, Werdhölzli and Glarnerland WWs were used to determine the derivatization efficiency of 200 μM TSH.

Peak areas were divided by the internal standard peak area of tramadol-d6 for correction of instrumental variability. Furthermore, the samples were blank corrected, and any benzaldehyde or cinnamaldehyde that might have been in the samples prior to spiking was accounted for. The slope and intercept (calculated with the LINEST function in Excel) of the benzaldehyde-TSH and cinnamaldehyde-TSH calibrations, concentrations were calculated in each sample matrix. The measured concentrations (conc.) were divided with the expected concentration (conc.) of 200 nM, and multiplied by 100 to obtain derivatization efficiencies in %, as depicted in equation 2.

$$\text{Derivatization efficiency (\%)} = \frac{\text{Measured conc.}}{\text{Expected conc.}} \times 100 \% \quad (2)$$

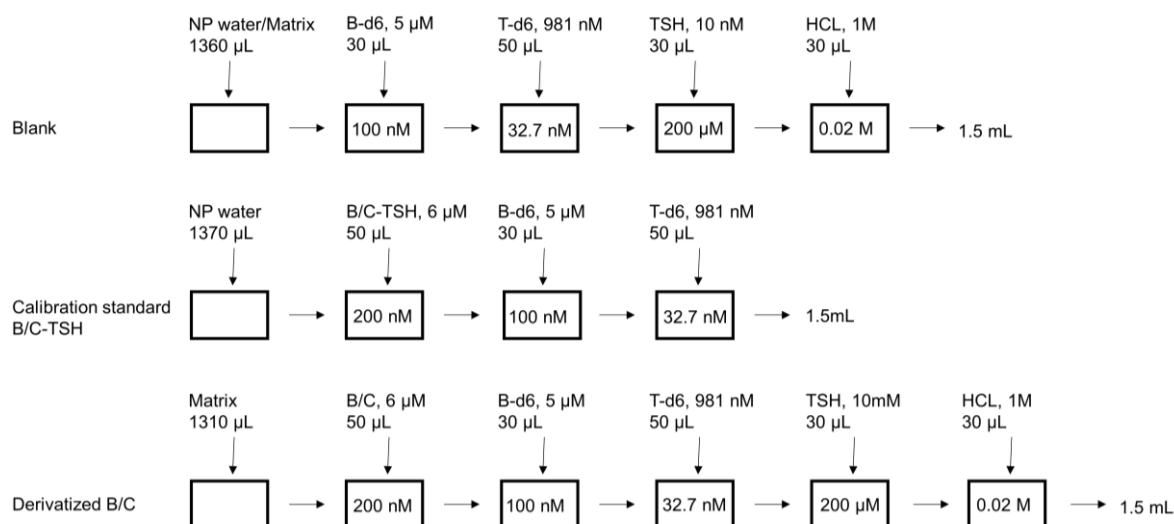


Figure 3. Scheme of sample preparation of a blank that was derivatized (TSH 200 μM , HCl 0.02 M), a benzaldehyde-TSH/cinnamaldehyde-TSH (B/C-TSH) calibration standard (200 nM) and a sample spiked with benzaldehyde/cinnamaldehyde (B/C) (200 nM) that was derivatized. All samples were spiked with the two internal standards benzaldehyde-d6 (B-d6) and tramadol-d6 (T-d6) and had a total volume of 1.5 mL.

Increasing carbonyl concentrations were observed with an increasing TSH concentration in blank samples, pointing to a contamination of TSH with carbonyl-TSH hydrazones. For this reason, acetone, butyraldehyde and 3-pentanone that were derivatized could not be quantified. More details regarding the contamination of TSH with carbonyls is provided in the SI Section S.2.

2.4.2 Influence of acid addition

NP water was spiked with a mix containing 100 nM of each of the 16 target carbonyl compounds used in this study. The total carbonyl compound concentration in the sample was therefore 1.6 μM . 30 μM TSH were used for derivatization. After the addition of TSH, different amounts of HCl (1M) were added as a reaction catalyst. The following HCl concentrations were tested: 0, 0.01, 0.02, 0.03, 0.04 and 0.05 M HCl. Derivatized glyoxal, glyoxylic acid and pyruvic acid could not be detected using these conditions (only 30 μM TSH).

2.4.3 Influence of reaction time

Four NP water samples spiked with 500 nM of each of the 16 target carbonyls were derivatized with 200 μM TSH and 0.02 M HCl. The total carbonyl concentration in the sample was 8 μM . The samples were stored at room temperature for varying reaction times: 10, 30, 60 and 120 minutes. Subsequently, the samples were stored in the fridge at around 4-8 $^{\circ}\text{C}$ until analysis. An internal standard of 500 nM benzaldehyde-d6 was added to the samples but was not used for correction of instrumental variability. The derivatized benzaldehyde-d6 peak areas would also have been affected by the derivatization reaction time, introducing a bias, and were thus unsuitable for internal standard correction.

2.4.4 Influence of derivatization on the detectability of carbonyl compounds

A mixture of carbonyls in NP water without derivatization was analysed separately in full scan mode with positive and negative ESI. For this, the instrument mass range was set to 55-550 Da.

The mixture of carbonyl compounds contained 250 nM crotonaldehyde, benzaldehyde, cinnamaldehyde, 4-hydroxy-2-methoxybenzaldehyde, cyclopentanone, decanal, indole-3-carboxaldehyde, methacrolein, 3,5-heptanedione and 1-acetyl-1-cyclohexene. It also contained glutaraldehyde (750 nM), glyoxal (3 μ M), pyruvic acid (1.5 μ M), acetaldehyde (3 μ M), glyoxylic acid (4.5 μ M) and formaldehyde (3 μ M). The total carbonyl concentration in the sample was 18.25 μ M. The same mixture of carbonyls was derivatized with 200 μ M TSH and 0.02 M HCl, and analysed separately in full scan mode with positive and negative ESI and a mass range of 100-1000 Da.

2.5 Method performance characteristics

2.5.1 Linearity ranges, limits of detection and quantification

The limits of detection (LOD) and quantification (LOQ) were estimated for each compound based on the slope of its calibration curve (s), the standard deviation of the y-intercept of the calibration curve (σ), and the equations $LOD = 3 \times \sigma/s$ and $LOQ = 10 \times \sigma/s$. The calibration range was chosen based on the following criteria: (i) the coefficient of determination (R^2) is above 0.995 and (ii) concentrations of carbonyls detected in ozonated WW samples are within the calibration range. The lowest calibration point, for which a clear increase in peak area was detected compared to the previous calibration point, was chosen as the lower limit of the calibration range. R^2 was calculated and if below 0.995, the highest concentration data point was discarded. This procedure was repeated until $R^2 \geq 0.995$ with a minimum of six data points. If this could not be achieved, calibration points were neglected at the lower range of the calibration, until a range with an $R^2 \geq 0.995$ was identified. R^2 values, the slope, intercept and the standard deviation of the intercept of the calibration curves were computed with the integrated function LINEST in Excel. For glyoxylic acid and formaldehyde, two calibration ranges were established so that the wide concentration range observed in WW could be covered. Peak areas were divided by the internal standard peak area of tramadol-d6 for correction of instrumental variability.

2.5.2 Analytical matrix effects

Analytical matrix effects on the measurement of derivatized carbonyl compounds using HRMS in ozonated and non-ozonated SRFA solutions and secondary treated WW effluent were investigated. Ozonated (specific ozone dose 1 mgO₃/mgDOC) and non-ozonated SRFA and WW Neugut samples (with DMSO) were derivatized with 200 μ M TSH and 0.02 M HCl. Unspiked samples and samples spiked with both benzaldehyde- and cinnamaldehyde-TSH hydrazones at 200nM were prepared. Benzaldehyde- and cinnamaldehyde-TSH hydrazones were spiked instead of benzaldehyde and cinnamaldehyde, so that analytical matrix effects without considering derivatization efficiencies could be determined. NP water was derivatized in the same manner and spiked with both benzaldehyde- and cinnamaldehyde-TSH hydrazones at 200nM as a calibration standard. A blank was prepared by adding 200 μ M TSH and 0.02 M HCl to NP water. All samples additionally contained 32.7 nM tramadol-d6 and 100 nM benzaldehyde-d6 as internal standards and were corrected using tramadol-d6. Furthermore, the samples were blank corrected. The analytical matrix effects were calculated according to equation 3:

$$\text{Matrix effect (\%)} = \frac{\text{Peak area}_{\text{spiked sample}} - \text{Peak area}_{\text{unspiked sample}}}{\text{Peak area}_{\text{calibration standard in NP water}}} \times 100 \quad (3)$$

2.5.3 Stability of derivatized carbonyl compounds

Experiments in this study involved the measurement of many samples over several days, which were prepared in one batch, derivatized and then stored at 4 °C until analysis. Therefore, it was crucial to determine the stability of the derivatized carbonyl compounds at 4 °C over the measurement duration. To investigate this, one NP water sample spiked with 100 nM of each of the 16 target carbonyl compounds was derivatized using 25 µM TSH and 0.02 M HCl. On each of five subsequent measurement days the sample was injected and analysed. A spiking with 100 nM was not enough for the detection for the following compounds: glyoxal, glyoxylic acid and pyruvic acid. This was caused by the generally higher LODs for these compounds and a reduced derivatization efficiency by addition of only 25 µM TSH. No internal standard was added, as this experiment was conducted in a preliminary stage of method development. In hindsight, the experiment could have been improved by preparing a larger volume of the sample (10 mL instead of 1.5 mL) and storing the sample at 4 °C. Each day a sample could have been spiked freshly with an internal standard, such as tramadol-d6 for example, to account for instrumental variability over time, by correcting the peak areas with the internal standard.

2.6 Data analysis and non-target workflow

For LCMS data analysis, the software Xcalibur (version 4.1), Trace Finder (EFS version 4.1) and Compound Discoverer (version 3.1) were used. Peak areas for the method development and quantification were obtained using Xcalibur or Trace Finder. Compound Discoverer was used for the development of a workflow to identify unknown carbonyls that were formed during ozonation. The Compound Discoverer workflow was based on the pre-defined workflow template “Untargeted environmental research ID workflow with statistics: Detect and identify unknown compounds with differential analysis” that was modified slightly (SI Section S.10). A crucial part of the workflow was the node “Compound Class Scoring”, which was linked to the node “Group Compounds”, and contained three signature fragments that originated from the derivatizing agent, and were used as signature fragments for derivatized carbonyls. The three signature fragments (Figure 4) had the exact masses of 139.0212, 155.0161 and 157.0318 Da.

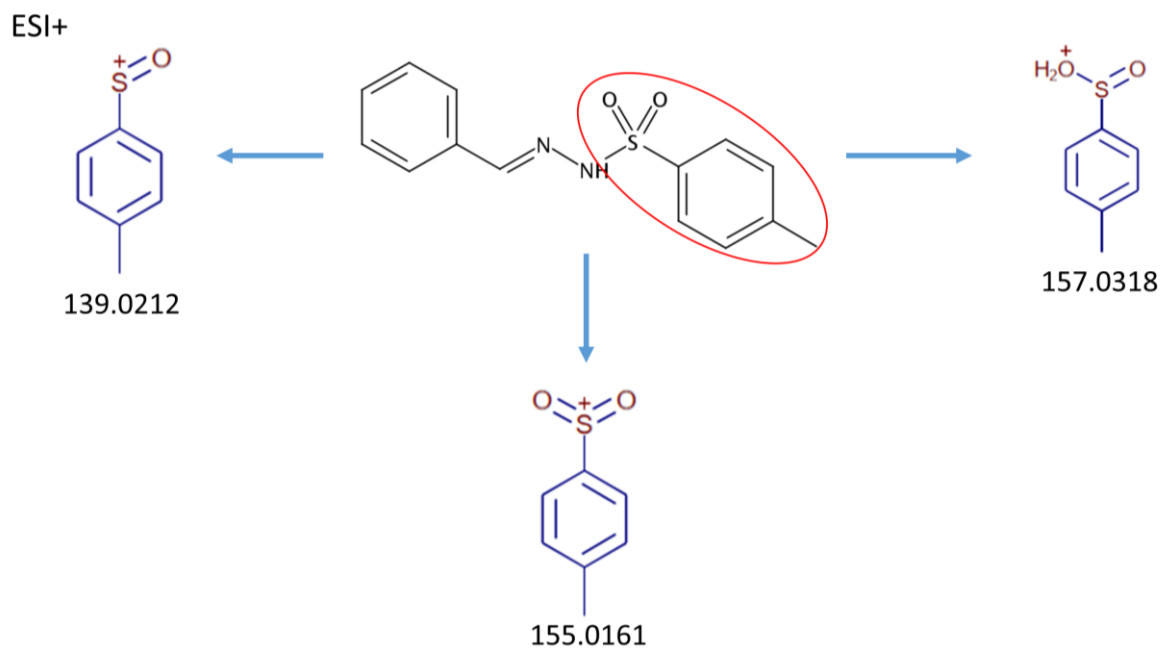


Figure 4. Signature fragments for derivatized carbonyl compounds originating from the derivatizing agent TSH with exact masses of 139.0212, 155.0161 and 157.0318 Da and structures in positive ESI.

The analysis results from Compound Discoverer were exported into excel files, where they were further processed. Details on the input files, grouping of samples and generated ratios in Compound Discoverer are shown in the SI (Section S.11). Several criteria were applied to screen for unknown carbonyl compounds that were formed during ozonation. In the “Predict Compositions” node a minimal elemental composition of $C_8H_{10}N_2O_2S$ was set, which is the molecular formula of formaldehyde (CH_2O , smallest carbonyl) derivatized with TSH. Furthermore, at least one of the three signature fragments (Figure 4) was required in the MS^2 data of a possible hit, which is equivalent to a compound class scoring of 33 or higher. Additionally, for a compound to be considered as a suspect, its group peak area had to be at least two-fold higher (defined arbitrarily) in the ozonated samples compared to the derivatized ozonated NP water blank. Moreover, the group peak area of the ozonated samples had to be at least five-fold (defined arbitrarily) than the group peak area in the non-ozonated samples, indicating that the carbonyl was formed during ozonation. Since the elemental compositions originating from TSH are respectively $C_7H_8N_2SO$ and $C_{14}H_{16}N_4S_2O_2$ for single and double derivatizations, only compounds with a predicted chemical formula that contained either two or three nitrogen and one sulphur atom (N_2S / N_3S) or four nitrogen and two sulphur atoms (N_4S_2) were considered. Triple derivatized compounds or other derivatized compounds containing additional phosphate, sulphur or nitrogen for example were not studied.

Python in the programming environment Spyder was used for plotting figures.

3. Results and discussion

3.1 Optimization of derivatization

3.1.1 Influence of TSH concentration

Figure 5a and 5b show the derivatization efficiencies at three TSH concentrations (100, 200 and 300 μM) for benzaldehyde and cinnamaldehyde, respectively. The derivatization efficiencies were between 82-98% for benzaldehyde and between 91-105% for cinnamaldehyde at a TSH concentration of 200 μM . Derivatization efficiencies at 100 μM TSH were 68-91% for benzaldehyde and 81-104% for cinnamaldehyde. This indicates that derivatization with 100 μM TSH was less efficient than with 200 μM TSH. With 300 μM TSH, efficiencies between 80-107% were obtained for benzaldehyde and 85-113% for cinnamaldehyde. The data points at 300 μM TSH are spread farther apart than at 200 μM TSH. There was no clear increase in derivatization efficiencies between 200-300 μM TSH. Therefore, 200 μM TSH was chosen as an optimal concentration for derivatization. Overall, derivatization efficiencies were slightly higher for cinnamaldehyde than for benzaldehyde.

Derivatization efficiencies obtained for NP water were within the same range as those obtained in the other water samples. This shows that there was no procedural matrix effect in terms of a combined effect of all components of a sample on the derivatization efficiencies. The small differences in derivatization efficiencies between the different matrices are negligible, and may be attributed to pipetting errors, minimal matrix effects or instrument variability.

The influence of even lower TSH concentrations (12.5-200 μM) on the derivatization of benzaldehyde, cinnamaldehyde and a few other target carbonyls in different water matrices was studied in a preliminary experiment and is shown in the SI (Section S.12). Concentrations and derivatization efficiencies could not be calculated in said experiment but peak areas still gave an indication about the derivatization efficiencies.

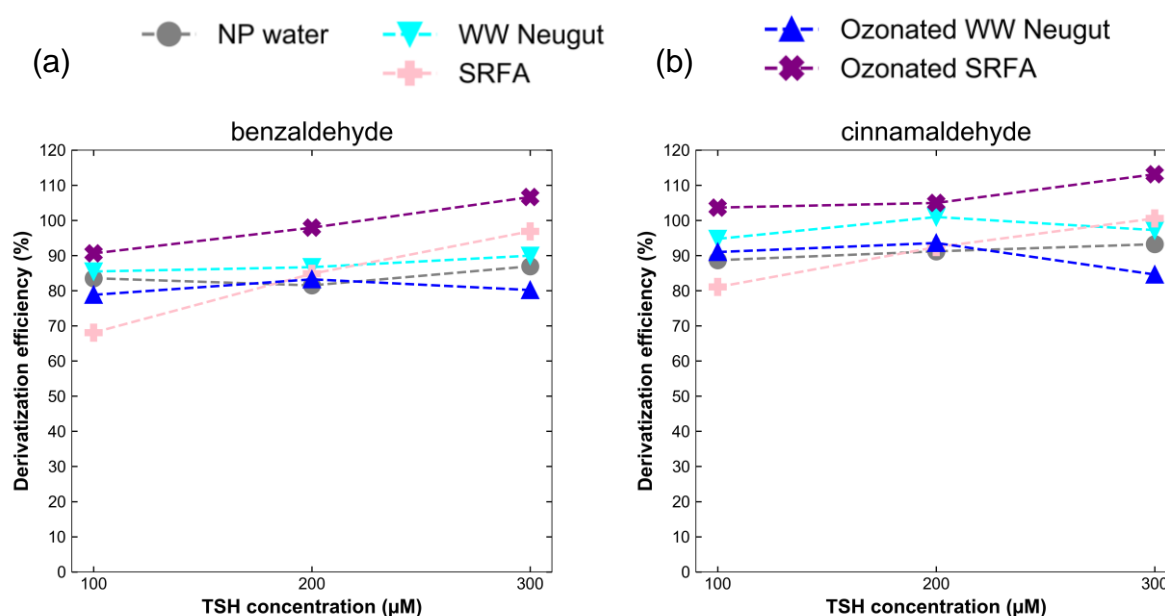


Figure 5. Influence of TSH concentration on the derivatization efficiency (%) of (a) benzaldehyde and (b) cinnamaldehyde in different water matrices.

3.1.2 Influence of acid concentration and reaction time

Figure 6a shows the influence of the HCl concentrations on the derivatization efficiency for 13 target carbonyl compounds. Figure 6b shows the influence of the reaction time at room temperature on the derivatization efficiency for 16 target carbonyl compounds.

Acid catalyses the reaction between TSH and carbonyl compounds (Marron et al., 2020; Siegel et al., 2014). In previous studies, different HCl concentrations were used for TSH derivatization. Marron et al., 2020 used a HCl concentration of 0.02 M for WW samples, whereas Siegel et al., 2014 used a HCl concentration of 0.04 M in biological samples (yeast cell sample extracts). The experiment conducted in this master thesis further highlights the need of an acid addition as a catalyst. For most carbonyl compounds (10 out of 13), a HCl dose as low as 0.01 M resulted in a considerable increase in derivatization efficiency compared to no HCl addition (Figure 6a). However, for some compounds including acetaldehyde, formaldehyde and decanal the derivatization efficiency decreased when adding 0.01 M HCl compared to no HCl addition. The derivatization efficiency for 3,5-heptanedione increased with increasing HCl dose and was highest at a HCl concentration of 0.05 M. The other 12 detected target carbonyls showed no difference or a slight decrease in derivatization efficiencies when applying HCl doses above 0.01 M. Since there was not an optimal HCl concentration for all target carbonyl compounds, a concentration of 0.02 M HCl was adopted.

The derivatization efficiencies were independent of the reaction time at room temperature (10 min-2 h) (Figure 6b). Minimal differences between samples may be attributed to pipetting errors or instrument variability. At spiking levels of 500 nM of each target carbonyl compound and derivatization with 200 μ M TSH and 0.02 M HCl, all 16 target carbonyl compounds were detected with peak areas in the order of 10^6 to 10^9 .

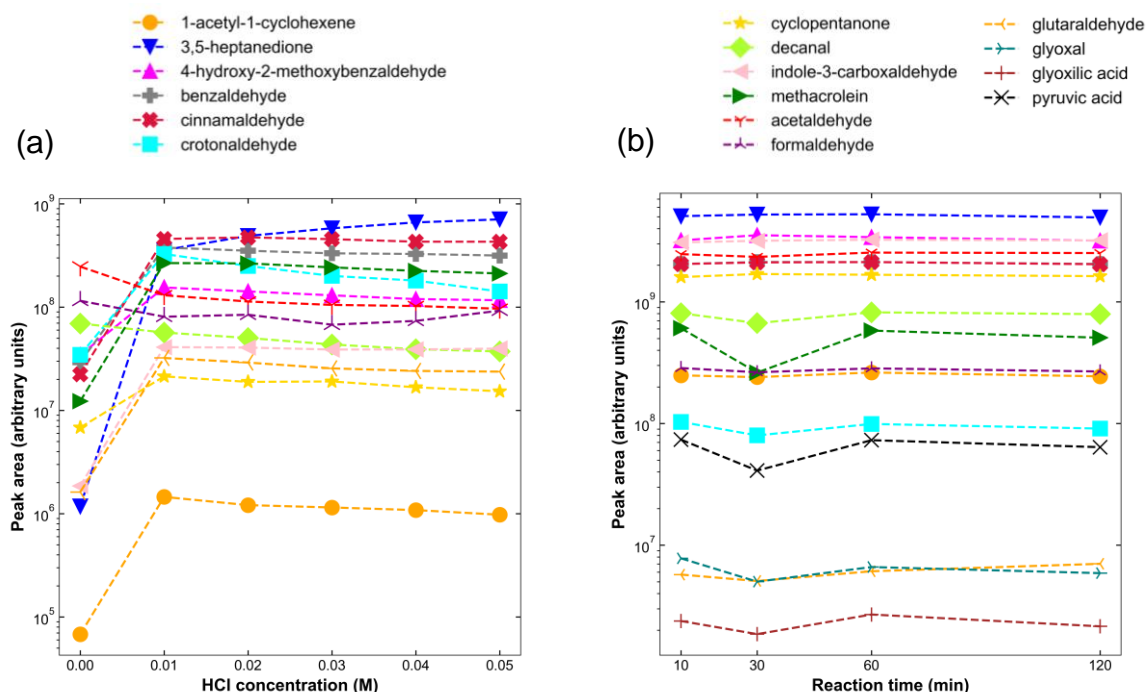


Figure 6. (a) Influence of HCl concentration on the derivatization efficiency for 13 target carbonyl compounds; (b) influence of reaction time at room temperature on the derivatization efficiency for 16 target carbonyl compounds.

3.1.3 Influence of derivatization on the detectability of carbonyls

Figure 7 shows the detectability of 16 target carbonyl compounds in positive and negative ESI modes with and without derivatization. For all 16 target carbonyl compounds in the mixture, the peak areas were highest when analysed in the positive mode after derivatization, with the exception of 1-acetyl-1-cyclohexene, whose peak area was about 2.6 times higher with positive ESI without derivatization than with derivatization. Formaldehyde, acetaldehyde, crotonaldehyde and 3,5-heptanedione were only detected in the positive mode with derivatization. Decanal, benzaldehyde, methacrolein, glyoxal and glutaraldehyde were only detected with derivatization in both the positive and negative modes. Cinnamaldehyde, cyclopentanone, and 1-acetyl-1-cyclohexene were detected in both modes when derivatized, and only in the positive mode without derivatization. Glyoxylic acid and pyruvic acid were detected in both modes when derivatized, and in the negative mode without derivatization. Indole-3-carboxaldehyde and 4-hydroxy-2-methoxybenzaldehyde were detected in all four conditions.

The detection of formaldehyde and acetaldehyde was not possible without derivatization since the monoisotopic masses of their molecular ions were outside the mass range (< 55 m/z). Moreover, these compounds are too polar to be separated on a C18 column. In general, aromatic compounds and cyclic compounds such as 4-hydroxy-2-methoxybenzaldehyde or cyclopentanone, respectively were detected more easily with LC-ESI-HRMS. The underivatized ketoacids (glyoxylic acid and pyruvic acid) were better detected with negative ESI than positive ESI, most likely due to their acidic (proton donor) nature.

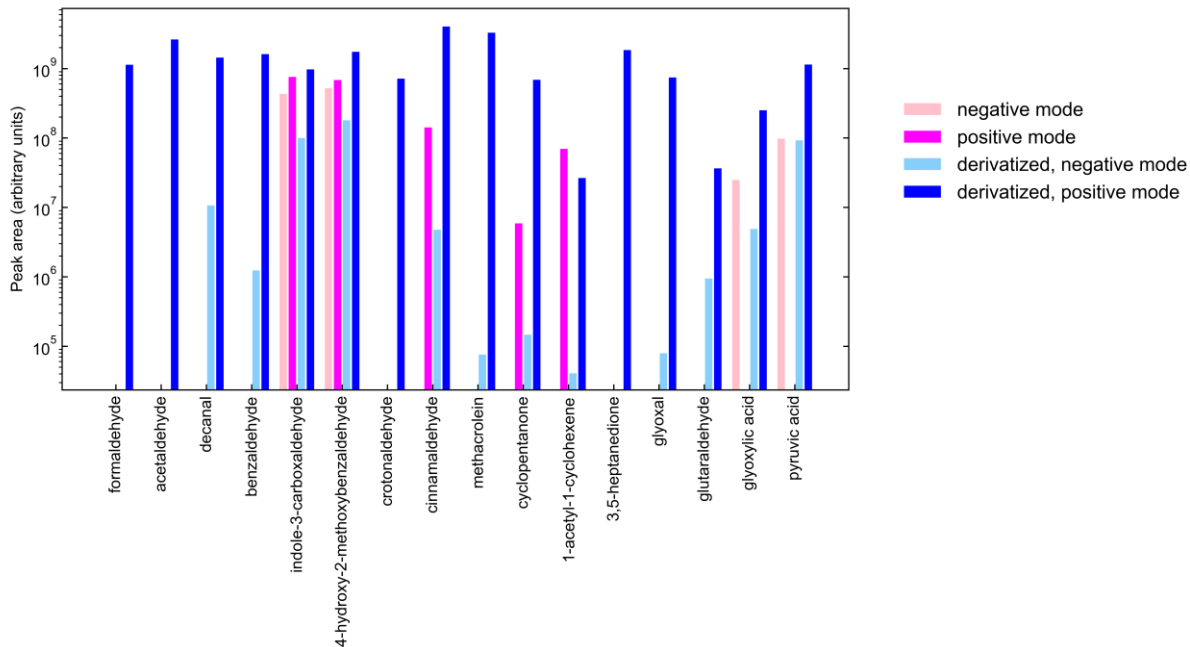


Figure 7. Detectability of 16 target carbonyl compounds in positive and negative ESI modes. The pink (negative mode) and magenta (positive mode) coloured bars refer to non-derivatized samples. The lightblue (negative mode) and blue (positive mode) coloured bars refer to derivatized samples.

The results for method performance characteristics such as linearity ranges, LODs and LOQs (Section S.4), analytical matrix effects (Section S.5) and the stability of derivatized carbonyl compounds (Section S.6) are described and discussed in the SI. Furthermore, the repeatability

of the internal standard spiking for benzaldehyde-d6 and tramadol-d6 is detailed in the SI (Section S.7).

3.2 Identification of unknown carbonyls by non-target analysis

Unknown carbonyl compounds were identified using a target and a non-target approach. First, the non-target approach will be laid out. Then, the non-target results for the ozonation (OH radical scavenged) of model compounds (olefins, phenols, β -diketone) will be shown, and tentative and probable structures assigned. Next, the quantified concentrations of the 16 target carbonyls in the different ozonated water matrices (with and without OH radical scavenging) as a function of the specific ozone dose will be displayed. Lastly, the non-target results for the different water matrices will be presented and discussed.

Figure 8 shows the workflow used for screening for unknown carbonyl compounds. The application of the different filtering criteria reduced considerably the number of unknown candidate carbonyl compounds. For most compounds, Compound Discoverer only proposed one single predicted composition formula and the mass error was very low (between - 1.5 and + 1.5 ppm). For a few compounds several predicted composition formulas were possible. Compound Discoverer ranked these predicted compositions based on an algorithm considering the mass error, isotope patterns, and fragments of a given compound. The proposed predicted compositions were checked to confirm that they were chemically valid with an acceptable mass error (less than 5 ppm) and had the minimum elements as derivatized carbonyl compounds.

Example WW Neugut (without OH radical scavenging)

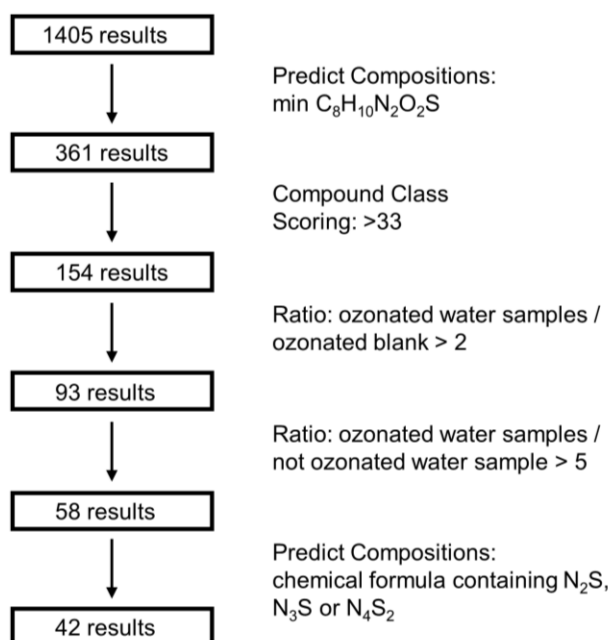


Figure 8. Scheme of the criteria applied to the outcome of the Compound Discoverer analysis for WW Neugut samples (without OH radical scavenging). With five criteria, 42 results were selected from initially 1405 results.

The remaining results from the workflow used for screening for unknown carbonyl compounds (Figure 8) were further processed using the workflow for the assignment of possible and probable structures (Figure 9). Chemical formulas of carbonyl compounds (Figure 9, tier (2)) were obtained by subtracting a substructure sum formula of the derivatizing agent from the derivatized predicted composition (Figure 9, tier (1)) obtained by the software Compound Discoverer. The numbers of nitrogen and sulphur atoms in the derivatized predicted composition formulas allowed determining whether a single or double derivatization occurred. A predicted composition formula containing one sulphur atom and two or three nitrogen atoms indicated that a single derivatization took place, while a formula containing two sulphur and four nitrogen atoms indicated that double derivatization took place. To account for the chemical formula of the carbonyl compound before derivatization, $C_7H_8N_2OS$ and $C_{14}H_{16}N_4O_2S_2$ were subtracted from the derivatized predicted composition formula for single and double derivatized compounds, respectively. At this stage, the identification of chemical formulas of carbonyls was of confidence level 3 (Schymanski et al., 2014).

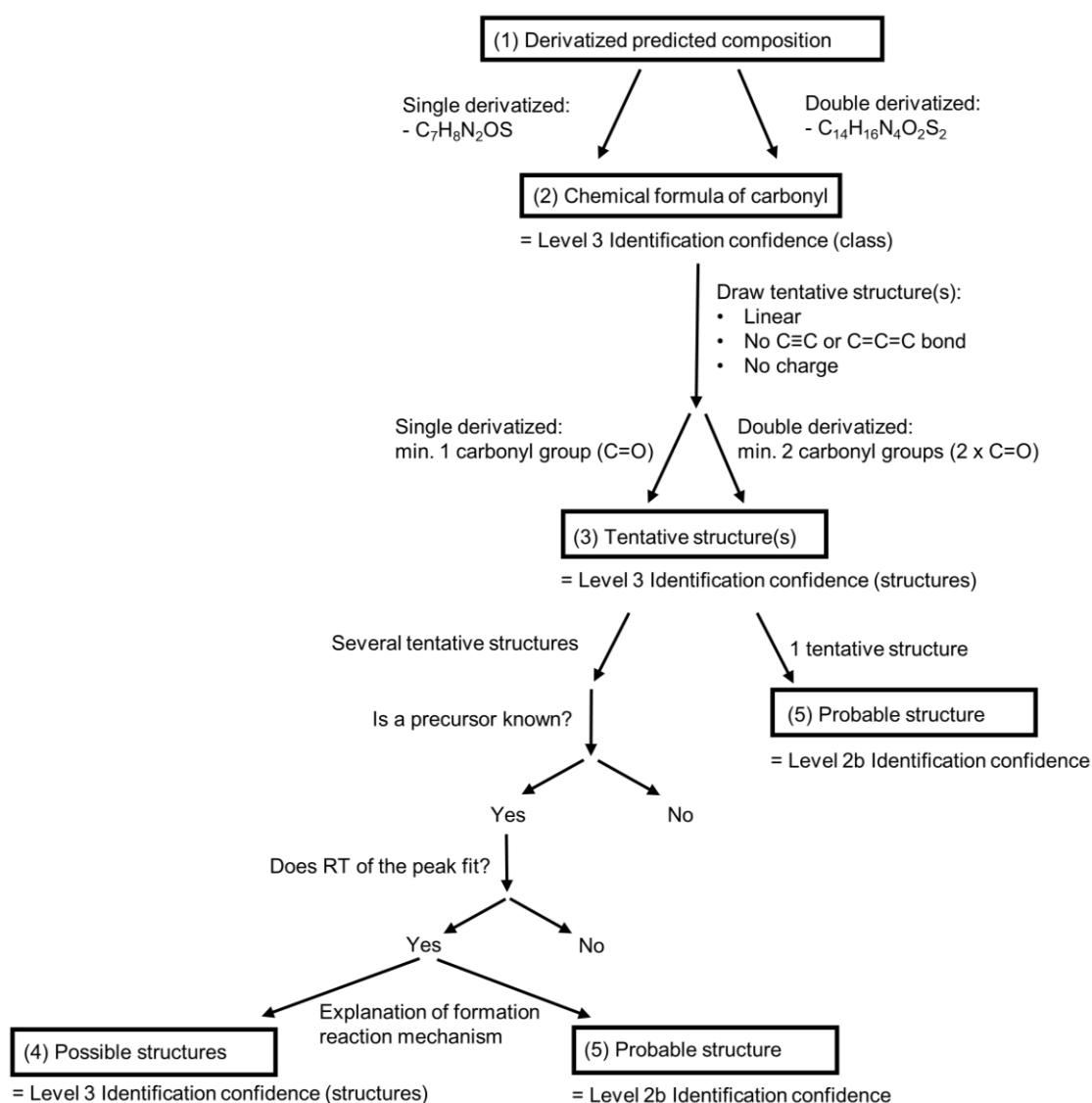


Figure 9. Scheme of workflow for assignment of possible and probable structures for unknown carbonyls. Confidence levels of identification according to Schymanski et al., 2014.

Out of the 16 target carbonyl compounds only glyoxal (C₂H₂O₂) was double derivatized. The chemical formulas of the other target carbonyls (single derivatized) were correctly (except 3,5-heptanedione) determined when subtracting of C₇H₈N₂OS from the predicted composition formulas. This further confirmed that the assignment of predicted composition formulas according to the workflow was reliable.

For 3,5-heptanedione (β -diketone) an H₂O loss occurring in the ion source of the MS was observed. Thus, it was assumed that 3,5-heptanedione is present in its enol rather than keto form in aqueous solutions. Keto-enol tautomerization has been extensively studied in the past (Emsley, 1984). Carbonyl compounds with at least one α -hydrogen atom can exist in two tautomeric forms (keto and enol), and the equilibrium position depends on the relative stability of the keto and enol form (Roy, 2017). Acetylacetone, the simplest member of the β -diketones, is predominantly found in its enol form in many cases (Lozada-Garcia et al., 2011). Due to the likeness in structure between 3,5-heptanedione and thus chemical properties it is likely that the enol form of 3,5-heptanedione is also more stable than its keto form. For acetylacetone the same H₂O loss was observed as for 3,5-heptanedione.

Tentative structures (Figure 14, tier (3)) for unknown carbonyl compounds were obtained by drawing linear, uncharged carbonyl compounds with no C \equiv C or C=C=C bonds because they are generally expected to react further with ozone. Single and double derivatized compounds had to contain at least one and two carbonyl groups, respectively. For some unknowns there was only one tentative structure possible and therefore a probable structure could be assigned (level 2b identification confidence, Figure 9, tier (5)) However, for many carbonyl compounds there were several tentative structures possible. The ozonation of the model compounds (cinnamic acid, sorbic acid, 3-buten-2-ol, acetylacetone, phenol, 4-ethylphenol, 4-methoxyphenol, Section 3.3) provided further information that could be used to deduce possible structures (confidence level 3 for identification (structure)) (Figure 9, tier (4)) and probable structures. For chemical formulas of carbonyl compounds that were formed both during the ozonation of WW, LW or SRFA and model compounds, it was checked if the RT matched. A shift in RT could be traced based on the RTs of the target carbonyl compounds glyoxal, acetaldehyde or formaldehyde in the samples. When the RTs matched, a possible carbonyl formation mechanism from the precursor (model compound) was investigated that would help to reduce the number of tentative structures based on the structure of the precursor and expected transformation during ozonation. A basic assumption was that the model compounds react according to the Criegee mechanism. To confirm possible and probable structures (levels 3 and 2b, respectively), reference standards would have to be purchased when commercially available, derivatized and analysed. By matching MS, MS/MS and retention time data of the possible or probable structure of an unknown carbonyl compound with the reference standard, a confirmed structure (level 1 identification confidence) would be achieved (Schymanski et al., 2014).

In the following sections, the results for the formation of targeted and non-targeted carbonyl compounds during ozonation of model compounds (Section 3.3) and ozonation of different water matrices (Section 3.4) are shown and discussed.

3.3 Carbonyl precursor evaluation and structure elucidation

The results from the ozonation of the carbonyl precursors (model compounds) cinnamic acid, sorbic acid, 3-buten-2-ol, acetylacetone, phenol, 4-ethylphenol and 4-methoxyphenol are presented here. This section is a preliminary assessment with further mechanistic evaluation needed. It is emphasized that all propositions for possible or probable structures are just tentative and more investigations are needed to verify or falsify them. Molecular formulas for carbonyl compounds produced during ozonation of the model compounds are listed in Table 6. Peak areas for a selection of carbonyl compounds that were formed in the ozonolysis of the model compounds as a function of the applied ozone doses are depicted in the SI Section S.15. Drawings (similar to Figure 10) of carbonyl products formed during ozonolysis of the model compounds according to the Criegee mechanism are shown in the SI Section S.16.

Whether formaldehyde was formed during ozonolysis (with DMSO) of the model compounds could not be decided because of the formaldehyde yield from the ozonolysis of DMSO. The calibration for formaldehyde that was established for quantification could not be applied here because a different TSH amount was used for derivatization. The ozonated model compounds were derivatized with 50 μM TSH whereas the formaldehyde calibration was established using a TSH concentration of 200 μM . Furthermore, a DMSO concentration of 1 mM was used for the ozonation of the model compounds, but ozonated blank samples (with DMSO) were only available at a DMSO concentration of 0.5 mM and derivatized with 200 μM TSH. Thus, a potential formation of formaldehyde would be difficult to claim and will therefore not be discussed in this section.

3.3.1 Olefinic carbonyl precursors

Cinnamic acid When applying the non-target workflow to the analysis of ozonated samples of cinnamic acid, benzaldehyde was the only carbonyl product that could be identified when OH radicals were scavenged (with DMSO). Based on the theoretical reaction mechanism benzaldehyde ($\text{C}_7\text{H}_6\text{O}$) and glyoxylic acid ($\text{C}_2\text{H}_2\text{O}_3$) are formed during ozonation of cinnamic acid (Leitzke et al., 2001). However, glyoxylic acid was not formed as expected or could not be identified with the non-target workflow. Glyoxylic acid might have reacted further with H_2O_2 and given rise to formic acid and carbon dioxide (Leitzke et al., 2001; Ramseier & von Gunten, 2009). Ramseier & von Gunten, 2009 experimentally confirmed the transformation of glyoxylic acid into formic acid and carbon dioxide. When OH radicals were not scavenged, apart from $\text{C}_7\text{H}_6\text{O}$ the following carbonyl sum formulas were identified: $\text{C}_3\text{H}_2\text{O}$, $\text{C}_4\text{H}_4\text{O}_3$, $\text{C}_5\text{H}_6\text{O}_3$, $\text{C}_7\text{H}_6\text{O}_2$, $\text{C}_7\text{H}_6\text{O}_3$ and $\text{C}_7\text{H}_6\text{O}_4$. $\text{C}_7\text{H}_6\text{O}_2$, $\text{C}_7\text{H}_6\text{O}_3$ and $\text{C}_7\text{H}_6\text{O}_4$ are likely benzaldehyde-like structures with additional hydroxyl groups at the aromatic ring.

Sorbic acid The formation of the following carbonyl compounds was expected from reactions of sorbic acid with ozone according to the Criegee mechanism: crotonaldehyde ($\text{C}_4\text{H}_6\text{O}$), glyoxylic acid ($\text{C}_2\text{H}_2\text{O}_3$), glyoxal ($\text{C}_2\text{H}_2\text{O}_2$), acetaldehyde ($\text{C}_2\text{H}_4\text{O}$) and 4-oxobut-2-enoic acid ($\text{C}_4\text{H}_4\text{O}_3$) (Figure 10). Crotonaldehyde and glyoxal were detected when ozonating sorbic acid (with DMSO) (Table 6). The ozone dose had an effect on the yield of crotonaldehyde. For ozone doses $\leq 25 \mu\text{M}$, the peak area was increasing (maximum peak area: $2.7\text{E}+08$). At an ozone dose of about 100 μM the peak area was smaller by two orders of magnitude ($2.7\text{E}+06$) and decreased even further at higher ozone doses. At higher ozone doses an attack

of ozone on the C=C bond of crotonaldehyde is expected giving rise to glyoxal and acetaldehyde. Therefore, it makes sense that crotonaldehyde is degraded at high ozone doses.

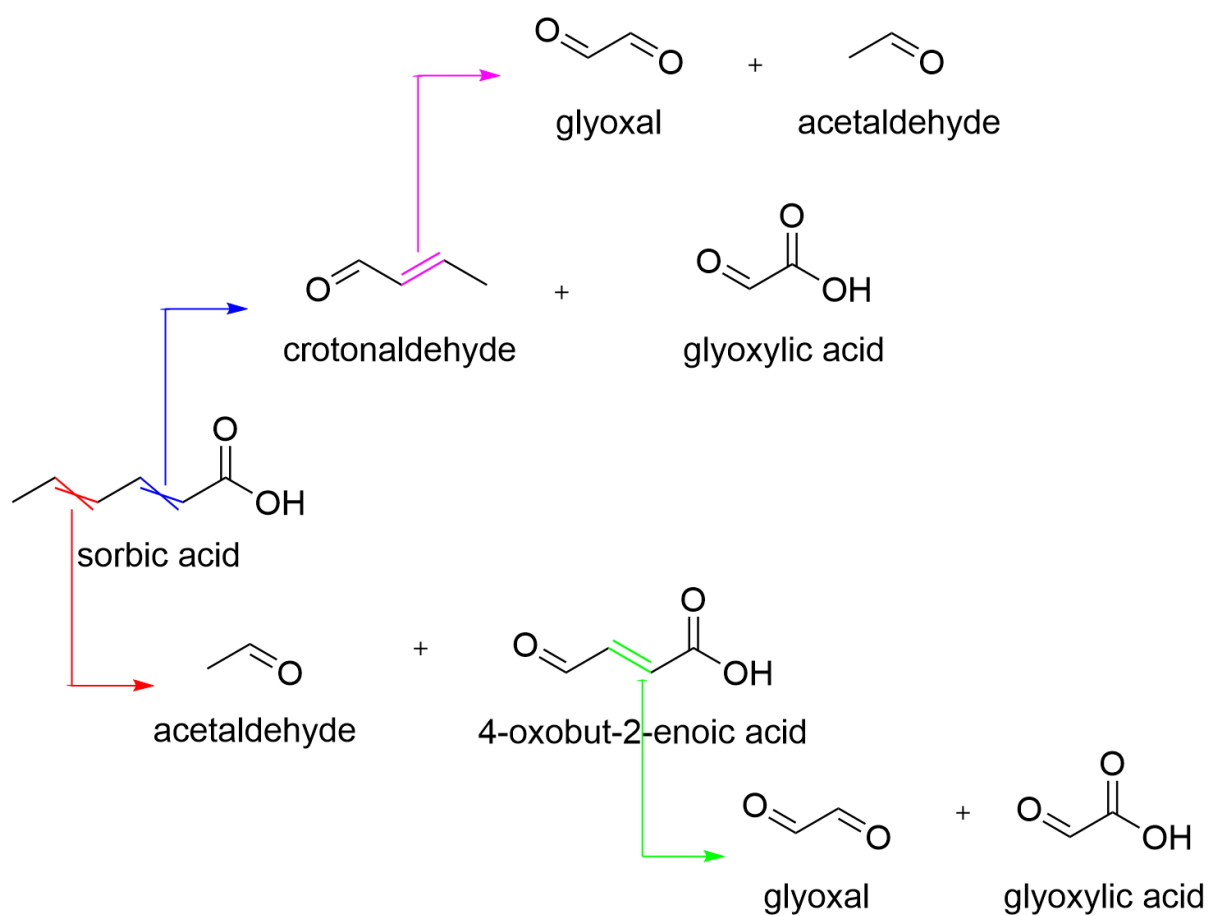


Figure 10. Scheme of product formation from reactions of sorbic acid with ozone according to the Criegee mechanism. Reaction arrows indicate an attack of ozone at the carbon double bond highlighted in the same color.

Table 6. Summary of molecular formulas and retention times for carbonyl compounds (excluding *N*-containing) that were identified (using non-target workflow) in ozonated WWs, SRFA and LW without OH radical scavenging (without DMSO) and from the ozonated model compounds (excluding cinnamic acid) with OH radical scavenging (with DMSO).

Molecular formula	Without OH radical scavenging (without DMSO)					With OH radical scavenging (with DMSO)					
	WW Neugut	WW Werdhölzli	WW Glarnerland	SRFA	LW Greifensee	Sorbic acid	3-Buten-2-ol	Acetylaceton	Phenol	4-Ethylphenol	4-Methoxyphenol
C ₂ H ₂ O	13.8	13.9	13.9	13.7	ND	ND	ND	13.9	ND	ND	ND
C ₂ H ₂ O ₂	16.3**	16.5**	16.4**	16.3**	ND	16.3**	ND	ND	16.6**, 17.3**	16.3**	16.3**
C ₂ H ₂ O ₃	13.5	ND	13.6	ND	ND	ND	ND	ND	ND	ND	13.5
C ₂ H ₄ O	ND	ND	ND	ND	ND	ND	13.9	ND	ND	13.7	ND
C ₂ H ₄ O ₂	ND	13.0	13.0	12.8	ND	12.8	ND	ND	13.1	ND	12.8
C ₃ H ₂ O	15.7	15.9	13.0, 15.8	15.7	15.7	ND	ND	ND	13.2, 16.0	ND	12.9, 15.7
C ₃ H ₂ O ₂	15.0	15.2	15.1, 16.8**	15.0	15.0	ND	ND	ND	15.3	14.9	15.0
C ₃ H ₂ O ₃	16.5**	16.7**	16.6**	16.5**	ND	16.5**	ND	ND	13.4, 16.8**	16.5**	16.5**
C ₃ H ₂ O ₄ #	ND	ND	ND	ND	ND	ND	ND	ND	ND	ND	17.9**
C ₃ H ₄ O	ND	ND	15.1, 16.3	ND	ND	ND	ND	ND	ND	ND	ND
C ₃ H ₄ O ₂	ND	ND	16.6**	16.5**	ND	ND	16.7**	16.6**	15.1**	ND	ND
C ₃ H ₄ O ₃	13.8, 16.4**	14.0	13.9, 16.5**	13.7, 16.4**	ND	13.5, 13.7	13.9	13.5, 13.9, 15.8	14.1	13.4, 13.7	13.5, 13.8, 14.5
C ₃ H ₆ O*	ND	ND	13.4	ND	ND	ND	ND	ND	ND	ND	ND
C ₃ H ₆ O ₂	13.0	13.2	13.1	13.0	13.0	ND	13.9	13.1	ND	ND	ND
C ₄ H ₂ O ₃ #	ND	ND	ND	ND	ND	ND	ND	ND	ND	ND	12.8, 13.1
C ₄ H ₄ O*	ND	14.0	13.9	16.4	13.8	16.4	ND	ND	14.1	ND	ND
C ₄ H ₄ O ₂	15.8	16.0	15.9	15.8	15.8	ND	ND	15.9	12.7, 14.1, 16.4**	ND	12.4, 14.9
C ₄ H ₄ O ₃	13.5	13.7	13.7, 14.5, 15.2	13.5, 14.3, 15.9**	12.7	ND	ND	ND	14.6, 15.4	ND	15.1
C ₄ H ₄ O ₄	ND	ND	ND	15.9**	ND	ND	ND	ND	13.4	ND	ND
C ₄ H ₆ O#	ND	ND	ND	ND	ND	15.7, 16.6	ND	ND	ND	ND	ND
C ₄ H ₆ O ₂	15.7	15.9, 16.9**	14.5, 15.8, 16.9**	15.7, 16.7**	15.7, 16.7**	ND	ND	15.8, 16.8**	ND	16.3	ND

C ₄ H ₆ O ₃	13.5, 13.8	13.7, 13.9	13.6, 13.9	13.5, 13.7	13.4	13.7	ND	13.9	13.8, 14.1	13.7, 14.3, 17.4	13.7, 14.3, 14.8
C ₄ H ₆ O ₄	12.8	13.0	12.9	12.7	ND	ND	ND	ND	ND	ND	ND
C ₄ H ₈ O ₂ #	ND	ND	ND	ND	ND	13.7	ND	14.0	ND	ND	ND
C ₅ H ₄ O ₂ #	ND	ND	ND	ND	ND	ND	ND	ND	ND	ND	13.2
C ₅ H ₄ O ₃	13.9	14.1	14.0	16.3	13.9	ND	ND	ND	14.2, 14.4, 15.3	ND	ND
C ₅ H ₄ O ₄	ND	ND	12.8	ND	ND	ND	ND	ND	ND	ND	ND
C ₅ H ₆ O	16.3	16.5	ND	17.0	ND	ND	ND	ND	ND	14.7, 17.1, 17.4	ND
C ₅ H ₆ O ₂	13.3, 14.4	13.5, 14.6	13.8, 14.6	14.4	14.4	ND	ND	ND	ND	16.6	ND
C ₅ H ₆ O ₃	ND	16.8**	14.3, 14.5, 16.7**	14.4	ND	ND	ND	ND	15.4	ND	ND
C ₅ H ₆ O ₄ *	ND	ND	ND	16.0**	ND	ND	ND	ND	ND	ND	ND
C ₅ H ₆ O ₅	ND	14.6	ND	ND		ND	ND	ND	ND	ND	ND
C ₅ H ₆ O ₆ #	ND	ND	ND	ND	ND	ND	ND	ND	ND	ND	13.7
C ₅ H ₈ O	17.1	ND	17.2	ND	ND	ND	ND	ND	ND	ND	ND
C ₅ H ₈ O ₂ #	ND	ND	ND	ND	ND	ND	ND	ND	ND	14.8, 16.3, 16.7	ND
C ₅ H ₈ O ₃	ND	14.1	14.0, 14.6	ND	ND	ND	ND	ND	ND	14.2, 14.3	ND
C ₅ H ₈ O ₄	ND	ND	13.0	ND	ND	ND	ND	ND	ND	ND	ND
C ₆ H ₄ O ₂ #	ND	ND	ND	ND	ND	ND	ND	ND	16.0	ND	ND
C ₆ H ₄ O ₃ #	ND	ND	ND	ND	ND	ND	ND	ND	ND	ND	14.4, 16.1
C ₆ H ₄ O ₄ #	ND	ND	ND	ND	ND	ND	ND	ND	ND	15.2	14.1
C ₆ H ₄ O ₅	13.0	13.2	ND	13.0	13.0	ND	ND	ND	13.4	ND	ND
C ₆ H ₆ O ₂ #	ND	ND	ND	ND	ND	ND	ND	ND	ND	16.0	ND
C ₆ H ₆ O ₄	14.9	ND	15.0	14.5	ND	ND	ND	ND	13.0, 13.2	14.4	12.7, 12.9, 13.7
C ₆ H ₆ O ₅	13.2	ND	13.1	ND	13.2	ND	ND	ND	ND	ND	13.2
C ₆ H ₈ O ₂	ND	ND	17.8**	ND	ND	ND	ND	ND	ND	15.8, 16.2	ND
C ₆ H ₈ O ₃ #	ND	ND	ND	ND	ND	ND	ND	ND	ND	14.9, 15.4, 15.9, 16.2	ND
C ₆ H ₈ O ₄	14.8, 16.5**	15.0, 16.7**	15.0, 16.6**	14.8	14.8	ND	ND	ND	ND	ND	14.3
C ₆ H ₁₀ O ₂	15.4	15.6	14.6, 15.5	ND	15.4	ND	ND	ND	ND	ND	ND
C ₆ H ₁₀ O ₃ #	ND	ND	ND	ND	ND	ND	ND	ND	ND	15.2	ND
C ₇ H ₆ O ₅ #	ND	ND	ND	ND	ND	ND	ND	ND	ND	ND	15.4

C ₇ H ₈ O ₄ #	ND	ND	ND	ND	ND	ND	ND	ND	ND	ND	14.4, 15.3
C ₇ H ₈ O ₂ #	ND	ND	ND	ND	ND	ND	ND	ND	ND	16.3	ND
C ₇ H ₈ O ₄ #	ND	ND	ND	ND	ND	ND	ND	ND	ND	15.2	ND
C ₇ H ₁₀ O*	ND	ND	17.0	ND	ND	ND	ND	ND	ND	ND	ND
C ₇ H ₁₀ O ₃	15.4	15.6	15.5, 17.1**	15.4	15.4	ND	ND	ND	ND	ND	ND
C ₇ H ₁₂ O ₂	ND	ND	15.2	ND	ND	ND	ND	ND	ND	ND	ND
C ₈ H ₁₀ O ₃ #	ND	ND	ND	ND	ND	ND	ND	ND	ND	14.6	ND
C ₈ H ₁₀ O ₅ #	ND	ND	ND	ND	ND	ND	ND	ND	ND	14.2, 14.4, 16.6	ND
C ₈ H ₁₂ O ₃ #	ND	ND	ND	ND	ND	ND	ND	ND	ND	16.4	ND
C ₈ H ₁₂ O ₅ #	ND	ND	ND	ND	ND	ND	ND	ND	ND	12.7	ND
C ₈ H ₁₆ O ₄	ND	ND	14.4	ND	ND	ND	ND	ND	ND	ND	ND
C ₈ H ₂₀ O ₄ *	ND	ND	ND	ND	16.6	ND	ND	ND	ND	ND	ND
C ₉ H ₁₂ O ₂ *	ND	ND	ND	ND	17.0	ND	ND	ND	ND	ND	ND
C ₁₀ H ₁₂ O ₅	ND	ND	14.8	ND	ND	ND	ND	ND	ND	ND	ND
C ₁₄ H ₁₀ O ₃	17.7	ND	ND	ND	ND	ND	ND	ND	ND	ND	ND
C ₁₄ H ₂₀ O ₄	ND	ND	18.6	ND	ND	ND	ND	ND	ND	ND	ND

* Molecular formulas which were not identified in ozonated WWs, SRFA and LW with OH radical scavenging but only without OH radical scavenging; ** Retention times of double derivatized carbonyls; # Molecular formulas which were only identified in ozonated model compounds and not in ozonated WWs, SRFA or LW.

Slight RT shifts were observed: Sorbic acid (+ 0.1 min), 3-buten-2-ol (+ 0.3 min), acetylacetone (+ 0.3 min), phenol (+ 0.4-0.5 min), 4-ethylphenol (+ 0.1 min), 4-methoxyphenol (+ 0.1-0.2 min).

Glyoxilic acid, actetaldehyde and 4-oxobut-2-enoic acid were not detected as expected from the Criegee mechanism (Figure 10). The product $C_2H_4O_2$ was identified in the ozonated sorbic acid samples. The only carbonyl structure that fitted this chemical formula was 2-hydroxyacetaldehyde. Additionally, the product $C_3H_2O_3$, which was double derivatized, was identified as 2-oxopropanedial. $C_3O_4O_3$ was also formed and is likely to be 3-hydroxy-2-oxopropanal based on a reaction mechanism suggested for ozone and acrylic acid (Figure 11) (von Sonntag & von Gunten, 2012). Hence, 2-hydroxyacetaldehyde, 2-oxopropanedial and 3-hydroxy-2-oxopropanal are probable structures (level 2b confidence) for carbonyls that are formed during ozonolysis of sorbic acid (with DMSO). Moreover, the products C_4H_4O , $C_4H_6O_3$ and $C_4H_8O_2$ were observed (with DMSO).

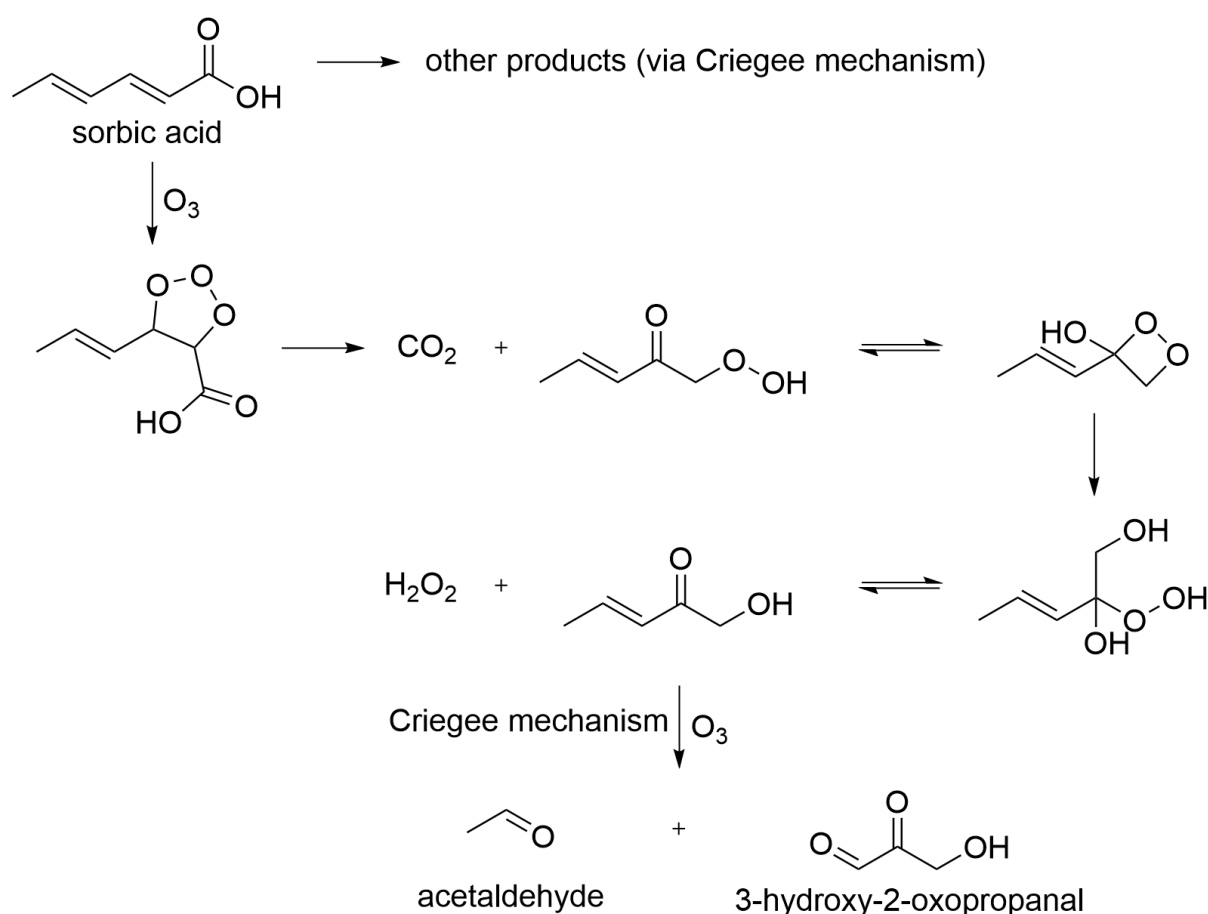


Figure 11. Scheme of tentative (not solely according to the Criegee mechanism) product formation from reactions of sorbic acid with ozone. Reaction mechanism is adapted from mechanism of ozonolysis of acrylic acid shown in von Sonntag & von Gunten (2012).

3-buten-2-ol During ozonolysis (with DMSO) of 3-buten-2-ol, acetaldehyde was detected and $C_3H_4O_3$, which could be pyruvic acid based on the RT of the peak considering the slight RT shift (+ 0.3 min) of the ozonated 3-buten-2-ol samples Figure 12. The acetaldehyde yield decreased with increasing ozone dose and reached a maximum at an ozone dose of about $25 \mu M$. 2-hydroxypropanal (probable structure for $C_3H_6O_2$) was formed as expected from the

Criegee mechanism. The yield of $C_3H_4O_3$ remained constant when applying ozone doses between 50 and 300 μM . Additionally, the product $C_3H_4O_2$ (double derivatized) was detected. The latter fits two tentative candidates: 2-oxopropanal (methyl glyoxal) and malonaldehyde. Based on the positions of hydroxyl group in 3-buten-2-ol, 2-oxopropanal seemed to be the more likely possible structure. Without OH radical scavenging, the following additional carbonyl compounds were identified: $C_2H_4O_2$ (2-hydroxyacetaldehyde), $C_3H_4O_4$, $C_4H_6O_2$ and $C_4H_6O_3$. The formation of $C_4H_6O_2$ and $C_4H_6O_3$ is interesting because carbonyl compounds contain four carbon atoms same as the precursor 3-buten-2-ol. Thus, they were formed without breaking the carbon skeleton of 3-buten-2-ol.

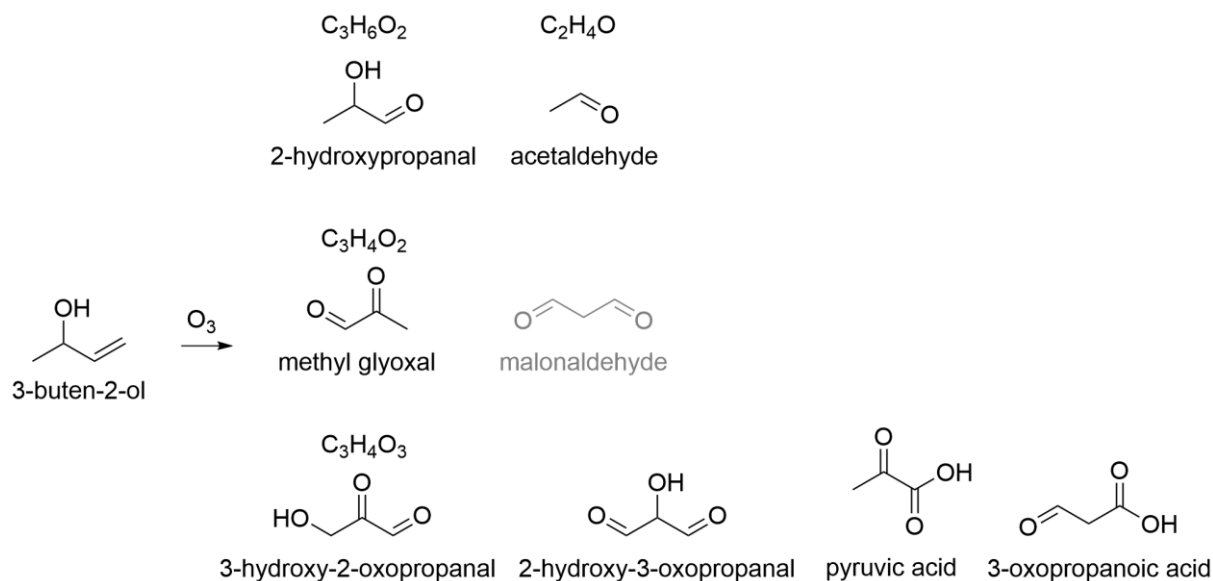


Figure 12. Scheme of possible and probable structures for carbonyl compounds that were formed during ozonolysis of 3-buten-2-ol in the presence of the OH radical scavenger DMSO. The tentative candidates in grey are less likely than the ones in black color (based on the structure of the precursor 3-buten-2-ol).

Acetylacetone A scheme of possible and probable structures for carbonyl compounds that were formed in the ozonolysis of acetylacetone in the presence of DMSO are shown in Figure 13. In ozonolysis of acetylacetone, 2-oxopropanal (methyl glyoxal, $C_3H_4O_2$) was observed double derivatized as expected from the Criegee mechanism. $C_4H_6O_2$ was observed single and double derivatized. $C_4H_6O_2$ (double derivatized) must contain two carbonyl groups and thus possible structures were: butane-2,3-dione, butanedial, 2-methylpropanedial, 2-oxobutanal and 3-oxobutanal. From these five diketones, butane-2,3 dione and 3-oxobutanal were the best candidates, because of the methyl group that should be attached to one carbonyl group (based on the structure of acetylacetone). Still, the structures butane-2,3-dione and 3-oxobutanal could not be traced back to the precursor compound due to the carbon skeleton and the positioning of the oxygen atoms based on the known reaction mechanisms. Therefore, it is important to highlight that further mechanistic evaluation is needed. Furthermore, $C_4H_6O_3$ was found, assuming that a methyl group is attached to a carbonyl group (based on the structure of acetylacetone) and that no ether is contained, the possible structures were: 3-oxobutanoic acid, 2-hydroxy-3-oxobutanal and 1-hydroxybutane-2,3-dione. Additionally, the product $C_4H_4O_2$ was identified, for which only structures with a $C=C$ or $C\equiv C$ bond were feasible. The product is less likely to contain a $C\equiv C$ bond than a $C=C$ bond. Moreover, $C_3H_6O_2$ was detected for which the best

candidate was 1-hydroxypropan-2-one based on the position of the ketone group. 3-hydroxypropanal would also be feasible based on the sum formula, but seemed less likely to relate back to acetylacetone as a precursor. 2-methoxyacetaldehyde was not a likely structure because it contains an ether. Lactaldehyde was also not considered a likely structure for $C_3H_6O_2$, because the RT did not match with the one for $C_3H_6O_2$ in the ozonated 3-buten-2-ol samples, for which the probable structure was lactaldehyde based on expectations from the Criegee mechanism. Ethenone is the probable structure for C_2H_2O .

In conclusion, the Criegee mechanism did not seem to be the only reaction mechanism occurring for olefins, despite being considered as the main one. It has also been stated that partial oxidation of olefins may be observed, which leads to the formation of products in which the carbon-carbon double bond is not fully cleaved (von Sonntag & von Gunten, 2012). However, the formation of carbonyl compounds through partial oxidation was only observed in organic solvents and not in water samples (von Sonntag & von Gunten, 2012). Furthermore, there seem to be cases where a homolytic cleavage instead of a heterolytic cleavage of the ozonide can occur for olefins, which may lead to the formation of carbonyls (von Sonntag & von Gunten, 2012). For some of the identified carbonyl compounds formed during the ozonolysis of the precursors, no reasonable explanation for their formation could be found yet. It would therefore make sense to enhance the quality control of the predicted molecular formulas even further and if the molecular formulas prove valid, to search for alternative reaction mechanisms occurring during ozonolysis.

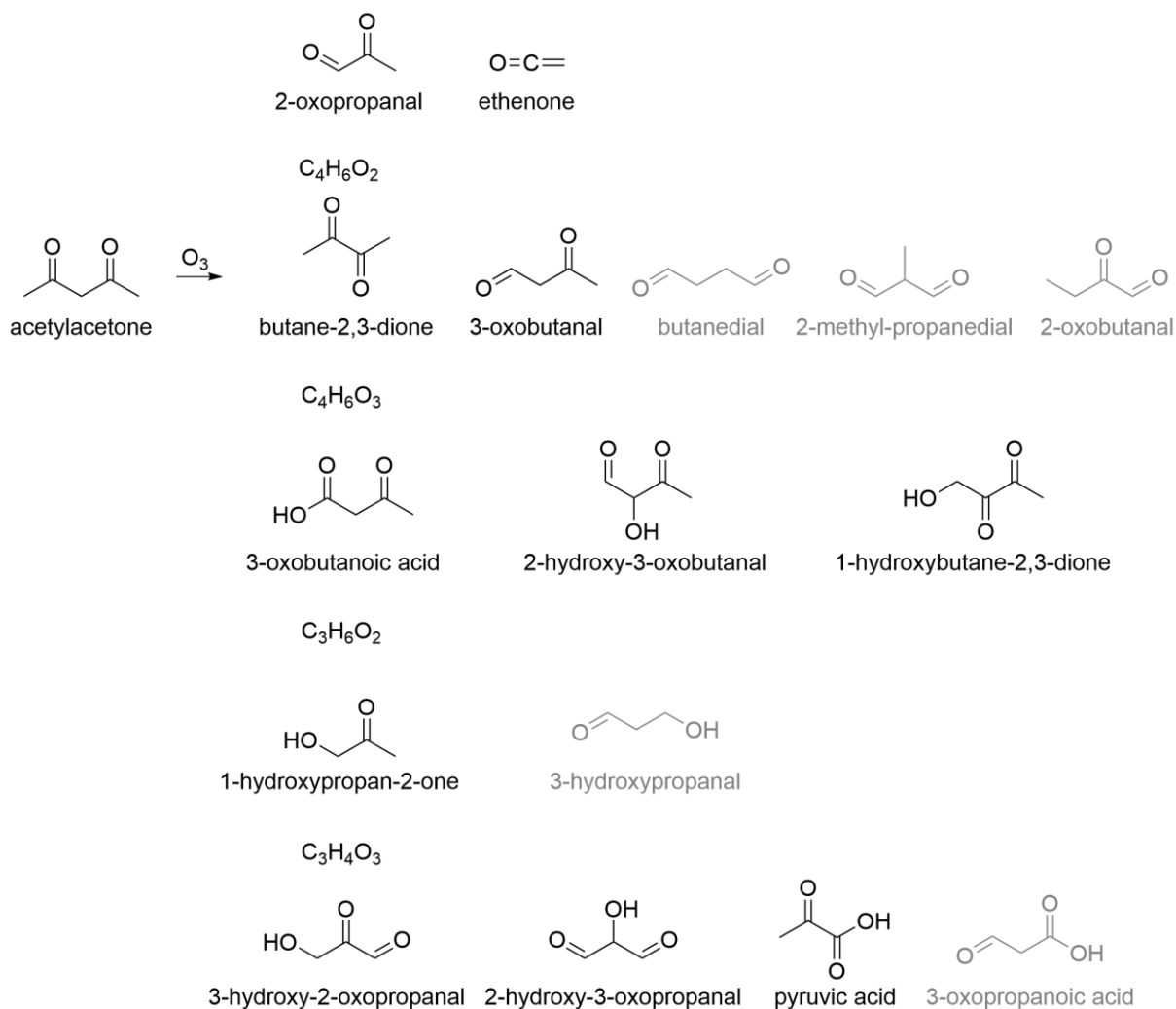


Figure 13. Scheme of possible and probable structures for carbonyl compounds that were formed during ozonolysis of acetylacetone in the presence of the OH radical scavenger DMSO. The tentative candidates in grey are less likely than the ones in black color (based on the structure of the precursor acetylacetone).

3.3.2 Phenolic carbonyl precursors

Phenols can react via different reaction pathways (von Sonntag & von Gunten, 2012). The first step in the reaction of ozone with aromatic compounds is the formation of an adduct (intermediate), which either forms an ozonide or reacts to other products (Ramseier & von Gunten, 2009; von Sonntag & von Gunten, 2012). These other products may only be formed because in aromatic systems the positive charge that develops through the adduct formation stabilises the adduct and sufficiently retards the collapse to the ozonide (von Sonntag & von Gunten, 2012). However, in the following the focus will be only about products that are expected from the Criegee mechanism and/or allow for assignment of possible and probable structures. Not all unknown carbonyls formed during ozonation of phenol, 4-ethylphenol and 4-methoxyphenol will be discussed here. A full overview over the unknown carbonyl compounds that were formed during the ozonolysis (with DMSO) of the phenolic carbonyl precursors is provided in Table 6.

Phenol

In total, 17 different chemical formulas for carbonyls were found in the ozonolysis (with DMSO) of phenol Table 6. The ozonation of phenol lead to the formation of

glyoxal, $C_4H_4O_3$ and $C_4H_4O_2$ as expected from the Criegee mechanism. Glyoxylic acid, which was expected as a product but was not found, likely reacted further with H_2O_2 giving rise to formic acid and carbon dioxide (Leitzke et al., 2001; Ramseier & von Gunten, 2009). Two peaks were detected for double derivatized glyoxal (RT: 16.6 and 17.3 min), which were likely the two E/Z-glyoxal TSH-hydrazones. The peak area at RT 17.3 minutes was smaller by two orders of magnitude compared to the peak area at RT 16.6 minutes. The yield of glyoxal was highest at the highest ozone dose (about 300 μM). The two isomers of $C_4H_4O_3$ were likely 4-oxobut-2-enoic acid and 2-hydroxyfumaraldehyde which are both expected from the Criegee mechanism. Otherwise, the two isomers could also be E/Z-TSH-hydrazones of either 4-oxobut-2-enoic acid or 2-hydroxyfumaraldehyde. The probable structure for $C_4H_4O_2$ was fumaraldehyde/malealdehyde. Furthermore, the product 2-hydroxyacetaldehyde was formed. Additionally, 2-oxopropanedial and $C_3H_4O_3$ (3-hydroxy-2-oxopropanal, 2-hydroxy-3-oxopropanal, pyruvic acid or 3-oxopropanoic acid) were formed. $C_3H_4O_2$ (double derivatized) was measured at a RT of 15.1 minutes, and its only two possible structures were 2-oxopropanal (methyl glyoxal) and propanedial. 2-oxopropanal (double derivatized) was likely formed in the ozonolysis of acetylacetone according to the Criegee mechanism and a peak was observed at 16.6 minutes. Because of the clear RT difference (1.5 minutes), $C_3H_4O_2$ that was produced in the ozonolysis of phenol must either be propanedial or the other E/Z-2-oxopropanal-TSH hydrazone.

4-ethylphenol 23 unknown carbonyl compounds were produced in the ozonolysis (with DMSO) of 4-ethylphenol (Table 6). The carbonyl compounds, which were expected to be formed based on the Criegee mechanism and for which a corresponding chemical formula was identified were: $C_8H_{10}O_3$, $C_6H_8O_3$, $C_6H_8O_2$ and glyoxal. The probable structures for $C_6H_8O_2$ and $C_6H_8O_3$ were 2-ethylfumaraldehyde/2-ethylmalealdehyde (E/Z isomers) and 4-oxohex-2-enoic acid, respectively (Figure 14). According to the Criegee mechanism, $C_8H_{10}O_3$ is formed as an initial product from the degradation of the ozonide 4-ethylphenol. Three different structures could theoretically be formed for the sum formula $C_8H_{10}O_3$, depending on the location where the ozone attacks the aromatic ring structure of 4-ethylphenol, but only one peak was observed. The peak area for $C_8H_{10}O_3$ was increasing with an increasing ozone dose $\leq 100 \mu M$, then it was decreasing (S14, SI). This trend was compatible with the suggested pathway, because the two C=C double bonds in $C_8H_{10}O_3$ are supposed to be attacked by ozone and lead to further product formation. The formation of $C_4H_4O_3$ and glyoxylic acid was expected from the Criegee mechanism, but it could not be confirmed in this experiment. Furthermore, acetaldehyde and 2-oxopropanedial were formed among many other carbonyl compounds.

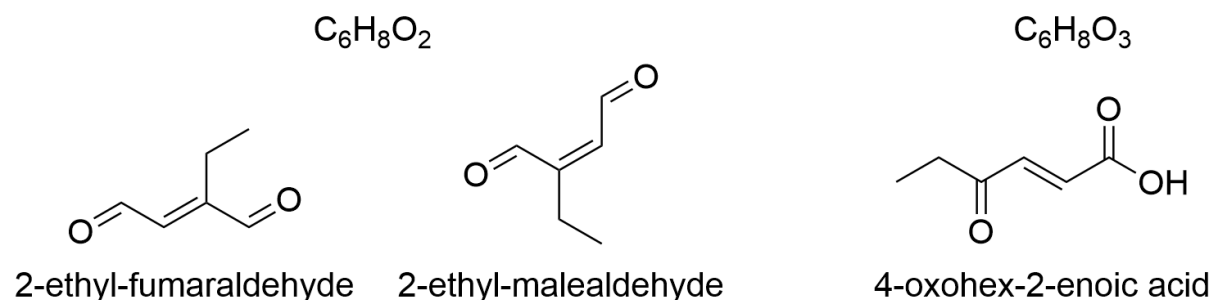


Figure 14. Tentative candidates for $H_6H_8O_2$ and $C_6H_8O_3$ formed during the ozonolysis of 4-ethylphenol based on the Criegee mechanism.

4-methoxyphenol 21 carbonyl compounds were identified in the ozonolysis (with DMSO) of 4-methoxyphenol (Table 6). The following compounds and sum formulas were expected based on the Criegee mechanism and found in ozonated (with DMSO) 4-methoxyphenol: glyoxal, glyoxylic acid, C₃H₄O₃, C₄H₄O₃ and C₇H₈O₄. The probable structure for C₃H₄O₃ was methyl-2-oxoacetate (Figure 15). The probable structure for C₄H₄O₃ (RT = 15.1 min) is 2-hydroxyfumaraldehyde, which was also found in the ozonolysis of phenol. For C₇H₈O₄ three structures were expected due to the three attack sites for ozone on the aromatic ring. Two peaks were measured for C₇H₈O₄ and the possible structures were: 4-methoxy-6-oxohexa-2,4-dienoic acid, methyl-4-hydroxy-6-oxohexa-2,4-dienoate and 2-hydroxy-5-methoxyhexa-2,4-dienedial (Figure 15). For several of the small carbonyl compounds that were formed during ozonation of 4-methoxyphenol, we could assign probable structures or tentative candidates. For C₃H₂O₄ (double derivatized) the probable structure is 2,3-dioxopropanoic acid (Figure 15), which is the only possible structure that has two carbonyl groups. Further, 2-hydroxyacetaldehyde and 2-oxopropandial were identified (probable structures).

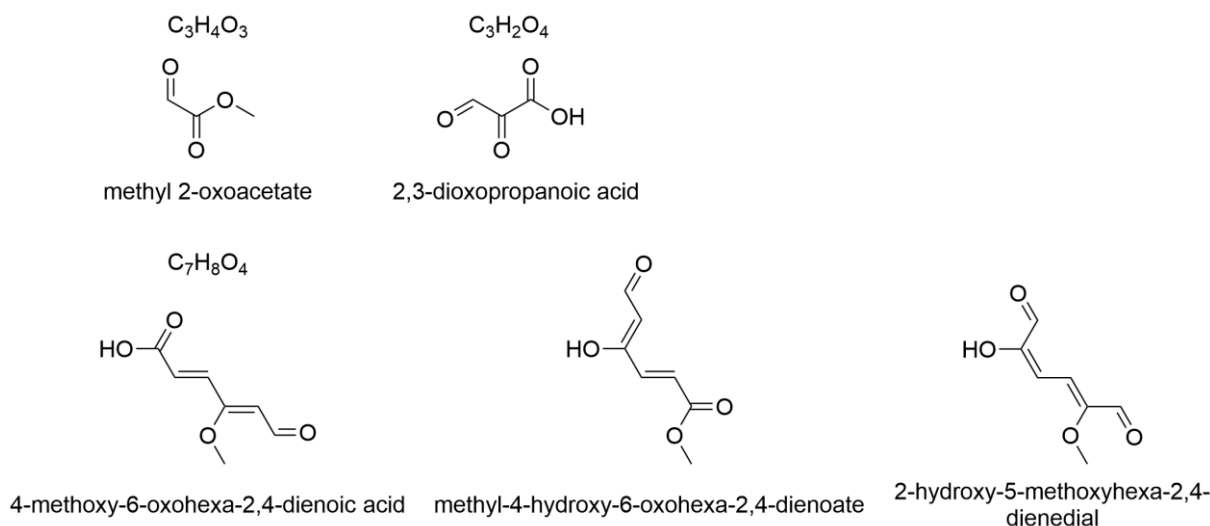


Figure 15. Tentative candidates for C₃H₄O₃ and C₇H₈O₄ formed during the ozonolysis of 4-methoxyphenol based on the Criegee mechanism.

3.4 Ozonation of different water matrices

3.4.1 Quantification of target carbonyl compounds

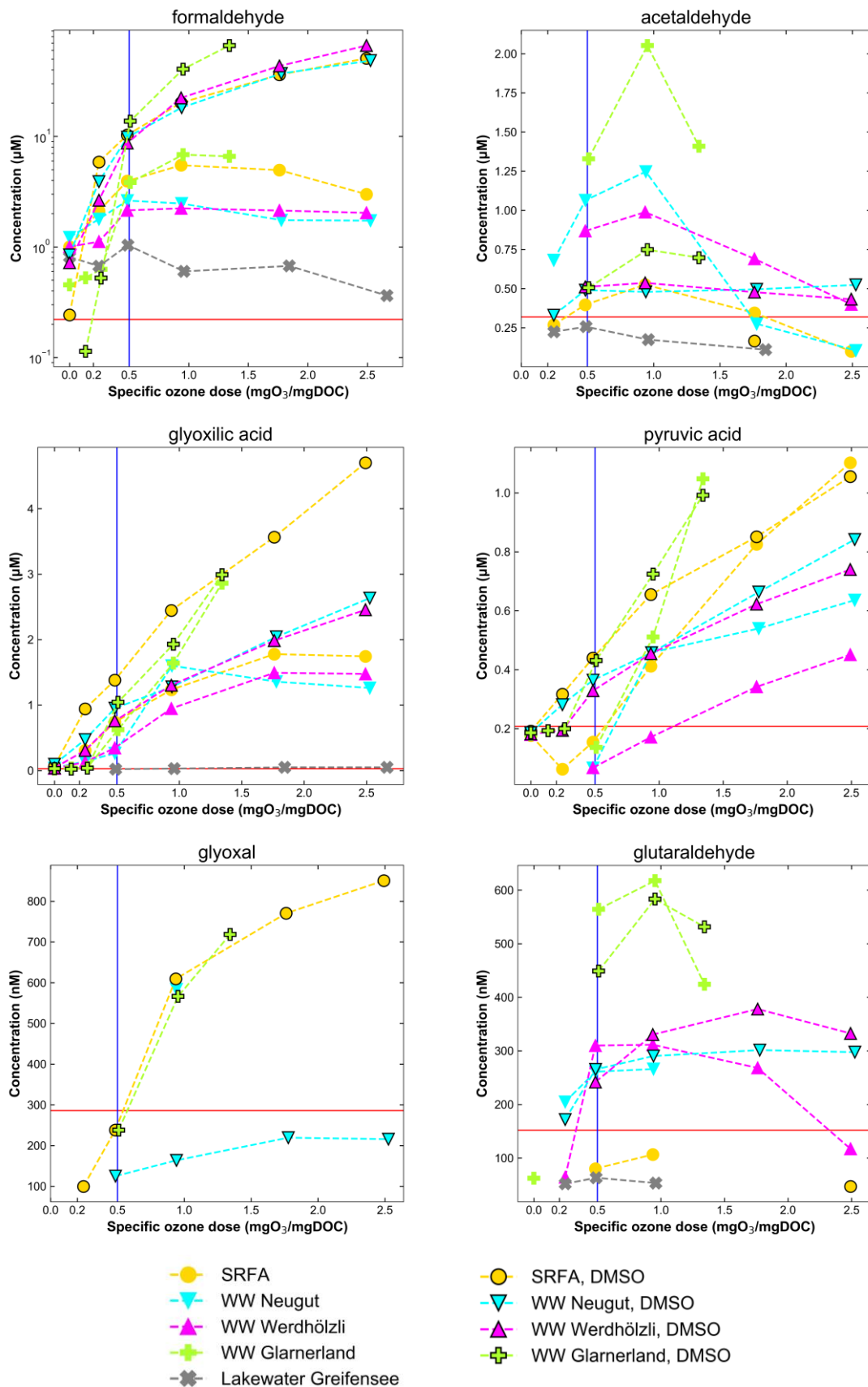


Figure 16. Quantification of formaldehyde, acetaldehyde, glyoxylic acid, pyruvic acid, glyoxal and glutaraldehyde in different ozonated water samples (without and with DMSO). The red horizontal line indicates the LOQ for each target carbonyl compound. The blue vertical line is drawn at a specific ozone dose of 0.5 mgO₃ / mgDOC, which is typically applied in WWTPs. The specific ozone dose (mgO₃ / mgDOC) is shown on the x-axis and the concentration on the y-axis (nM or μM). The y-axis for formaldehyde is presented in a logarithmic scale. Concentrations below the LODs are not shown.

Considerable amounts of formaldehyde, acetaldehyde, glyoxylic acid, pyruvic acid, glyoxal and glutaraldehyde were detected in the selected ozonated waters (Figure 16). The red horizontal lines (Figure 16) indicate the LOQs for each target carbonyl. Concentrations below the calculated LODs are not shown. The required average 80% micropollutant abatement in WWTPs is reached at around a specific ozone dose of 0.5 mgO₃/mgDOC (Bourgin et al., 2018). Therefore, a specific ozone dose of 0.5 mgO₃/mgDOC (blue vertical line in Figure 16) or doses in this range are typically applied for ozonation. At the WWTP Neugut, for example, a specific ozone dose of 0.33-0.5 mgO₃ / mgDOC is applied (Schachtler & Hubaux, 2016). The data displayed in Figure 16 refers to a measurement series containing 34 samples. In the SI (Section S.13) the quantified concentrations for formaldehyde, acetaldehyde, glyoxylic acid, pyruvic acid, glyoxal and glutaraldehyde are listed and their structures are shown. Concentrations above the LOD were also obtained for benzaldehyde and 1-acetyl-1-cyclohexen for some ozonated samples. However, the concentrations for benzaldehyde were all below the LOQ and concentrations for 1-acetyl-1-cyclohexene were mostly below the LOQ. All other target carbonyl compounds were not detected in the ozonated samples. In LW Lake Greifensee (without DMSO), much smaller carbonyl compound concentrations were measured compared to the WWs, likely because the DOC was lower (3.4 mg/L). Small concentrations of formaldehyde, acetaldehyde, glyoxylic acid and glutaraldehyde were found. However, only formaldehyde was contained at levels above the LOQ.

In the following, the quantified target carbonyl compounds are discussed for the different matrices and experimental conditions.

Formaldehyde The highest formaldehyde concentration that was found in an ozonated blank was 0.39 μM (ozone dose 5, with DMSO). As stated in Section 2.2.2, a slightly higher formaldehyde concentration of about 2 μM was expected in blanks containing DMSO (0.5 mM). The formaldehyde yield from the ozonolysis of DMSO was subtracted from the quantified amounts (blank correction was applied). Formaldehyde was already detected in most non-ozonated samples at low concentrations, up to 1.2 μM for WW Neugut (without DMSO). Formaldehyde concentrations were much higher in the ozonated samples with DMSO than without DMSO. Formaldehyde concentrations for OH radical scavenged samples (with DMSO) were between about 18-66 μM for specific ozone doses between 1-2.5 mgO₃ / mgDOC. In samples without DMSO, formaldehyde was contained in the few μM range. At a specific ozone dose of 0.5 mgO₃ / mgDOC (without DMSO) WW Glarnerland and SRFA contained the highest concentrations (about 3.8-3.9 μM; 114-117 μg/L) of formaldehyde among the different matrices. Overall, formaldehyde was formed at greater concentrations than the other target carbonyl compounds. Similarly, Wert et al., 2007 observed that formaldehyde was formed in higher amounts (up to 3.1 μM) than six other carbonyl compounds (among them acetaldehyde and glyoxal) during ozonation of WW. Wert et al., 2007 found that formaldehyde concentrations were high-

est, followed by glyoxal and lastly acetaldehyde. Furthermore, the authors attributed the formaldehyde formation mostly to OH radical exposure because O_3/H_2O_2 produced greater concentrations than O_3 . However, in this thesis smaller formaldehyde concentrations were detected when OH radicals were present (without DMSO) compared to when OH radicals were quenched.

Acetaldehyde Acetaldehyde concentrations were highest when a specific ozone dose of around $1 \text{ mgO}_3 / \text{mgDOC}$ was applied (without DMSO). At higher specific ozone doses, acetaldehyde was degraded again or other reaction pathways were favoured that lead to a lower acetaldehyde formation. In WW prior to ozonation, no acetaldehyde above the LOD concentration was detected. At a specific ozone dose of $0.5 \text{ mgO}_3 / \text{mgDOC}$ the following concentrations of acetaldehyde were detected: $1.3 \text{ }\mu\text{M}$ ($52 \text{ }\mu\text{g/L}$) in WW Glarnerland, $1.1 \text{ }\mu\text{M}$ ($44 \text{ }\mu\text{g/L}$) in WW Neugut, $0.87 \text{ }\mu\text{M}$ ($35 \text{ }\mu\text{g/L}$) in WW Werdhölzli and $0.4 \text{ }\mu\text{M}$ ($16 \text{ }\mu\text{g/L}$) in experiments with SRFA. In contrast to formaldehyde, acetaldehyde concentrations were higher when OH radicals were not scavenged during ozonation (without DMSO) (S10, SI). For WW Neugut, for example, $1.1 \text{ }\mu\text{M}$ (without DMSO) and $0.49 \text{ }\mu\text{M}$ (with DMSO) acetaldehyde were quantified when applying a specific ozone dose of around $0.5 \text{ mgO}_3/\text{mgDOC}$.

Glyoxylic acid and pyruvic acid For both glyoxylic acid and pyruvic acid, the quantified concentrations were slightly higher in the ozonated samples when DMSO was added as a scavenger. At a specific ozone dose of around $1 \text{ mgO}_3 / \text{mgDOC}$, concentrations in the range of $0.95\text{-}1.6 \text{ }\mu\text{M}$ (without DMSO) and $1.3\text{-}2.4 \text{ }\mu\text{M}$ (with DMSO) were obtained for glyoxylic acid in WWs and SRFA. At the same specific ozone dose, concentrations for pyruvic acid were in the range of $0.17\text{-}0.51 \text{ }\mu\text{M}$ (without DMSO) and $0.45\text{-}0.72$ (with DMSO) in WWs and SRFA. Hence, it is likely that precursors of glyoxylic acid and pyruvic acid follow slightly different reaction pathways when OH radicals are present, leading to a smaller product yield. Additionally, the ozone exposure changes when an OH scavenger is used (von Sonntag & von Gunten, 2012), which may have resulted in higher product formation in samples with DMSO. With increasing specific ozone doses, the concentrations of glyoxylic and pyruvic acid increased steadily. At a specific ozone dose of around $0.5 \text{ mgO}_3 / \text{mgDOC}$ (with DMSO) the highest concentrations were found in SRFA and WW Glarnerland, $1.4 \text{ }\mu\text{M}$ ($104 \text{ }\mu\text{g/L}$) and $1.0 \text{ }\mu\text{M}$ ($74 \text{ }\mu\text{g/L}$) for glyoxylic acid and $0.44 \text{ }\mu\text{M}$ ($39 \text{ }\mu\text{g/L}$) and $0.43 \text{ }\mu\text{M}$ ($38 \text{ }\mu\text{g/L}$) for pyruvic acid, respectively.

Glyoxal Glyoxal was found at concentrations above the LOQ for a specific ozone dose of around $1 \text{ mgO}_3 / \text{mgDOC}$ for WW Glarnerland ($0.61 \text{ }\mu\text{M}$; $35 \text{ }\mu\text{g/L}$) and SRFA ($0.57 \text{ }\mu\text{M}$; $33 \text{ }\mu\text{g/L}$), when DMSO was added as a scavenger. At this specific ozone dose, it was also detected in WW Neugut (with DMSO) below the LOQ. In Werdhölzli WW (with DMSO), however, no glyoxal was measured above the LOD at any specific ozone dose. In the absence of an OH radical scavenger (without DMSO), no glyoxal was measured above the LOD in all water samples (with one exception). The reason for this was unknown. Surprisingly, glyoxal was present in one water sample (without DMSO). $0.58 \text{ }\mu\text{M}$ glyoxal was quantified in WW Neugut (without DMSO) at a specific ozone dose of around $1 \text{ mgO}_3 / \text{mgDOC}$. Due to an error during sample preparation, the sample was derivatized freshly two days after ozonation was conducted. The ozonated sample had been stored in the dark in the refrigerator for the period

of these two days. This freshly derivatized WW Neugut sample (without DMSO) was analysed in LC-HRMS within a few hours, while the other samples were only measured after 1-2 days after derivatization during which they were stored at 4° C. Therefore, the question arises whether derivatized glyoxal (double derivatized) is indeed stable for more than a few hours. Although the stability of some derivatized carbonyl compounds over the period of five days was evaluated (Section 3.2.3), the stability of derivatized glyoxal could not be studied due to too low spiking levels of glyoxal. Further experiments are needed to test the stability of derivatized glyoxal.

Glutaraldehyde Glutaraldehyde was found at similar quantifiable levels with and without OH radical quenching in LW Lake Greifensee, WW Werdhölzli and WW Neugut. Thus, the presence of OH radicals did not influence the glutaraldehyde yield. The highest glutaraldehyde concentrations, 0.62 µM (62 µg/L, without DMSO) and 0.58 µM (58 µg/L, with DMSO), were observed for WW Glarnerland at a specific ozone dose of around 1 mgO₃/mgDOC. At very high ozone doses glutaraldehyde concentrations decreased again, similar to what was observed for acetaldehyde.

3.4.2 Identification of non-target carbonyl compounds

Overall, up to 70 carbonyl compounds were detected in the different ozonated water matrices, among them many unknown carbonyl compounds and some of the 16 selected target carbonyl compounds (Table 7). Table 7 shows the count of total compounds (including *N*-containing) for the different ozonated water samples (without DMSO and with DMSO). The identified In Table 6. Summaries of molecular formulas and retention times for carbonyl compounds (excluding *N*-containing) that were identified (using non-target workflow) in the different water matrices without OH radical scavenging (without DMSO) and with OH radical scavenging (with DMSO) are shown in Table 6 and in the SI Section S.14, respectively. Identified *N*-containing compounds are listed in the SI (Section S.17).

Here, the results for the ozonated samples without DMSO are discussed, as they are more relevant for real ozonation processes occurring in WWTPs. The highest number of unknown carbonyl compounds was found in WW Glarnerland (without DMSO) with a total of 70 carbonyl compounds, among which 18 carbonyl compounds were nitrogen-containing compounds. Isomers with the same molecular formula but different RTs were counted separately. WW Neugut (without DMSO) and WW Werdhölzli (without DMSO) contained a total of 40 and 45 different carbonyl compounds, respectively. Thus, the number of carbonyls after ozonation (without DMSO) were decreasing as follows: WW Glarnerland > WW Werdhölzli > WW Neugut.

In SRFA (without DMSO) and LW Greifensee (without DMSO), only three nitrogen-containing carbonyl compounds were detected, whereas in the ozonated WW samples (without DMSO) between 12 and 18 nitrogen-containing carbonyl compounds were detected (Table 7). Past research showed that in WW effluent organic matter samples, the dissolved organic nitrogen is present in higher concentrations than in natural organic matter such as SRFA or lake water (Nam & Amy, 2008). Also, considering the low nitrogen content in the elemental composition of SRFA (0.67% nitrogen), only a limited formation of nitrogen-containing carbonyl compounds can be expected.

Table 7. Count of total compounds (including *N*-containing) and *N*-containing results for the different ozonated water samples (without DMSO and with DMSO). ND (not determined) indicates that this value was not obtained.

		WW Neugut	WW Werdhölzli	WW Glarner- land	SRFA	LW Greifensee
Without DMSO	Total	40	45	70	37	21
	N containing	12	15	18	3	3
With DMSO	Total	36	41	43	31	ND
	N containing	9	13	10	3	ND

In the following section, a selection of unknown carbonyl molecular formulas will be discussed. The peak areas as a function of the specific ozone dose of eight unknown carbonyl compounds, which were formed in ozonated WW, LW and SRFA (without OH scavenging) and identified by non-target analysis, are shown in Figure 17. The peak areas were extracted using the software Trace Finder and were corrected using the internal standard benzaldehyde-d6-TSH. The blue vertical line (Figure 17) is drawn at a specific ozone dose of 0.5 mgO₃/mgDOC, which is typically applied for ozonation in WWTPs (Schachtler & Hubaux, 2016). The following sum formulas were assigned to the eight unknown carbonyl compounds: C₃H₂O, C₃H₂O₂, C₃H₅NO₂, C₄H₄O₂, C₄H₄O₃, C₄H₆O₃, C₅H₇NO₄. As an overall trend, an increase of peak areas was observed with an increasing specific ozone dose in all ozonated water samples. This further confirmed that these unknown carbonyl compounds were formed during ozonation. For some of the unknown carbonyl compounds a slight decrease in peak areas was observed at a very high specific ozone dose (about 2.5 mgO₃/mgDOC). All eight carbonyl compounds occurred in ozonated SRFA, the three different ozonated WWs and in ozonated LW Lake Greifensee. In LW Lake Greifensee they were less abundant probably due to a lower DOC concentration.

Liu et al., 2020 characterized carbonyl OBP during ozonation among other oxidation processes. The authors identified the three oxoacids 3-oxobutanoic acid (C₄H₆O₃), 3-methyl-2-oxobutanoic acid (C₅H₈O₃) and 9-oxononanoic acid (C₉H₁₆O₃) in treated drinking water. C₄H₆O₃ and C₅H₈O₃ were also identified using the non-target workflow presented in this thesis. C₄H₆O₃ was identified in all three ozonated WWs, ozonated LW Greifensee and SRFA, and in the ozonolysis of sorbic acid, acetylacetone, phenol, 4-ethylphenol and 4-methoxyphenol. Hence, C₄H₆O₃ (3-oxobutanoic acid) seems to be a very abundant OBP. C₅H₈O₃ was identified in ozonated WW Werdhölzli, WW Glarnerland and 4-ethylphenol. Unsaturated oxoacids are an important class of products in the ozonolysis of phenol and are formed by phenolic benzene ring opening (Tentscher et al., 2018). 3-oxobutanoic acid, 3-methyl-2-oxobutanoic acid and 9-oxononanoic acid are most likely derived from the cleavage of the phenyl ring in macromolecular phenols (Liu et al., 2020). This hypothesis is supported by the finding that both C₄H₆O₃ (3-oxobutanoic acid) and C₅H₈O₃ (3-methyl-2-oxobutanoic acid) were identified as products from the ozonation of phenolic compounds (in this thesis).

Remucal et al., 2020 provide molecular-level evidence for the selectivity of ozone as an oxidant within DOM. The authors established reactions between model compounds and ozone or OH radicals. These reactions were for example an addition of one to two oxygen atoms in reaction

with ozone or an addition of one oxygen atom and decarboxylation for reactions with OH radicals (Remucal et al., 2020). These reactions produced highly oxidized DOM with a O:C ratio > 1.0. Furthermore, Remucal et al., 2020 provide a table of ozonation products of DOM that were previously identified using target approaches. Several molecular formulas that were identified in this thesis were also mentioned on said table. The following identified carbonyls are thus likely to be found in ozonated WWS: glycolaldehyde (C₂H₄O₂), propanal/acetone (C₃H₆O), methylglyoxal (C₃H₄O₂), dimethylglyoxal/isomer of 2,3-butanedione (C₄H₆O₂), 5-ketohexanal (C₇H₁₂O₂).

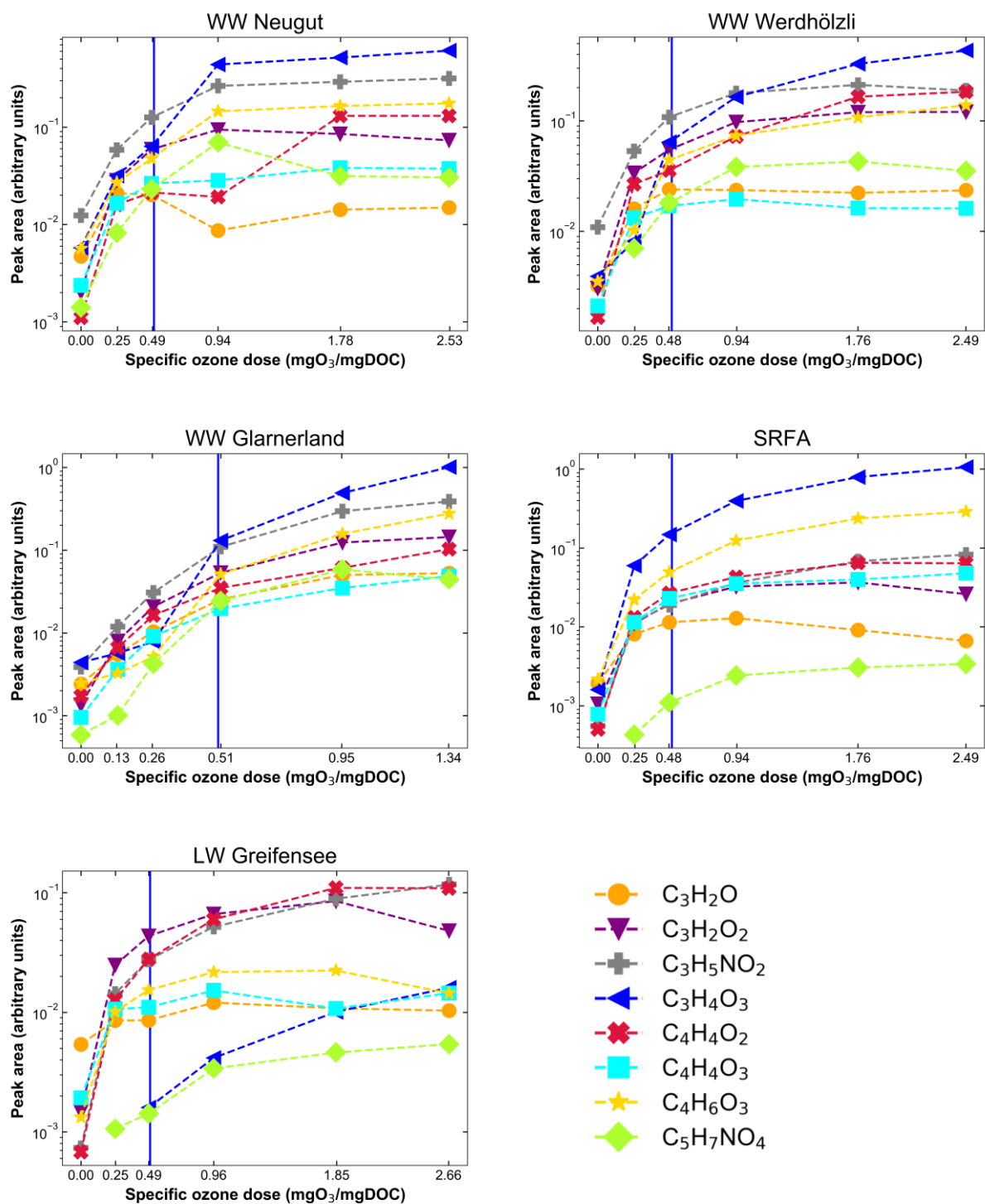


Figure 17. Peak areas (arbitrary units, y-axis) of eight carbonyl compounds that were identified in ozonated WW, LW and SRFA (without DMSO) as a function of the specific ozone dose (mgO₃/mgDOC, x-axis). The blue vertical line is drawn at a specific ozone dose of 0.5 mgO₃/mgDOC, which is typically applied in WWTPs.

3.5 Limitations

The contamination of the derivatizing agent TSH with carbonyl-TSH compounds such as formaldehyde-TSH, acetaldehyde-TSH, acetone-TSH, 3-pentanone-TSH and butyraldehyde-TSH was a major limitation to this method. Derivatized acetone, 3-pentanone and butyraldehyde could therefore not be quantified at concentrations relevant in WW. Derivatized formaldehyde and acetaldehyde could be quantified but relatively higher LOD and LOQs were obtained for these two target carbonyl compounds due to the contamination. Even a purification of the TSH product through recrystallization did not reduce this contamination.

Typically, all major fragments in the MS² spectra belonged to the derivatizing agent. These signature fragments were valuable for the identification of carbonyl compounds. However, the use of the MS² information for the structure elucidation was limited, as there were no characteristic fragments or neutral losses allowing to distinguish aldehydes, ketones and ketoacids from one another.

In this thesis, the pool of tentative structural candidates, which were considered for unknown carbonyls was compiled based on entries from the Pubchem database as well as by manual drawing. Comprehensive search for carbonyl compounds in chemical databases or manual drawing of tentative structures by hand for compounds with a high carbon atom number ($\geq C_5$) becomes very time intensive. Compiling of tentative structures was thus only feasible for small carbonyl compounds ($\leq C_4$) or double derivatized carbonyls, for which there is a relatively small number of tentative structures. Possible or probable structures of carbonyl compounds with high carbon atom number could only be assigned based on the precursor evaluation and the knowledge from the Criegee mechanism.

Due to a limited time for this master thesis and an elaborate, time-intensive method development, it was not possible to obtain replicates for the ozonated WW, LW and SRFA samples.

4. Conclusions and outlook

The derivatization of carbonyl compounds with the derivatizing agent TSH was optimized by using the following concentrations: 200 μ M of TSH, 0.02 M of HCl. A reaction time of 10 minutes to 2 hours at room temperature was sufficient for complete derivatization. All 16 target carbonyl compounds were detectable after derivatization when analysed LC-ESI-HRMS with positive ESI. Positive ESI was better suited than negative ESI for detection of the derivatized carbonyl compounds. 9 out of 16 target carbonyl compounds were only detectable after derivatization. Linear calibration ranges of the derivatized carbonyls could be established with LODs in the range of 2-96 nM and LOQs in the range of 5-320 nM. There was no analytical or procedural matrix effect observed. By using a TSH concentration of 200 μ M derivatization efficiencies between 82 and 105% were obtained in different water matrices (for benzaldehyde and cinnamaldehyde).

Formaldehyde, acetaldehyde, glyoxylic acid and pyruvic acid were observed at relatively high concentrations (total concentration of 3.7 - 6.3 μ M) after ozonation (0.5 mgO₃ / mgDOC) of different WWs (without quenching OH radicals). As a general trend, the formation of carbonyl

compounds increased when applying increasing ozone doses. By tracking signature fragments (m/z 139.0212, 155.0161 and 157.0318) originating from the TSH moiety of derivatized carbonyl compounds using a non-target workflow, many molecular formulas of unknown carbonyl compounds could be identified in ozonated WWs, LW and SRFA. The ozonation of precursors such as olefins, phenols and β -diketones provided further indications on the reaction pathways occurring during ozonation and facilitated the structure elucidation of unknown carbonyl compounds. Possible and probable structures (identification confidence levels 3 and 2b, respectively) could be assigned to some carbonyl compounds. Identified probable structures were 2-hydroxyacetaldehyde, 3-hydroxy-2-oxopropanal, 2-oxopropanedial, 2-hydroxypropanal, fumaraldehyde/malealdehyde, 4-oxohex-2-enoic acid, 2-ethylfumaraldehyde/2-ethylmalealdehyde, methyl-2-oxoacetate, 2,3-dioxopropanoic acid and ethenone. Moreover, several molecular formulas that were identified in this thesis were previously reported such as $C_2H_4O_2$, $C_4H_6O_3$, $C_5H_8O_3$ and $C_7H_{12}O_2$. This confirmed that the non-target workflow and the derivatization approach was working well, even though further quality assurance is needed. Over 40 different (including isomers) carbonyl compounds were detected in each analysed WW. The effectiveness of biological post-treatment after ozonation should thus be monitored in water treatment facilities.

As a next step, the commercially available probable structures and tentative candidates that were discussed in this thesis should be purchased, derivatized and analysed. In this way, a confirmed identification (confidence level 1) of these carbonyl compounds could be achieved (Schymanski et al., 2014). These confirmed carbonyl compounds could then become target compounds that may be quantified in WW and other matrices.

The optimal HCl concentration of 0.02 M and the stability of the derivatized carbonyl compounds should be confirmed for a derivatization with 200 μ M TSH and spiking of carbonyl compounds clearly above their determined LOQs. For example, the stability of double derivatized glyoxal over several days at 4 °C is still uncertain. Further, the ozonation experiments should be replicated to evaluate the repeatability and consolidate the available datasets.

The subtraction of $C_7H_8N_2OS$ and $C_{14}H_{16}N_4O_2S_2$ from the predicted composition formulas for single and double derivatized carbonyl compounds, respectively was done manually in excel. The non-target workflow could be further automated by elaborating and incorporating a scripting node dedicated for this effect using Compound Discoverer.

Moreover, it would be valuable to develop a tool that can provide a list of tentative structures (uncharged) that are possible for a molecular formula of a carbonyl compound. Additional filters could be incorporated that would allow for selection of linear compounds for example.

Additionally, it would be interesting to develop a method for the quantification of the total carbonyl compound content in WW. This could be achieved by adding a polymer-bound carbonyl to a sample after derivatization. The TSH excess that was added for derivatization would then be cleared away by reacting with the polymer-bound carbonyl compounds. By determining the sulphur content originating from TSH with ICP-MS (by establishing the difference of sulphur content before and after derivatization for example) the total carbonyl compounds concentration could be estimated. This estimation would be based on the assumption

that each carbonyl compound binds to one TSH molecule, neglecting that some dicarbonyls bind to two TSH molecules. Preliminary experiments with a polymer-bound carbonyl compound were conducted during this thesis. However, removal of the excess TSH from the derivatized sample was not successful in the aqueous phase. By using a mixed water and solvent matrix, a successful binding of the excess TSH to the polymer-bound carbonyl compounds might be achieved. Further investigation along this line are needed.

5. Acknowledgements

I would like to thank PhD candidate Joanna Houska, postdoctoral researcher Dr. Tarek Manasfi and Prof. Dr. Urs von Gunten for their great supervision of my master thesis. I thank Prof. Dr. Urs von Gunten for giving me the opportunity to do my master thesis in his research group. I very much thank all of my supervisors for the many inspiring discussions, their advice, critical input and support during my time at Eawag. I would also like to thank them for proofreading my master thesis. I especially thank Joanna Houska for her close supervision of my thesis, for always finding the time to answer my many questions and for supporting me with the ozonation experiments. I especially thank Dr. Tarek Manasfi for introducing me to the analytical software and for his advice regarding the experimental setup and the LC-ESI-HRMS measurements.

Furthermore, I want to thank Bernadette Vogler for introducing me to the LC-ESI-HRMS instrument and for helping me with troubleshooting. I would also like to thank Philipp Longree for his technical support. I thank Elisabeth Salhi for the introduction to the laboratory and Ursula Schönenberger for the introduction to the HPLC. I would like to thank Michael Patrick for the introduction to Trace Finder. I thank Dr. Jennifer Schollee for her support regarding the analysis of the fragments in the MS² data. Additionally, I would like to thank Franz Werder and Daniel Pellanda for their technical IT support and Claire Wedema for the administration. A big thank you to Dr. Samuel Derrer who synthesized cinnamaldehyde tosylhydrazone for me. Also, I would like to thank Joanna Houska and Dr. Samuel Derrer for attempting to purify the TSH chemical via recrystallization.

A big thank you goes to the whole Drinking Water Chemistry group lead by Prof. Dr. Urs von Gunten for the group discussions, lunch and coffee breaks, and for making my time at Eawag very enjoyable. A special thank you goes to Joanna Houska and Sung Eun Lim for the lovely teatime and encouraging words. I greatly appreciated the supportive, familiar and professional atmosphere in this group.

Lastly, I would also like to thank my friends and family for their great emotional support during the course of my thesis.

6. References

Publications

- Benigni, R., Conti, L., Crebelli, R., Rodomonte, A., & Vari, M. R. (2005). Simple and α,β -unsaturated aldehydes: Correct prediction of genotoxic activity through structure-activity relationship models. *Environmental and Molecular Mutagenesis*, 46(4), 268–280. <https://doi.org/10.1002/em.20158>
- Bourgin, M., Beck, B., Boehler, M., Borowska, E., Fleiner, J., Salhi, E., Teichler, R., von Gunten, U., Siegrist, H., & McArdell, C. S. (2018). Evaluation of a full-scale wastewater treatment plant upgraded with ozonation and biological post-treatments: Abatement of micropollutants, formation of transformation products and oxidation by-products. *Water Research*, 129, 486–498. <https://doi.org/10.1016/j.watres.2017.10.036>
- Buffle, M. O., Schumacher, J., Salhi, E., Jekel, M., & von Gunten, U. (2006). Measurement of the initial phase of ozone decomposition in water and wastewater by means of a continuous quench-flow system: Application to disinfection and pharmaceutical oxidation. *Water Research*, 40(9), 1884–1894. <https://doi.org/10.1016/j.watres.2006.02.026>
- Buxton, G. V., Dainton, F. (1968). The radiolysis of aqueous solutions of oxybromine compounds; the spectra and reactions of BrO and BrO₂. *Proceedings of the Royal Society of London. Series A. Mathematical and Physical Sciences*, 304(1479), 427–439. <https://doi.org/10.1098/rspa.1968.0095>
- Cal/EPA. (2010). *Drinking Water Notification Levels and Response Levels: An Overview*. 1–14. www.cdph.ca.gov/certlic/drinkingwater/Documents/Notificationlevels/notificationlevels.pdf
- Criegee, R. (1975). Mechanismus der Ozonolyse. *Angewandte Chemie - International Edition*, 87(21), 765–771.
- Eggen, R. I. L., Hollender, J., Joss, A., Schärer, M., & Stamm, C. (2014). Reducing the discharge of micropollutants in the aquatic environment: The benefits of upgrading wastewater treatment plants. *Environmental Science and Technology*, 48(14), 7683–7689. <https://doi.org/10.1021/es500907n>
- Emsley, J. (1984). The composition, structure and hydrogen bonding of the β -diketones. *Complex Chemistry*, 57, 147–191. <https://doi.org/10.1007/bfb0111456>
- Feron, V. J., Til, H. P., de Vrijer, F., Woutersen, R. A., Cassee, F. R., & van Bladeren, P. J. (1991). Aldehydes: occurrence, carcinogenic potential, mechanism of action and risk assessment. *Mutation Research/Genetic Toxicology*, 259(3–4), 363–385. [https://doi.org/10.1016/0165-1218\(91\)90128-9](https://doi.org/10.1016/0165-1218(91)90128-9)
- Flyunt, R., Leitzke, A., Mark, G., Mvula, E., Reisz, E., Schick, R., & Von Sonntag, C. (2003). Determination of $\cdot\text{OH}$, $\text{O}_2\cdot^-$, and hydroperoxide yields in ozone reactions in aqueous solution. *Journal of Physical Chemistry B*, 107(30), 7242–7253. <https://doi.org/10.1021/jp022455b>
- Leitzke, A., Reisz, E., Flyunt, R., & Von Sonntag, C. (2001). The reactions of ozone with cinnamic acids: Formation and decay of 2-hydroperoxy-2-hydroxyacetic acid. *Journal of the Chemical Society, Perkin Transactions 2*, 5, 793–797.

<https://doi.org/10.1039/b009327k>

- Liu, X., Liu, R., Zhu, B., Ruan, T., & Jiang, G. (2020). Characterization of Carbonyl Disinfection By-Products during Ozonation, Chlorination, and Chloramination of Dissolved Organic Matters. *Environmental Science and Technology*, *54*(4), 2218–2227. <https://doi.org/10.1021/acs.est.9b04875>
- Lopachin, R. M., Barber, D. S., & Gavin, T. (2008). Molecular mechanisms of the conjugated α,β -unsaturated carbonyl derivatives: Relevance to neurotoxicity and neurodegenerative diseases. *Toxicological Sciences*, *104*(2), 235–249. <https://doi.org/10.1093/toxsci/kfm301>
- Lopachin, R. M., & Gavin, T. (2014). Molecular mechanisms of aldehyde toxicity: A chemical perspective. *Chemical Research in Toxicology*, *27*(7), 1081–1091. <https://doi.org/10.1021/tx5001046>
- Lozada-Garcia, R. R., Ceponkus, J., Chin, W., Chevalier, M., & Crépin, C. (2011). Acetylacetone in hydrogen solids: IR signatures of the enol and keto tautomers and UV induced tautomerization. *Chemical Physics Letters*, *504*(4–6), 142–147. <https://doi.org/10.1016/j.cplett.2011.01.055>
- Marron, E. L., Prasse, C., Buren, J. Van, & Sedlak, D. L. (2020). Formation and Fate of Carbonyls in Potable Water Reuse Systems. *Environmental Science and Technology*. <https://doi.org/10.1021/acs.est.0c02793>
- Nam, S. N., & Amy, G. (2008). Differentiation of wastewater effluent organic matter (EfOM) from natural organic matter (NOM) using multiple analytical techniques. *Water Science and Technology*, *57*(7), 1009–1015. <https://doi.org/10.2166/wst.2008.165>
- Ramseier, M. K., & von Gunten, U. (2009). Mechanisms of phenol ozonation-kinetics of formation of primary and secondary reaction products. *Ozone: Science and Engineering*, *31*(3), 201–215. <https://doi.org/10.1080/01919510902740477>
- Remucal, C. K., Salhi, E., Walpen, N., & Von Gunten, U. (2020). Molecular-level transformation of dissolved organic matter during oxidation by ozone and hydroxyl radical. *Environmental Science and Technology*, *54*(16), 10351–10360. <https://doi.org/10.1021/acs.est.0c03052>
- Richardson, S. D., Caughran, T. V., Poiger, T., Guo, Y., & Gene Crumley, F. (2000). Application of DNPH derivatization with LC/MS to the identification of polar carbonyl disinfection by-products in drinking water. *Ozone: Science and Engineering*, *22*(6), 653–675. <https://doi.org/10.1080/01919510009408805>
- Roy, P. (2017). Computational Studies on the Keto-Enol Tautomerism of Acetylacetone. *International Research Journal of Natural Sciences*, *II*(June), 1–9.
- Schymanski, E. L., Jeon, J., Gulde, R., Fenner, K., Ruff, M., Singer, H. P., & Hollender, J. (2014). Identifying small molecules via high resolution mass spectrometry: Communicating confidence. *Environmental Science and Technology*, *48*(4), 2097–2098. <https://doi.org/10.1021/es5002105>
- Siegel, D., Meinema, A. C., Permentier, H., Hopfgartner, G., & Bischoff, R. (2014). Integrated quantification and identification of aldehydes and ketones in biological samples. *Analytical Chemistry*, *86*(10), 5089–5100. <https://doi.org/10.1021/ac500810r>

- Tentscher, P. R., Bourgin, M., & Von Gunten, U. (2018). Ozonation of Para -Substituted Phenolic Compounds Yields p -Benzoquinones, Other Cyclic α,β -Unsaturated Ketones, and Substituted Catechols. *Environmental Science and Technology*, 52(8), 4763–4773. <https://doi.org/10.1021/acs.est.8b00011>
- Tomkins, B. A., McMahon, J. M., Caldwell, W. M., & Wilson, D. L. (1989). Liquid chromatographic determination of total formaldehyde in drinking water. *Journal - Association of Official Analytical Chemists*, 72(5), 835–839. <https://doi.org/10.1093/jaoac/72.5.835>
- Von Gunten, U. (2018). Oxidation Processes in Water Treatment: Are We on Track? *Environmental Science and Technology*, 52(9), 5062–5075. <https://doi.org/10.1021/acs.est.8b00586>
- von Sonntag, C., & von Gunten, U. (2012). Chemistry of Ozone in Water and Wastewater Treatment: From Basic Principles to Applications. In *Chemistry of Ozone in Water and Wastewater Treatment: From Basic Principles to Applications*. <https://doi.org/10.2166/9781780400839>
- Weinberg, H. S., Glaze, W. H., Krasner, S. W., & Scilimenti, M. J. (1993). Formation and removal of aldehydes in plants that use ozonation. *Journal / American Water Works Association*, 85(5), 72–85. <https://doi.org/10.1002/j.1551-8833.1993.tb05988.x>
- Wert, E. C., Rosario-Ortiz, F. L., Drury, D. D., & Snyder, S. A. (2007). Formation of oxidation byproducts from ozonation of wastewater. *Water Research*, 41(7), 1481–1490. <https://doi.org/10.1016/j.watres.2007.01.020>
- Yurkova, I. L., Schuchmann, H. P., & Von Sonntag, C. (1999). Production of OH radicals in the autoxidation of the Fe(II)-EDTA system. *Journal of the Chemical Society. Perkin Transactions 2*, 10, 2049–2052. <https://doi.org/10.1039/a904739e>

Website and PDF sources

- Abwasserverband Glarnerland (2020). *Zahlen und Fakten*. Retrieved December 28, 2020, from <http://avglarnerland.ch/anlage/zahlen-fakten/>
- ARANEugut (2020). *ARANEugut*. Retrieved December 28, 2020, from <http://www.neugut.ch/index.php/1/Home>
- Encyclopaedia Britannica (2019, November 28). *Urea*. Retrieved January 10, 2020, from <https://www.britannica.com/science/urea>
- Micropoll (2019, December). *Ozonung Klärwerk Werdhölzli, Zürich* [PDF file]. Retrieved December 28, 2020, from https://micropoll.ch/wp-content/uploads/2020/06/2019_VSA_S_Projektsteckbrief-ARA-Werdh%C3%B6lz_d.pdf
- Schachtler, M., Hubaux, N. (2016, March). *Switzerland's first facility for the removal of micropollutants* [PDF file]. ARANEugut. Retrieved December 28, 2020, from http://www.neugut.ch/scms/upload/Text/Ozonung/ARA_Factsheet_EN_01.pdf

Stadt Zürich (2020). *Werdhölzli*. Retrieved December 28, 2020, from https://www.stadt-zuerich.ch/ted/de/index/entsorgung_recycling/sauberer_wasser/klaerwerk/werdhoelzli.html

Swisswater AG (2020). *Stadt Zürich, ARA Werdhölzli*. Retrieved December 28, 2020, from <https://www.swisswater.ch/referenzen/schweiz/ara-werdhoelzli>

Supporting Information (SI)

Section S.1 Abbreviations

ACN: Acetonitrile

AGC: Automatic gain control

DOM: Dissolved organic matter

DMSO: Dimethylsulfoxide

DNPH: 2,4-Dinitrophenylhydrazine

FA: Formic acid

LC-ESI-HRMS: Liquid chromatography coupled to electrospray ionization high-resolution mass spectrometry

LOD: Limit of detection

LOQ: Limit of quantification

LW: Lakewater

MeOH: Methanol

m/z: Mass-to-charge ratio

NCE: Normalized collision energy

OBP: Ozonation byproducts

OTP: Ozonation transformation products

RT: Retention time

TSH: *p*-toluenesulfonylhydrazine

US EPA: United States Environmental Protection Agency

WPA: Waters Protection Act

WW: Wastewater

WWTP: Wastewater treatment plant

R²: Coefficient of determination

SI: Supporting Information

Section S.2 Impurities in TSH chemical

The derivatizing agent *p*-toluenesulfonylhydrazide was only available at 97% purity. It contained several impurities, among them also carbonyl-TSH hydrazones. Initially, acetone, butyraldehyde and 3-pentanone were also selected as target carbonyl compounds. Unfortunately, peaks for acetone, butyraldehyde and 3-pentanone after derivatization were detected in blanks at peak areas in the order of magnitude of 10⁸-10⁹ when using 200 μM TSH for derivatization. Concentrations in the different water matrices (e.g. ozonated WW) were not high enough for these compounds to be considerably above the concentration levels of the impurities in the blanks. Thus, these compounds were excluded from the list of target carbonyl compounds due to difficulties in quantification stemming from the blank contamination. There was also a considerable contamination with formaldehyde-TSH hydrazone and acetaldehyde-TSH hydrazone

in the blanks. However, formaldehyde and acetaldehyde were contained at high enough levels in the different water matrices, so that a linear calibration and quantification could be achieved in the relevant concentration range. Peak areas for the other target carbonyls after derivatization were negligible or undetectable in the blanks. Several factors were tested to gain insight into the source of this blank contamination: (i) replacing NP water with LC/MS grade water for sample preparation, (ii) enhanced rinsing of the glassware (four times with NP water and then four times with ACN), (iii) fresh preparation of the HCl stock solution in LC/MS grade water, (iv) fresh preparation of the TSH stock solution (directly from the solid chemical by weighing in), (v) fresh preparation of the TSH stock solution (directly from the solid chemical by weighing in) in a different laboratory hood to avoid contamination from air, (vi) fresh preparation of the TSH stock solution (directly from the solid chemical by weighing in) in NP water or MeOH instead of ACN, (vii) replacing FA in the eluents with acetic acid, (viii) replacing the column (already used with dirty matrices) with a new clean column. All these measures did not lead to a reduction in blank contamination with carbonyl-TSH hydrazones. Furthermore, an increase in blank contamination was observed with an increasing TSH concentration used. This leads to the hypothesis that the contamination was coming from the solid TSH chemical itself. The increase of contamination with acetaldehyde-, acetone-, butyraldehyde-, formaldehyde- and 3-pentanone-TSH hydrazones as a function of increasing TSH concentrations spiked to blanks (NP water) is depicted in Figure S.1.

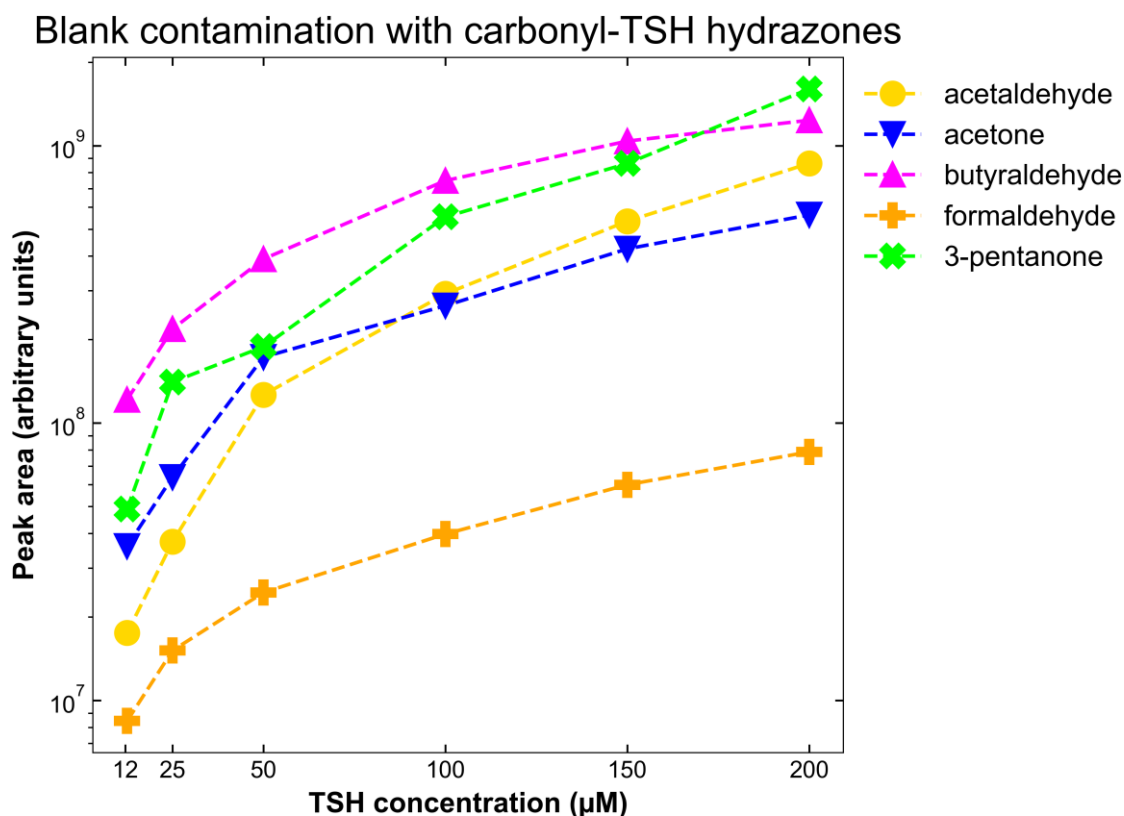


Figure S.1. Contamination with acetaldehyde-, acetone-, butyraldehyde-, formaldehyde- and 3-pentanone-TSH hydrazones as a function of increasing TSH concentrations (µM) spiked to blanks (NP water).

Section S.3 Volumes of ozone stock solution spiked to different water matrices

Table S.1. Volumes (μL) of ozone stock solution (1.69 mM) spiked to different water matrices.

Matrix	Spiked ozone stock solution (μL)					
	Dose 0	Dose 1	Dose 2	Dose 3	Dose 4	Dose 5
SRFA	0	260	510	1020	2040	3060
WW Neugut	0	230	470	940	1870	2810
WW Werdhölzli	0	260	510	1020	2040	3060
WW Glarnerland	0	280	560	1110	2220	3330
LW Greifensee	0	160	320	630	1260	1890

Section S.4 Linearity ranges, limits of detection and quantification

The method for the determination of the linearity ranges, LODs and LOQs is described in section 2.5.1. The results are presented here. R^2 values higher than 0.995 were obtained for all target carbonyl compounds with the exception of glyoxylic acid when applying the criteria for the selection of the linearity range and are shown in Table S.2. For glyoxylic acid a linear calibration range between 15-750 nM with an R^2 value of 0.9999 was established based on four data points. When additional higher calibration points were included, the R^2 value decreased to below 0.995, thus not fulfilling the criteria for linearity. Since relatively high concentrations of glyoxylic acid were expected in ozonated WW (based on preliminary laboratory tests), a second linear calibration range (75-2250 nM) was defined for quantification of higher concentrations of glyoxylic acid with an R^2 value of 0.9977. Moreover, concentrations for glyoxylic acid were extrapolated for two data points at concentrations >2250 nM. For formaldehyde two calibration ranges were established as well (0.05-3 and 3-50 μM). The lower calibration range was linear, and for the upper calibration range (3-50 μM) an exponential function was used.

The linearity ranges, LODs (nM and $\mu\text{g/L}$) and LOQs (nM and $\mu\text{g/L}$) are shown in Table S.2. The LODs of the target carbonyl compounds were below 10 nM with a few exceptions: formaldehyde (66 nM), acetaldehyde (96 nM), glutaraldehyde (46 nM), glyoxal (86 nM) and pyruvic acid (62 nM). The LOQs were between 150 and 320 nM for formaldehyde, acetaldehyde, glutaraldehyde, glyoxal and pyruvic acid. The LOQs for the rest of the target carbonyl compounds were below 32 nM.

Table S.2. R², LODs, LOQs and linearity ranges for all target carbonyl compounds.

Target carbonyl compound	R ²	LOD (nM)	LOD (ug/L)	LOQ (nM)	LOQ (ug/L)	Range (nM)	Range (ug/L)
Formaldehyde	0.9984	66	2.0	220	6.6	50-3000	1.5-90
Acetaldehyde	0.9967	96	4.2	320	14.1	50-3000	2.2-132
Decanal	0.9985	5	0.8	16	2.5	0.1-250	0.016-39
Benzaldehyde	0.9986	5	0.5	16	1.7	0.1-250	0.011-27
Indole-3-carboxy-aldehyde	0.9983	3	0.4	11	1.6	0.05-150	0.0073-22
4-Hydroxy-2-methoxybenzaldehyde	0.9965	8	1.2	25	3.8	0.1-250	0.015-38
Crotonaldehyde	0.9992	2	0.1	5	0.4	0.1-75	0.0070-5.3
Cinnamaldehyde	0.9998	2	0.3	6	0.8	0.1-250	0.013-33
Methacrolein	0.9997	2	0.1	7	0.5	0.05-250	0.0035-18
Cyclopentanone	0.9987	4	0.3	14	1.2	0.05-250	0.004-21
1-Acetyl-1-cyclohexen	0.9978	5	0.6	17	2.1	0.1-200	0.012-25
3,5-Heptanedione	0.9970	10	1.3	32	4.1	25-200	3.2-26
Glyoxal	0.9974	86	5.0	290	16.6	50-3000	2.9-174
Glutaraldehyde	0.9957	46	4.6	150	15.2	150-750	15-75
Glyoxylic acid	0.9999	8	0.6	27	2.0	15-750	1.1-56
Pyruvic acid	0.9958	62	5.5	210	18.2	250-1000	22-88

Section S.5 Analytical matrix effects

The approach and equation for the calculation of the analytical matrix effect (without the influence of derivatization efficiencies) are described in section 2.5.2. The results are presented here. A matrix effect of 100% would be obtained in an ideal situation were there is absolutely no ion suppression or enhancement due to the matrix constituents in a sample. The calculated analytical matrix effects were 106-108% and 112-117% for ozonated and non-ozonated water matrices respectively (Table S.3). Thus, there was no considerable analytical matrix effect in terms of ion suppression or enhancement for benzaldehyde- and cinnamaldehyde-TSH hydrazones. Due to the partial structural similarity among derivatized carbonyl compounds it was assumed that other carbonyl-TSH hydrazones would behave in a similar manner. Furthermore, it was assumed that experiments with other WWs would lead to similar results. Siegel et al., 2014 evaluated matrix effects for carbonyl compounds derivatized with TSH in biological samples with a different approach. They computed matrix effects of around 100% for cinnamaldehyde (103 ± 5), glyoxal (100 ± 5), glyoxylic acid (112 ± 10) and pyruvic acid (93 ± 11). This further supports the assumption that analytical matrix effects for carbonyl compounds derivatized with TSH are negligible.

Table S.3. Analytical matrix effects (%) for benzaldehyde- and cinnamaldehyde-TSH hydrazones in different water matrices.

Matrix	Analytical matrix effects (%)	
	Benzaldehyde-TSH hydrazone	Cinnamaldehyde-TSH hydrazone
SRFA	113	112
Ozonated SRFA	107	106
WW Neugut	117	115
Ozonated WW Neugut	108	108

Section S.6 Stability of derivatized carbonyl compounds

The method for the determination of the linearity ranges, LODs and LOQs is described in section 2.5.3. The results are presented here. Some derivatized carbonyl compounds (decanal, crotonaldehyde, 3,5-heptanedione) showed a decrease or increase in peak area over the time period of 5 days, during which the sample was stored at 4 °C in the autosampler (Figure S.2). Decanal and crotonaldehyde that were derivatized showed a decrease in peak area over time (-69% and -57% of the initial value respectively), whereas derivatized 3,5-heptanedione showed an increase over time (+242% of the initial value). However, for most derivatized carbonyl compounds the peak areas remained stable for a typical period of a measurement series. Considering the peak areas for derivatized formaldehyde, glutaraldehyde and 1-acetyl-1-cyclohexene for example, some variability between the days with no clear trend (40 - 50% decrease from the biggest to smallest peak area) could be detected. Overall, most derivatized carbonyl compounds were stable but some were not so much. Therefore, samples were analysed as quickly as possible. The stability of derivatized glyoxal, glyoxylic acid and pyruvic acid could not be determined because of too low levels of spiking for these carbonyl compounds.

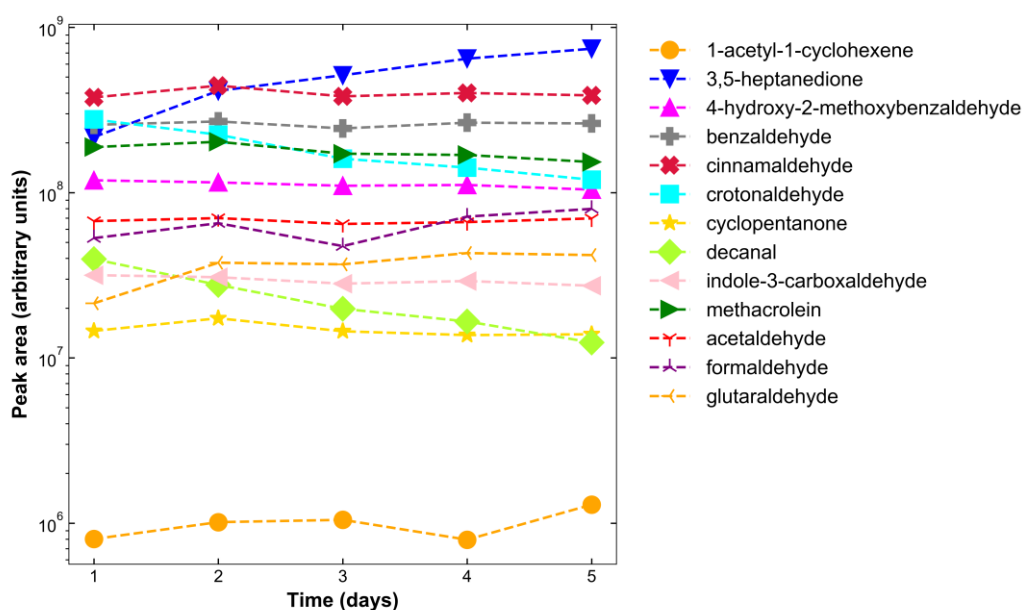


Figure S.2. Stability of 13 derivatized target carbonyl compounds in a sample stored at 4 °C in the autosampler that was analysed every day during a measurement series of five days.

Section S.7 Repeatability of internal standard spiking

The relative standard deviation of peak areas of the internal standards benzaldehyde-d6 (derivatized) and tramadol-d6 was calculated based on peak areas in 65 samples that were spiked with benzaldehyde-d6 (100nM) and tramadol-d6 (32.7 nM) and derivatized with 200 μ M TSH and 0.02 M HCl. The samples were measured over the course of 5 days and contained different (ozonated and non-ozonated) WW, LW and SRFA samples (with and without DMSO). The relative standard deviation for benzaldehyde-d6 and tramadol-d6 were 6% and 7%, respectively. The highest peak area was 1.37-fold and 1.39-fold higher than the smallest peak area for benzaldehyde-d6 and tramadol-d6, respectively.

Section S.8 Dilution factors applied for correction for quantification of target carbonyl compounds

Dilution factors were applied for correction of the calculated concentrations of target carbonyl compounds in the different water matrices to correct for dilution from (i) spiking of TSH and HCl stock solutions to the samples and (ii) spiking of ozone stock solution to the samples. The dilution factor for spiking of TSH (200 μ M) and HCl (0.02 M) stock solutions was 1.103 for all derivatized samples. The dilution factor for spiking of specific ozone doses to the different water matrices is shown in Table S.4.

Table S.4. Dilution factor for correction of concentrations of target carbonyls in different water matrices that were spiked with specific ozone doses.

Matrix	Dilution factors for spiking of specific ozone doses					
	Dose 0	Dose 1	Dose 2	Dose 3	Dose 4	Dose 5
SRFA	1.000	1.017	1.034	1.068	1.136	1.204
WW Neugut	1.000	1.016	1.032	1.062	1.125	1.187
WW Werdhölzli	1.000	1.017	1.034	1.068	1.136	1.204
WW Glarnerland	1.000	1.019	1.037	1.074	1.148	1.222
LW Greifensee	1.000	1.010	1.021	1.042	1.084	1.126

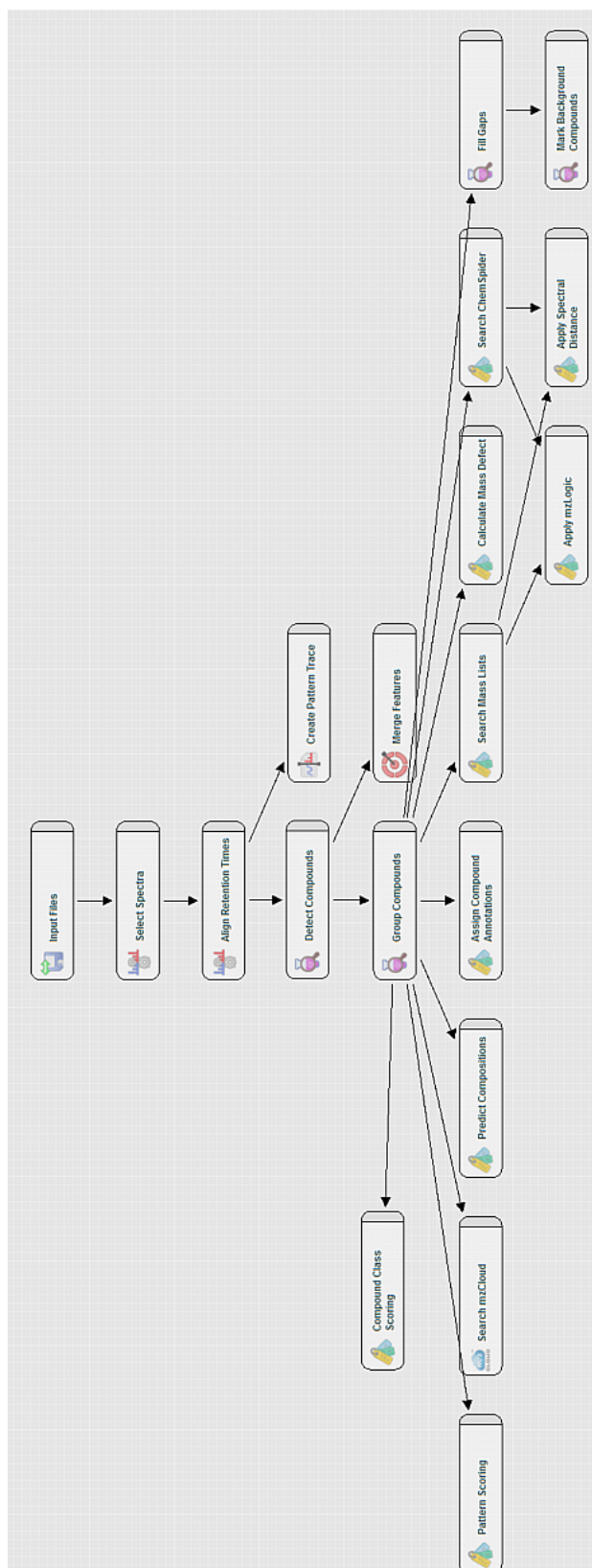
Section S.9 Applied ozone doses for ozonation of carbonyl precursors

Table S.5. Spiked volumes (theoretical values) (μ L) of ozone stock solution (1.59 mM), applied ozone doses (theoretical) (μ M), actual ozone doses in samples (μ M) and molar ratio ozone to compound spiking.

Ozone dose (theoretical) (μM)	25	50	100	200	300
Molar ratio ozone to compound	0.5	1	2	4	6
Ozone spiking (theoretical) (μL)	78	157	314	628	941
Actual ozone dose in sample (μM)	25	49	94	178	253

Section S.10 Compound Discoverer workflow

The Compound Discoverer workflow was based on the pre-defined workflow template “Untargeted environmental research ID workflow with statistics: Detect and identify unknown compounds with differential analysis” (Figure S.3) to which a few adaptations were made (Table S.6).



Description: Performs retention time alignment, unknown compound detection, and compound grouping across all samples. Predicts elemental compositions for all compounds, and hides chemical background (using Blank samples). Identifies compounds using mzCloud (ddMS² and/or DIA), ChemSpider (exact mass or formula) and local database searches against Mass Lists (exact mass with or without RT). Performs spectral similarity search against mzCloud for compounds with ddMS². Creates pattern trace from defined isotopic pattern. Flags compounds matching specified isotopic pattern by the Pattern Scoring node. Applies mzLogic to rank order structure candidates from ChemSpider and mass list matches. Applies spectral distance scoring to mass list and ChemSpider matches. Generates mass defect values in the Compounds table based on selected mass defect type (Kendrick for identifying polymers). Fill gaps by redetecting the peaks by the Fill Gaps node. Performs differential analysis on detected compounds.

Figure S.3. Nodes and description of pre-defined Compound Discoverer workflow template “Untargeted environmental research ID workflow with statistics: Detect and identify unknown compounds with differential analysis”.

Table S.6. Modifications to pre-defined workflow from Compound Discoverer

Predict Compositions	Compound Class Scoring
1. Prediction Settings	Compound Classes: Fragments with exact masses of 139.0212, 155.0161 and 157.0318 Da (Figure 4).
Max. Element Counts: C90 H190 N10 O18 S5	S/N Threshold: 5
Min. Element Counts: C8 H10 N2 O S	

Section S.11 Input files, grouping and ratios in Compound Discoverer

Sample	File	Sample Identifier	Sample Type	Treatment
S1	F1	20200919_B2	Sample	Blank_MQ
S2	F2	20200919_MQ1	Blank	MQ
S3	F3	20200923_M0	Sample	N_blank
S4	F4	20200923_M0+	Sample	N_blank_p
S5	F5	20200923_M1+	Sample	O_blank_p
S6	F6	20200923_M2+	Sample	O_blank_p
S7	F7	20200923_M3	Sample	O_blank
S8	F8	20200923_M3+	Sample	O_blank_p
S9	F9	20200923_M4+	Sample	O_blank_p
S10	F10	20200923_M5+	Sample	O_blank_p
S11	F11	20200923_S0	Sample	N_SRFA
S12	F12	20200923_S0+	Sample	N_SRFA_p
S13	F13	20200923_S1	Sample	O_SRFA
S14	F14	20200923_S1+	Sample	O_blank_p
S15	F15	20200923_S2	Sample	O_SRFA
S16	F16	20200923_S2+	Sample	O_SRFA_p
S17	F17	20200923_S3	Sample	O_SRFA
S18	F18	20200923_S3+	Sample	O_SRFA_p
S19	F19	20200923_S4	Sample	O_SRFA
S20	F20	20200923_S4+	Sample	O_SRFA_p
S21	F21	20200923_S5	Sample	O_SRFA
S22	F22	20200923_S5+	Sample	O_SRFA_p
S23	F23	20200926_S0_under	Sample	Under_N_SRFA
S24	F24	20200926_S3_under	Sample	Under_O_SRFA

Figure S.4. Input files, sample type and treatment for analysis of SRFA (exemplary) samples in Compound Discoverer analysis.

Samples:

S1: NP water (derivatized), TSH (200 μ M) and HCl (0.02 M)

S2: NP water only

S3: Derivatized NP water (non-ozonated) with phosphate buffer

S4: Derivatized NP water (non-ozonated) with phosphate buffer and DMSO

S7: Derivatized NP water (ozonated at middle specific ozone dose) with phosphate buffer

S5/S6/S8/S9/S10: Derivatized NP water (ozonated at different specific ozone doses) with phosphate buffer and DMSO

S11: Derivatized SRFA (non-ozonated) with phosphate buffer

S12: Derivatized SRFA (non-ozonated) with phosphate buffer and DMSO

S13/S15/S17/S19/S21: Derivatized SRFA (ozonated at different specific ozone doses) with phosphate buffer

S14/S16/S18/S20/S22: Derivatized SRFA (ozonated at different specific ozone doses) with phosphate buffer and DMSO

S23: Underivatized SRFA (non-ozonated) with phosphate buffer

S24: Underivatized SRFA (ozonated at middle specific ozone dose) with phosphate buffer

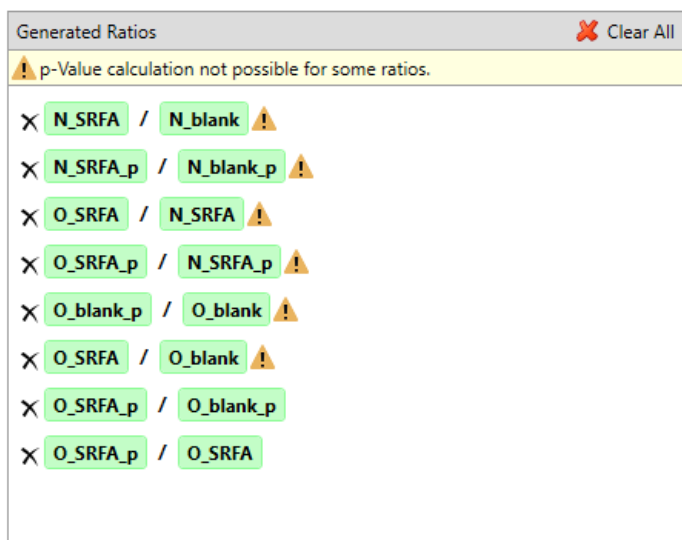


Figure S.5. Generated ratios for treatments in Compound Discoverer analysis.

Section S.12 Influence of TSH concentration on derivatization efficiencies in different water matrices

Benzaldehyde, cinnamaldehyde, 1-acetyl-acetone, 3-5-heptanedione, 4-hydroxy-2-methoxybenzaldehyde and cyclopentanone were spiked at a concentration of 100nM each. The plots for decanal, methacrolein and indole-3-carboxaldehyde look similar. Tramadol-d6 was not spiked to the samples and thus no internal standard correction could be applied. For formaldehyde and acetaldehyde spiking levels were not high enough for peak detection. For glutaraldehyde, crotonaldehyde, pyruvic acid, glyoxal and glyoxilic acid some decreases in peak areas were observed at high TSH concentrations in the SRFA and WW Neugut samples.

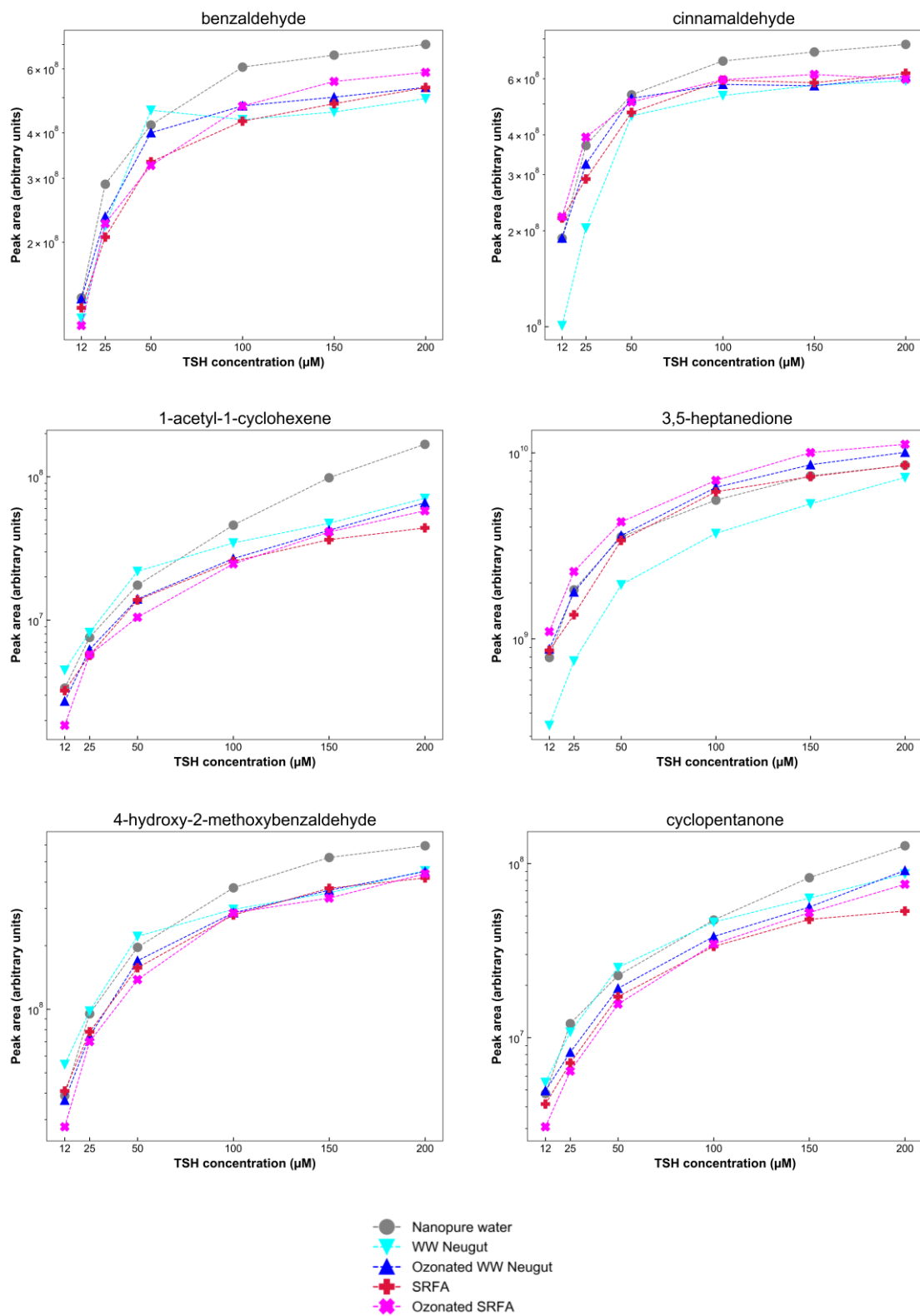


Figure S.6. Influence of TSH concentration on the derivatization efficiencies of several target carbonyl compounds in different water matrices.

Section S.13 Quantified concentrations of target carbonyl compounds in different water matrices

Table S.7. Quantified formaldehyde concentrations (μM) in different water matrices.

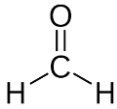
Formaldehyde							
		Specific ozone dose					
		Dose 0	Dose 1	Dose 2	Dose 3	Dose 4	Dose 5
Matrix	DMSO	Formaldehyde concentration (μM)					
SRFA	no	1.0	2.1	3.9	5.5	5.0	3.0
	yes	0.24	5.9	10.3	20.2	36.1	50.9
WW Neugut	no	1.2	1.8	2.6	2.5	1.7	1.7
	yes	0.84	3.9	9.8	18.2	37.1	48.5
WW Werdhölzli	no	1.0	1.1	2.1	2.2	2.1	2.0
	yes	0.72	2.6	8.7	22.3	43.4	66.4
WW Glarnerland	no	0.45	0.53	0.63	3.8	6.8	6.6
	yes	<LOD	0.11	0.52	13.7	40.6	66.4
Greifensee	no	0.81	0.67	1.0	0.60	0.67	0.36

Table S.8. Quantified acetaldehyde concentrations (μM) in different water matrices.

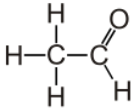
Acetaldehyde							
		Specific ozone dose					
		Dose 0	Dose 1	Dose 2	Dose 3	Dose 4	Dose 5
Matrix	DMSO	Acetaldehyde concentration (μM)					
SRFA	no	<LOD	0.27	0.40	0.53	0.35	0.10
	yes	<LOD	<LOD	<LOD	<LOD	0.16	<LOD
WW Neugut	no	<LOD	0.68	1.1	1.2	0.28	0.11
	yes	<LOD	0.33	0.49	0.48	0.50	0.52
WW Werdhölzli	no	<LOD	<LOD	0.87	0.99	0.69	0.40
	yes	<LOD	<LOD	0.51	0.54	0.48	0.43
WW Glarnerland	no	<LOD	<LOD	<LOD	1.3	2.1	1.4
	yes	<LOD	<LOD	<LOD	0.51	0.75	0.70
Greifensee	no	<LOD	0.22	0.26	0.17	0.11	<LOD

Table S.9. Quantified glyoxylic acid concentrations (μM) in different water matrices.

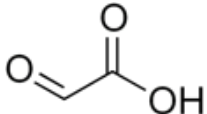
		Specific ozone dose					
		Dose 0	Dose 1	Dose 2	Dose 3	Dose 4	Dose 5
Glyoxylic acid							
Matrix	DMSO	Glyoxylic acid concentration (μM)					
SRFA	no	<LOD	0.31	0.74	1.2	1.8	1.7
	yes	0.068	0.94	1.4	2.4	3.6	4.7
WW Neugut	no	0.037	0.14	0.26	1.6	1.4	1.3
	yes	0.095	0.47	0.95	1.3	2.0	2.6
WW Werdhölzli	no	0.032	0.13	0.35	0.95	1.5	1.5
	yes	0.041	0.31	0.76	1.3	2.0	2.5
WW Glarnerland	no	0.023	0.038	0.045	0.62	1.6	2.9
	yes	0.029	0.021	0.035	1.0	1.9	3.0
Greifensee	no	<LOD	<LOD	0.022	0.031	0.050	0.049

Table S.10. Quantified pyruvic acid concentrations (μM) in different water matrices.

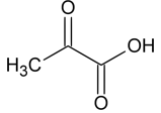
		Specific ozone dose					
		Dose 0	Dose 1	Dose 2	Dose 3	Dose 4	Dose 5
Pyruvic acid							
Matrix	DMSO	Pyruvic acid concentration (μM)					
SRFA	no	0.18	0.062	0.15	0.41	0.83	1.1
	yes	0.19	0.32	0.44	0.66	0.85	1.1
WW Neugut	no	0.18	<LOD	0.066	0.46	0.54	0.64
	yes	0.19	0.28	0.27	0.46	0.66	0.84
WW Werdhölzli	no	0.18	<LOD	0.067	0.17	0.34	0.45
	yes	0.18	0.19	0.33	0.45	0.62	0.74
WW Glarnerland	no	0.18	<LOD	<LOD	0.14	0.51	1.0
	yes	0.19	0.19	0.20	0.43	0.72	0.99
Greifensee	no	<LOD	<LOD	<LOD	<LOD	<LOD	<LOD

Table S.11. Quantified glyoxal concentrations (nM) in different water matrices.

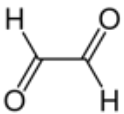
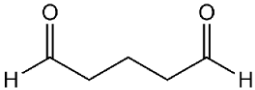
		<div style="text-align: center;">  </div>					
		Specific ozone dose					
		Dose 0	Dose 1	Dose 2	Dose 3	Dose 4	Dose 5
Matrix	DMSO	Glyoxal concentration (nM)					
SRFA	no	<LOD	<LOD	<LOD	<LOD	<LOD	<LOD
	yes	<LOD	100	240	610	770	850
WW Neugut	no	<LOD	<LOD	<LOD	580	<LOD	<LOD
	yes	<LOD	<LOD	130	160	220	220
WW Werdhölzli	no	<LOD	<LOD	<LOD	<LOD	<LOD	<LOD
	yes	<LOD	<LOD	<LOD	<LOD	<LOD	<LOD
WW Glarnerland	no	<LOD	<LOD	<LOD	<LOD	<LOD	<LOD
	yes	<LOD	<LOD	<LOD	240	570	720
Greifensee	no	<LOD	<LOD	<LOD	<LOD	<LOD	<LOD

Table S.12. Quantified glutaraldehyde concentrations (nM) in different water matrices.

		<div style="text-align: center;">  </div>					
		Specific ozone dose					
		Dose 0	Dose 1	Dose 2	Dose 3	Dose 4	Dose 5
Matrix	DMSO	Glutaraldehyde concentration (nM)					
SRFA	no	<LOD	<LOD	80	110	<LOD	<LOD
	yes	<LOD	<LOD	<LOD	<LOD	<LOD	47
WW Neugut	no	<LOD	210	260	270	<LOD	<LOD
	yes	<LOD	170	270	290	300	300
WW Werdhölzli	no	<LOD	64	310	310	270	120
	yes	<LOD	<LOD	240	330	380	330
WW Glarnerland	no	62	<LOD	<LOD	560	620	420
	yes	<LOD	<LOD	<LOD	450	580	530
Greifensee	no	<LOD	52	63	53	<LOD	<LOD

Section S.14 Identified (using non-target workflow) carbonyl compounds in different ozonated waters with OH radical scavenging

Table S.13. Summary of molecular formulas and retention times for carbonyl compounds (excluding *N*-containing) that were identified (using non-target workflow) in ozonated WWs and SRFA with OH radical scavenging (with DMSO).

Molecular formula	With OH radical scavenging (with DMSO)			
	WW Neugut	WW Werdhölzli	WW Glarnerland	WW SRFA
CH ₂ O*	13.1, 13.4	13.3, 13.6	13.5	13.1, 13.4
C ₂ H ₂ O	13.8	13.9	13.9	13.7
C ₂ H ₂ O ₂	16.3**	16.5**	16.4**	16.3**
C ₂ H ₂ O ₃	13.5	ND	13.6	ND
C ₂ H ₄ O ₂	ND	ND	13.0	12.8
C ₃ H ₂ O	15.7	15.9	13.0, 15.8	15.7
C ₃ H ₂ O ₂	15.0	15.2	15.1	15.0
C ₃ H ₂ O ₃	16.5**	16.7**	16.6**	13.0, 16.5**
C ₃ H ₂ O ₄ *	ND	ND	ND	17.9**
C ₃ H ₄ O	15.0	ND	15.1, 16.3	ND
C ₃ H ₄ O ₂	ND	ND	16.6**	16.5**
C ₃ H ₄ O ₃	13.8, 16.4**	14.0	13.9, 16.5**	13.7, 16.4**
C ₃ H ₆ O ₂	13.0	13.2	13.1	13.0
C ₄ H ₄ O ₂	15.8	16.0	15.9	13.5, 15.8
C ₄ H ₄ O ₃	13.5	12.9, 14.5	13.7, 15.2	15.9**
C ₄ H ₄ O ₄	ND	ND	ND	15.9**
C ₄ H ₆ O ₂	16.7**	15.9, 16.9**	15.8, 16.9**	15.7, 16.7**
C ₄ H ₆ O ₃	13.5, 13.8	13.7, 13.9	13.6, 13.9	13.5, 13.7
C ₄ H ₆ O ₄	12.8	13.0	12.9	12.7
C ₅ H ₄ O ₃	13.9	14.1	14.0	16.3
C ₅ H ₄ O ₄	ND	ND	12.8	14.2
C ₅ H ₆ O	16.3	16.5	16.4	ND
C ₅ H ₆ O ₂	13.3	13.5, 14.6	13.8, 14.6	14.4
C ₅ H ₆ O ₃	ND	16.8**	14.3, 14.5, 16.7**	ND
C ₅ H ₆ O ₅	ND	14.6	14.5	14.4
C ₅ H ₆ O ₆ *	ND	ND	ND	13.6
C ₅ H ₈ O	17.1	ND	14.6, 17.2	17.0
C ₅ H ₈ O ₃	13.9	14.1	14.0, 14.6	ND
C ₅ H ₈ O ₄	ND	ND	13.0	ND
C ₆ H ₄ O ₅	13.0	13.2	13.1	13.0
C ₆ H ₆ O ₄	14.9	15.1	15.0	14.5
C ₆ H ₆ O ₅	13.2	ND	ND	ND
C ₆ H ₈ O ₂	ND	ND	17.8**	ND
C ₆ H ₈ O ₄	14.8, 16.5**	16.7**	15.0, 16.6**	14.8
C ₆ H ₁₀ O ₂	15.4	15.6	14.6, 15.5	ND
C ₇ H ₆ O ₆ *	ND	ND	ND	13.9
C ₇ H ₈ O ₄ *	ND	15.0, 15.4	ND	ND
C ₇ H ₁₀ O ₃	15.4	15.6	15.5, 17.1**	15.4
C ₇ H ₁₂ O ₂	ND	ND	15.2	ND
C ₇ H ₁₄ O*	18.6	18.8	ND	ND
C ₈ H ₁₄ O ₂ *	ND	16.6	ND	ND
C ₈ H ₁₆ O ₄	ND	ND	ND	14.3
C ₁₀ H ₁₂ O ₅	ND	ND	14.8	ND
C ₁₁ H ₂₂ O*	ND	ND	20.8	ND
C ₁₄ H ₁₀ O ₂ *	ND	18.5	ND	ND
C ₁₄ H ₁₀ O ₃	17.7	ND	ND	ND
C ₁₄ H ₂₀ O ₃ *	ND	ND	18.6	ND

$C_{14}H_{20}O_4$	ND	ND	18.6	ND
-------------------	----	----	------	----

* Molecular formulas which were not identified in ozonated WWs, SRFA and LW without OH radical scavenging but only with OH radical scavenging; ** Retention times of double derivatized carbonyls

Section S.15 Carbonyl compounds that were formed in the ozonolysis of model compounds as a function of applied ozone dose

A selection of carbonyl compounds that were formed in the ozonolysis (with DMSO) of sorbic acid, 3-buten-2-ol, acetylacetone, phenol, 4-ethylphenol, 4-methoxyphenol as a function of applied ozone dose is shown in Figure S.7-Figure S.12. The degradation of sorbic acid and acetylacetone in its keto ($C_5H_8O_2$) and enol form (to which an H_2O loss occurred in the ion source of the MS (C_5H_6O)) is depicted as well. Among the selection of carbonyl compounds are mostly compounds predicted from the Criegee mechanism or to which confirmed or probable structures could be assigned. The RT of the selected isomer (highest peak area) is indicated for compounds for which more than one isomer was formed during ozonation. Peak areas were blank corrected.

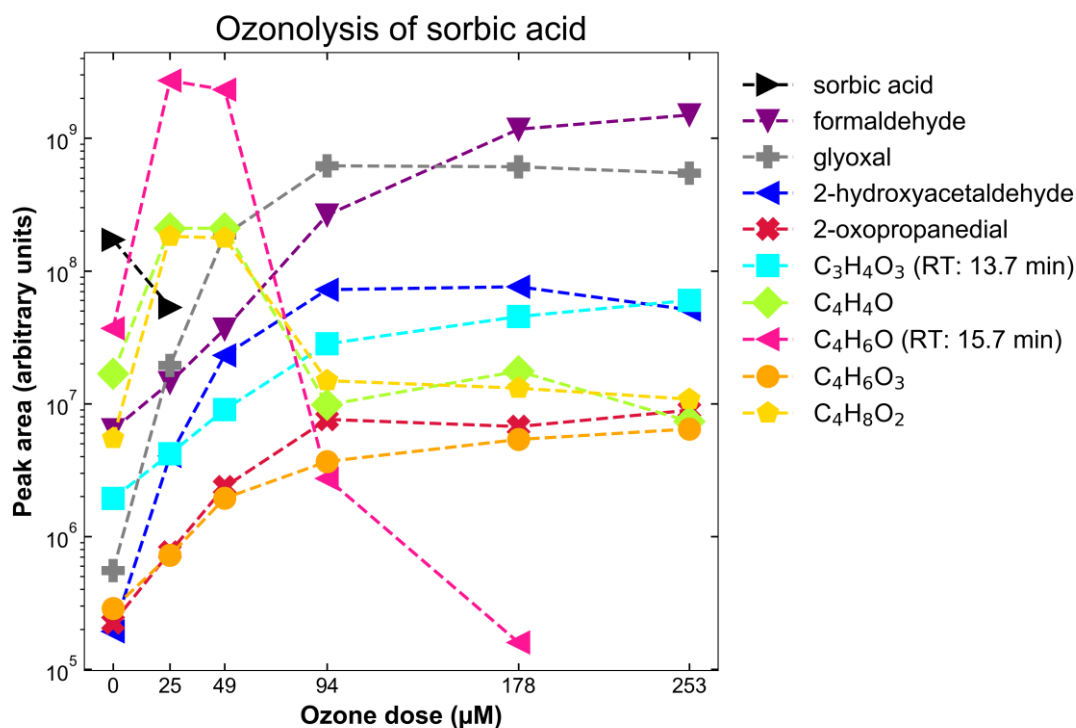


Figure S.7. Peak areas for a selection of carbonyl compounds that were formed during ozonolysis (with DMSO) of sorbic acid as a function of ozone dose (μM).

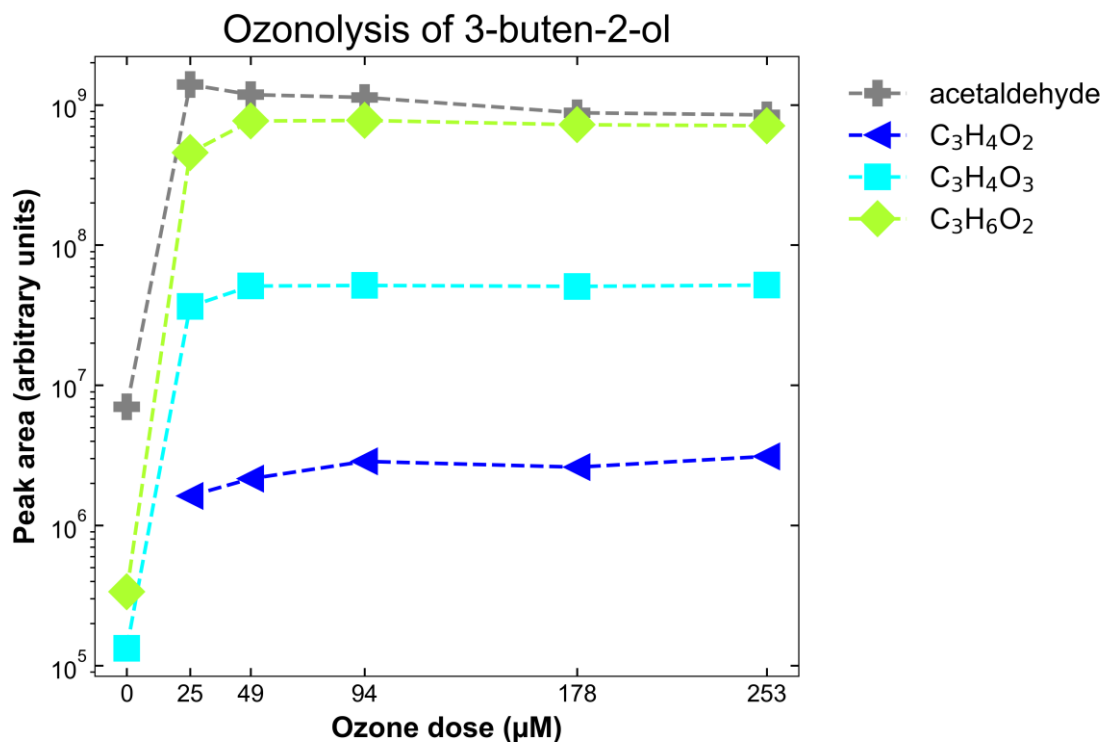


Figure S.8. Peak areas for all of carbonyl compounds that were formed during ozonolysis (with DMSO) of 3-buten-2-ol as a function of ozone dose (μM).

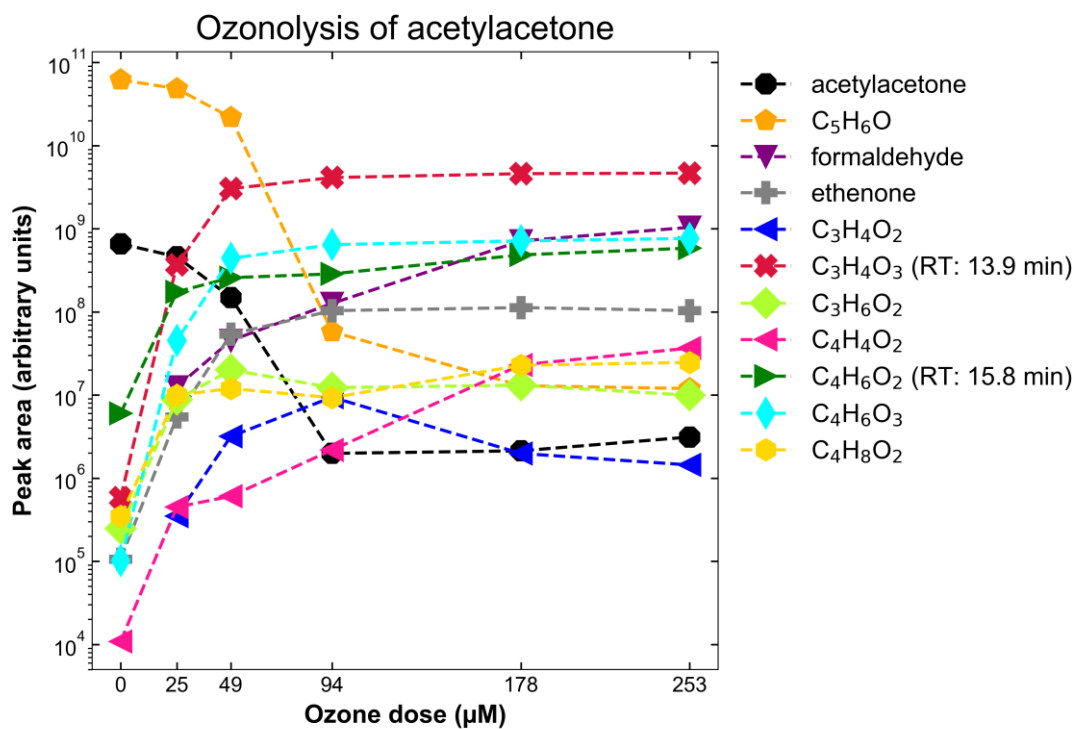


Figure S.9. Peak areas for a selection of carbonyl compounds that were formed during ozonolysis (with DMSO) of acetylacetone as a function of ozone dose (μM).

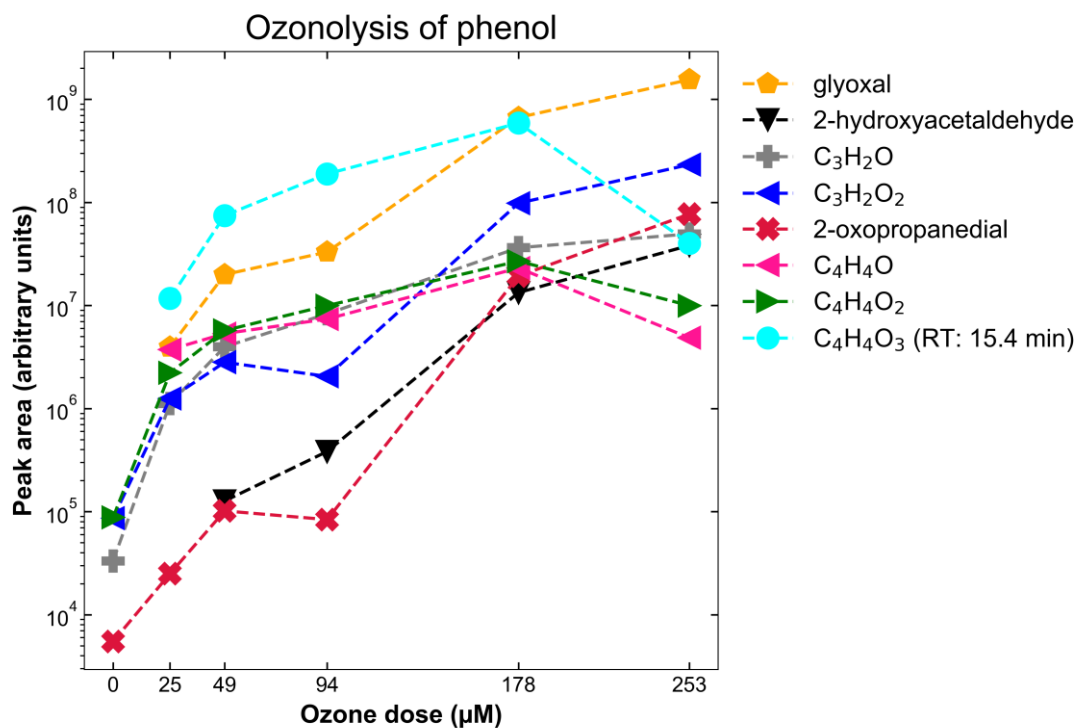


Figure S.10. Peak areas for a selection of carbonyl compounds that were formed during ozonolysis (with DMSO) of phenol as a function of ozone dose (μM).

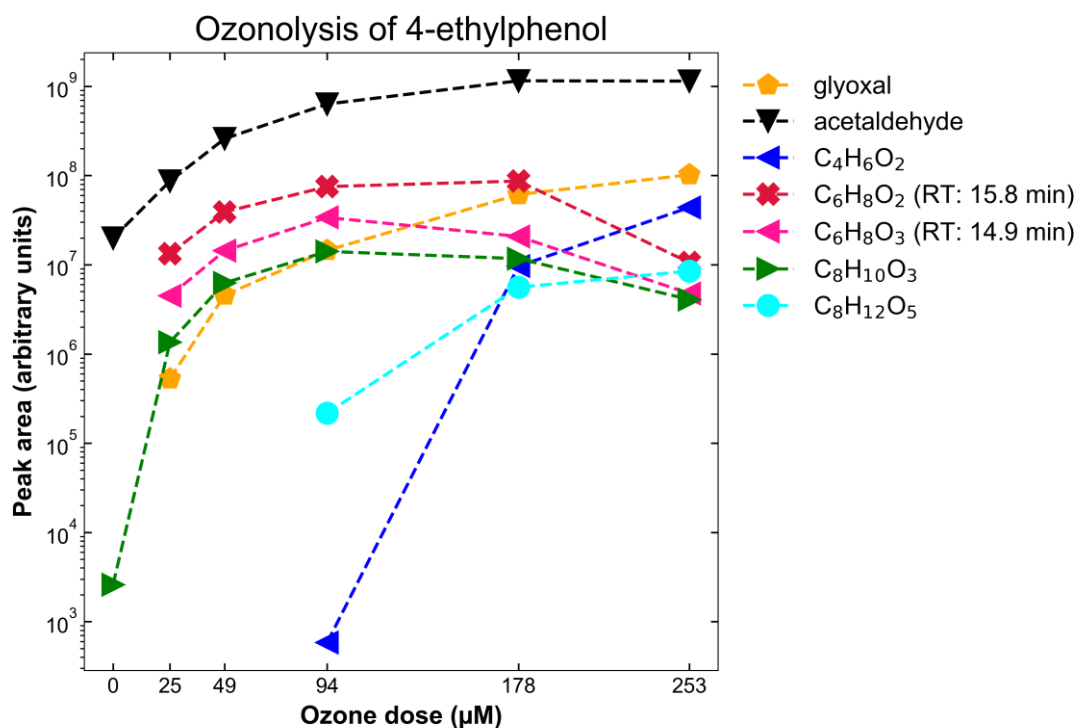


Figure S.11. Peak areas for a selection of carbonyl compounds that were formed during ozonolysis (with DMSO) of 4-ethylphenol as a function of ozone dose (μM).

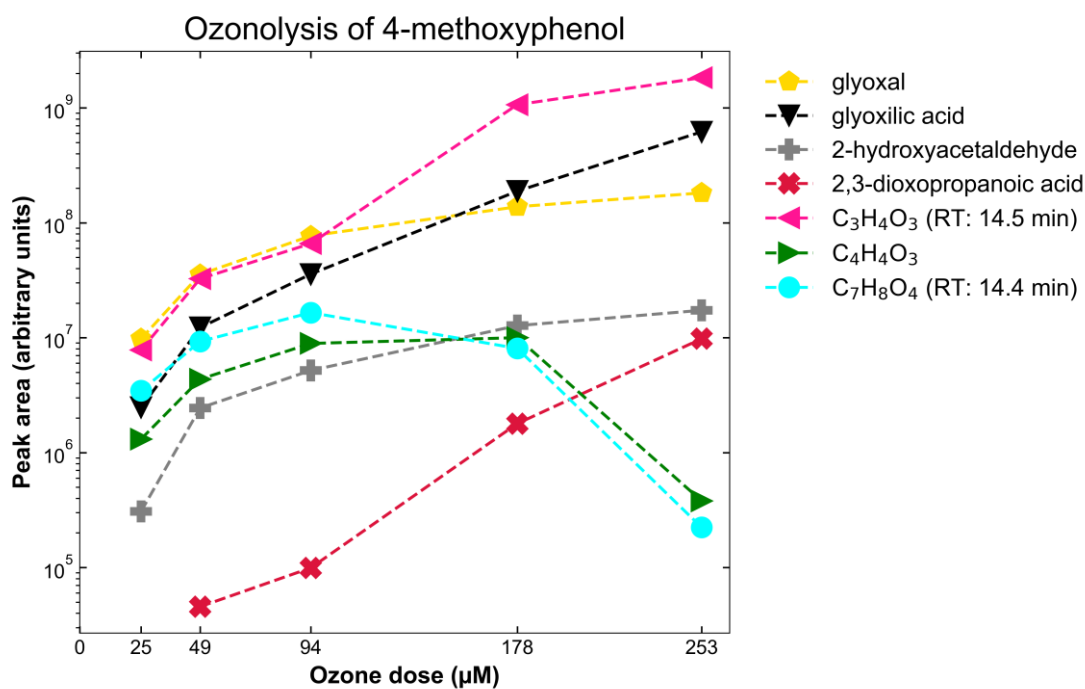


Figure S.12. Peak areas for a selection of carbonyl compounds that were formed during ozonolysis (with DMSO) of 4-methoxyphenol as a function of ozone dose (μM).

Section S.16 Drawings of carbonyl compound products formed during ozonolysis of model compounds according to Criegee mechanism

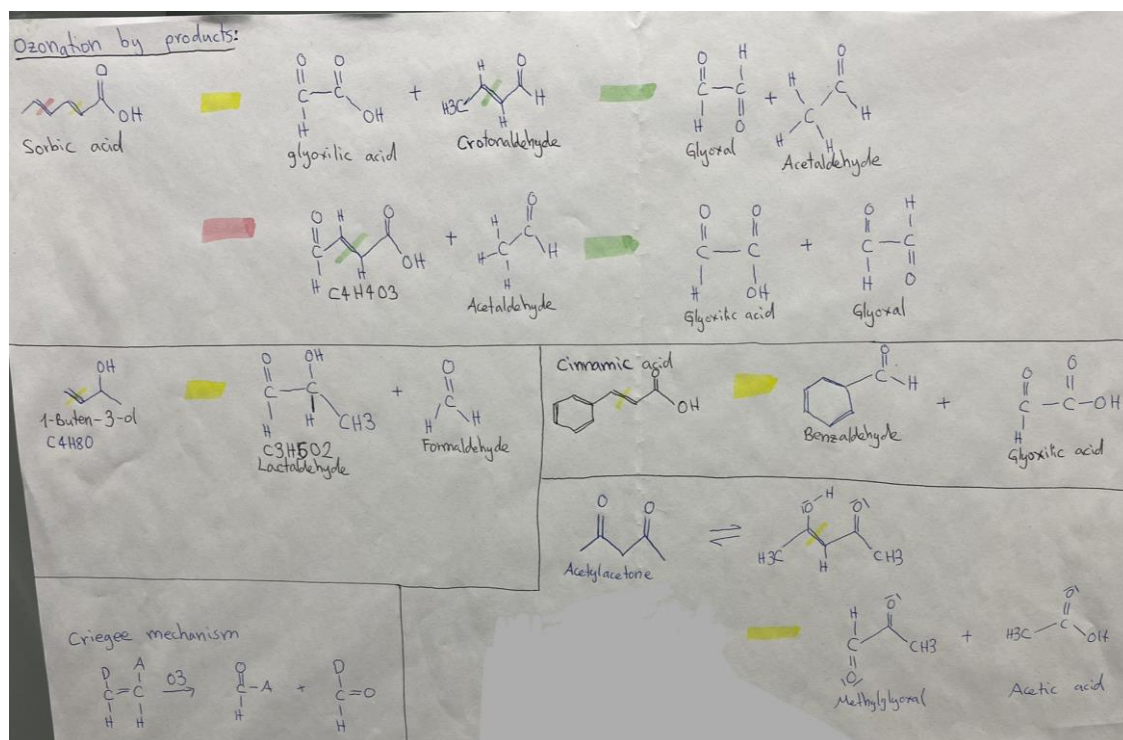


Figure S.13. Carbonyl compounds formed during ozonolysis of cinnamic acid, sorbic acid, 3-buten-2-ol and acetylacetone according to Criegee mechanism.

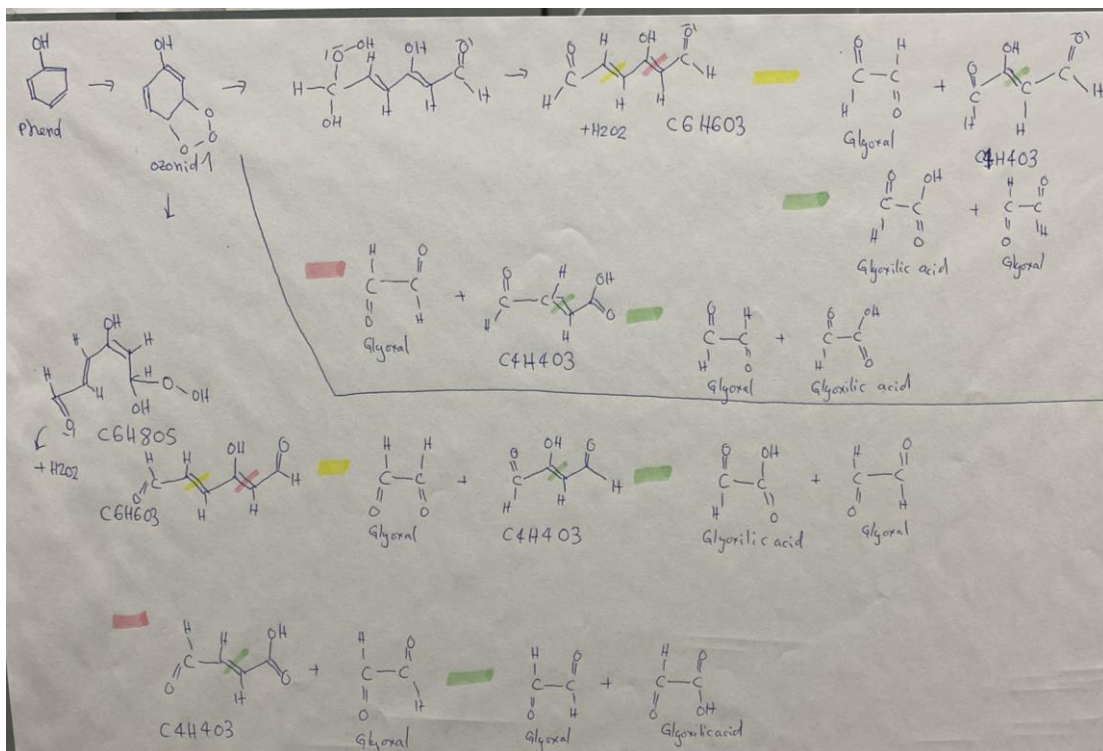


Figure S. 16. Carbonyl compounds formed during ozonolysis of phenol (ozonide 1) according to Criegee mechanism.

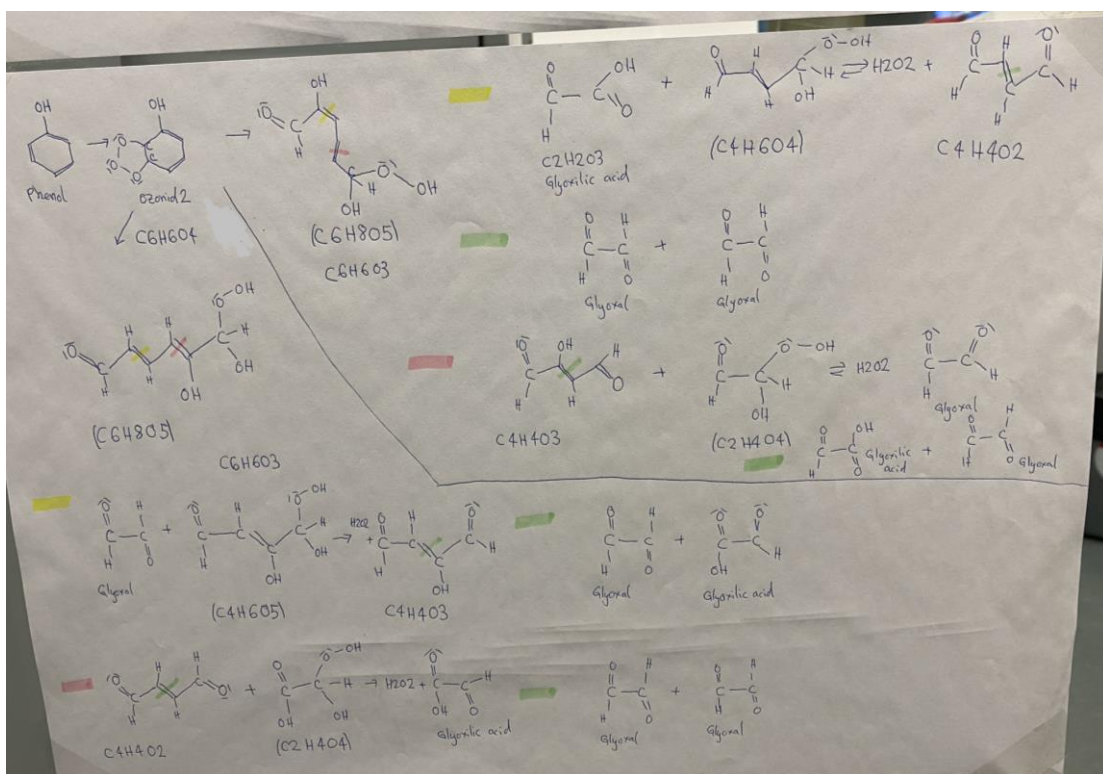


Figure S.17. Carbonyl compounds formed during ozonolysis of phenol (ozonide 2) according to Criegee mechanism.

Section S.17 Identified (using non-target workflow) N-containing carbonyl compounds in different water matrices

Table S.14. Molecular formulas and RTs of identified (using non-target workflow) N-containing carbonyl compounds in different water matrices.

Without OH radical scavenging (without DMSO)					
	WW Neugut	WW Werdhölzli	WW Glarnerland	WW SRFA	LW Greifensee
Molecular formula	Retention time(s)				
C ₂ H ₃ NO ₂	13.2	13.4	13.3	13.2	ND
C ₃ H ₅ NO ₂	13.3	13.5	13.5	13.3	13.3
C ₄ H ₅ NO ₄	13.5	ND	13.6	ND	ND
C ₄ H ₇ NO ₂	13.9	14.1, 14.5	14.0, 14.5	ND	ND
C ₄ H ₇ NO ₃	14.7	14.9	14.9	ND	14.7
C ₄ H ₉ NO ₂	ND	ND	10.6	ND	ND
C ₅ H ₇ NO ₂	12.7	12.9	12.9	ND	ND
C ₅ H ₇ NO ₄	13.7	13.9	13.8	ND	ND
C ₅ H ₇ NO ₆	ND	ND	ND	12.7	ND
C ₅ H ₉ NO ₃	15.1	15.3	15.3	ND	ND
C ₅ H ₁₁ NO	10.1	10.3	10.2	ND	ND
C ₆ H ₅ NO ₂	ND	12.9	12.9	ND	ND
C ₆ H ₉ NO ₄	ND	ND	14.0	ND	ND
C ₆ H ₁₁ NO ₃	11.6	11.8	11.7	ND	ND
C ₇ H ₁₁ NO ₂	16.0	16.2	ND	ND	ND
C ₇ H ₁₃ NO	ND	ND	10.9	ND	ND
C ₇ H ₁₃ NO ₄	ND	ND	11.1	ND	ND
C ₈ H ₁₁ NO ₆					12.6
C ₈ H ₁₅ NO ₄	ND	ND	11.0	ND	ND
C ₉ H ₁₃ NO ₅	15.0	14.7	15.1	ND	ND

Furthermore, N₂-containing carbonyl compounds were identified in different water matrices. These are the molecular formulas for N₂-containing carbonyl compounds identified in WW Glarnerland (without DMSO): CH₄N₂O, C₂H₂N₂O, C₂H₄N₂O, C₃H₂N₂O₃, C₄H₄N₂O₃, C₄H₆N₂O, C₅H₆N₂O₂, C₅H₆N₂O₃, C₆H₁₀N₂O, C₉H₈N₂O₃. CH₄N₂O is likely to be urea, which occurs in the urine, blood and milk of all mammals, and is also used widely as fertilizer or as starting material for the manufacture of plastics and drugs (Encyclopaedia Britannica, 2019). For N₂-containing carbonyl compounds with a higher number of carbon atoms there are many tentative structures which will not be discussed further here.

Declaration of originality



Eidgenössische Technische Hochschule Zürich
Swiss Federal Institute of Technology Zurich

Declaration of originality

The signed declaration of originality is a component of every semester paper, Bachelor's thesis, Master's thesis and any other degree paper undertaken during the course of studies, including the respective electronic versions.

Lecturers may also require a declaration of originality for other written papers compiled for their courses.

I hereby confirm that I am the sole author of the written work here enclosed and that I have compiled it in my own words. Parts excepted are corrections of form and content by the supervisor.

Title of work (in block letters):

Formation of carbonyl compounds during ozonation of wastewater: Method development for non-target screening and precursor evaluation
--

Authored by (in block letters):

For papers written by groups the names of all authors are required.

Name(s):

Gebhardt

First name(s):

Isabelle

With my signature I confirm that

- I have committed none of the forms of plagiarism described in the '[Citation etiquette](#)' information sheet.
- I have documented all methods, data and processes truthfully.
- I have not manipulated any data.
- I have mentioned all persons who were significant facilitators of the work.

I am aware that the work may be screened electronically for plagiarism.

Place, date

Zurich, 09.01.2021

Signature(s)

For papers written by groups the names of all authors are required. Their signatures collectively guarantee the entire content of the written paper.